The Properties of Thin Oxide Films in Relation to the Corrosion and Oxidation of Metals

Submitted for the degree of Ph.D.
in
The University of London

by

IJAZ HUSAIN KHAN

Department of Metallurgy
Royal School of Mines
Imperial College of Science and Technology
London.

1966.

ABSTRACT

For the present investigation the oxide films studied were produced by anodic oxidation. A number of techniques have been employed simultaneously. The growth characteristics of these films were studied and found to vary with the nature and pH of the electrolyte, surface treatment, growth current density and/or time of its decay at voltage. Oxide films with precisely controlled thickness can be produced on prepared aluminium specimens in electrolytes such as ammonium borate, citrate and tartrate solutions under specified conditions. Spectrophotometry has been found to be a very quick, most precise and a non-destructive method for measuring the thickness of oxide films both on and off the metal base. The chemical reactions involved in stripping films of oxide from aluminium using iodine in methanol and from zirconium using bromine in ethyl acetate do not significantly alter the optical properties or the thickness of the films. The dielectric constant of alumina formed on prepared surfaces has been found to be 9.8 ± 0.35 and that of zirconia 25.0 ± 1.0 under these conditions. Electron microscopic and electron diffraction studies showed development of $\tilde{\gamma}$ - alumina inclusions within the amorphous oxide as the oxide thickness exceeds about 1000Å. Recrystallisation of the amorphous oxide has been shown to depend upon surface preparation and ultimate thickness of the oxide.

The effect of various ions such as H^+, OH^-, Cl^-, CrO_4^{--}, SO_4^{--}, HCO_3^- and CO_3^{--} and molecular ligand NH_3 has been studied. It is suggested that H^+, OH^-, Cl^- and CrO_4^{--} ions and NH_3 ligands are strongly adsorbed on aluminium oxide. Some of these ions such as OH^-/H^+, Cl^-/H^+ and OH^-/H^+ and/or NH_3 ligands are incorporated into the oxide without changing its

structure. In alkaline solutions thinning of aluminium oxide has been observed in addition to the uptake of these ions. It is believed that adsorbed CrO_4^{--} ions tend to hinder the penetration of other ions. The electrical resistance of the oxide decreases due to the entry of ions. This effect is more pronounced due to the entry of H^+ or OH^- ions under conditions of direct current polarization.

Chloride ions possibly penetrate very rapidly at the crystalline spots of the oxide and produce substantial change in the resistance of the oxide locally. This effect is not significantly dependent upon the pH of the chloride solution. Chloride ions cause enhanced thinning of alumina in alkaline solutions. Permeation of Cl^- ions through stripped films of alumina was possibly preceded by pore formation.

TABLE OF CONTENTS

TABLE OF CONTENTS CONT'D.

TABLE OF CONTENTS CONT'D.

TABLE OF CONTENTS CONT'D.

SECTION I

INTRODUCTION

I - 1 Statement of Problem:

The majority of metals used in modern technology tend to oxidize spontaneously in all of the environments normally encountered. Aqueous corrosion is a widely occurring oxidation phenomenon; a generalized example of this type of corrosion is given below:

$$2M + xH_2O \rightarrow M_2O_x + xH_2 \quad \ldots\ldots\ldots\ldots\ldots\ldots\ldots\ldots (I - 1)$$

where M is an x valent metal.

The rate of oxidation may be controlled by the properties of the oxidation product. If the oxide formed is porous or non - adherent, corrosion will go on unchecked. On the other hand a non - porous and adherent oxide layer will reduce the rate of further oxidation by physically isolating the reactants. The diffusion of reacting species through the protective oxide layer becomes the rate controlling step in the oxidation process and this is the case for metals such as Al, Zr, Ti, U and Ta.

The characteristics of oxide films formed on these metals have been studied by numerous workers.[1 - 14] Many of the properties of these oxide films have been observed to be different from those of the bulk oxides. Several papers[1 - 6] have stressed the importance in corrosion of the characteristics of thin oxide films rather than those of the bulk oxides.

The corrosion product hydrogen plays an important role in the aqueous corrosion processes. For example enhanced corrosion rates have been observed in some cases, which are believed to be associated with the presence of hydrogen. Two general mechanisms have been put forward to explain how this deleterious effect of hydrogen can arise:

a) hydrogen (as ions or atoms) may diffuse through the oxide to be evolved as molecular hydrogen at the oxide - metal interface and so cause the mechanical failure of the film;[7,10]

b) hydrogen entry into the oxide may change the electrical conductivity[8 - 10] of the film by acting as a donor impurity. An increase in the electrical conductivity of the oxide may enhance the diffusion of ions , resulting in higher corrosion rates.

The hydrogen which has diffused through the oxide may also dissolve in the metal or form a metal hydride. These processes are known to cause embrittlement of the metal. This is often more damaging than loss of strength of the metal, due to reduction in area of the metal by corrosion. The exact mechanism of hydrogen embrittlement is a matter of some debate but its occurrance is beyond question.

Attempts have been directed towards the developement of improved corrosion resistant alloys by reducing the diffusion constants in the oxide film and by increasing the protective thickness of the oxide. These developments have been limited because of insufficient data regarding the mechanical and electrical characteristics of, and diffusion in, the thin oxide films.

Impedance studies supported by other physical methods such as optical[8,11] techniques, electron diffraction[9,11 - 12] and weight[13 - 14] gain measurements have been applied to the investigation of the rates of corrosion and diffusion processes through oxide layers formed on metals and alloys. The oxide has been considered not only as an ionic diffusion barrier but also as an electrolyte and a semi - conductor. It has been suggested that the electronic conductivity may alter the ionic diffusion rates, the protective thickness of the film and the hydrogen pick - up of the metal. All these factors change the corrosion behaviour of the metal.

I - 2 Present investigation:

Present work was designed to study the thin oxide films in relation to the corrosion and oxidation of the metals. Attention was focussed on the transport processes through thin oxide films, on metals such as aluminium and zirconium, and the effects on these transport processes of such factors as pH and composition of the electrolyte; and the nature and thickness of the films were studied.

For this investigation the films studied were produced by anodic oxidation. These films were chosen in preference to films produced by corrosion or thermal oxidation as it was believed that such films were produced more easily and consistently than corrosion films. As the work progressed it became clear that these anodic films were neither as reproducible nor as free from defects as was originally believed. As a result of this a substantial effort was devoted to the study of thin anodic oxide films, their properties, and how to produce films free from gross defects.

SECTION II

LITERATURE SURVEY

II - 1 Introduction:-

Pilling and Bedworth (1923)[15] first introduced the concept of oxide volume ratio to predict whether the oxide formed will be protective or non - protective. This ratio is defined by the equation:

$$\phi = \frac{\text{volume of oxide containing 1gm. atom of metal}}{\text{atomic volume of metal}} \quad (II - 1)$$

The theory by which ϕ is related to the stresses in the oxide, and hence to the oxide failure, is not applicable to oxidation kinetics where outward movement of metal ions takes place.

Measurements of weight gain and changes in thickness of the oxide were earlier employed[16 - 20] to investigate the rate of oxidation of a metal. Three basic laws (linear, parabolic and logarithmic), with some sub - forms, have been found to apply to the oxidation kinetics.

Oxide films have been examined for chemical[6,16,20] composition, structural features[5,12,16,20 - 23] and mechanical defects such as pores, micro - cracks and blisters.[10,16,20] Recently[19,24 - 27] stress has been laid on the importance of electrical, mechanical and diffusion characteristics of films for understanding the mechanisms of corrosion and oxidation of metals.

There is a shortage of data on diffusion characteristics of, and in inorganic compounds, particularly the oxides formed during corrosion. The present work was started to investigate the diffusion characteristics and related properties of alumina and zirconia formed anodically.

The literature survey includes a brief review of anodic films and their characteristics, and a more detailed consideration of the following:

a) the behaviour of the oxide and its electrical properties in aqueous environmental conditions;

b) diffusion and migration processes through the oxide during corrosion.

II - 2 Anodic Oxide Films.

II - 2 - (I) Introduction:

The work of Güntherschulze and Betz[29] initiated much of the present interest in the anodic films. Johansen et al.[28] and Young[29] have compiled the recent literature on the subject, The anodic behaviour of most metals is very sensitive to surface preparations, impurities, nature of electrolyte and forming conditions. A pre - existing film may affect the optical properties of the anodic film and its adhesion to the substrate in certain cases.[30]

The weight of the oxide is generally both current and time dependent, but the final thickness may be modified by the nature of the electrolyte, which may dissolve some of the oxide. Most of the valve metals give films with bright interference colours.

The non - ionic current usually evolves oxygen if the potential is above the reversible value for oxygen evolution and predominates at very low fields. Young[29] has introduced the concept of oxide - overpotential analogous to the hydrogen - overpotential. This is related to the driving force available for the oxide growth.

The growth of the anodic film is primarily a process of ionic conduction at high field strengths, complicated by ⁺ transfer processes at metal oxide and oxide-solution interfaces. The rate of increase of thickness of the oxide film is given by the equation overleaf:

$$\frac{dt}{dt_m} = \frac{iM}{\rho zF} \quad \text{.....(II - 2)}$$

where t = film thickness

t_m = time

i = ionic current density

M = molecular weight of the oxide

ρ = density of the oxide

zF = number of faradays per mole

If the differential field strength ($E_d = \frac{dv}{dt}$ where v = voltage) is assumed to be constant, then:

$$\frac{dv}{dt_m} = \frac{E_d dt}{dt_m} = \frac{iE_d M}{\rho zF} \quad \text{.....(II - 3)}$$

It is suggested[29] that the ionic current density (i) and the field (E) are related by the following expression:

$$i = A\exp(BE) \quad \text{.....(II - 4)}$$

where A and B are constants.

This equation also expresses ionic transport processes

Films produced at high current probably have high leakage current. This may imply more imperfections, but the film, due to its greater ability to deform in the presence of ionic fluxes, is often more free of mechanical flaws.

II - 2 - (2) Oxide Film Thickness Measurements:

Measurement of film thickness is of fundamental importance in the study of growth kinetics and other properties of oxides. Several workers,[31 - 36] using optical and other methods, have determined the thickness of barrier-type anodic alumina films. The spectrophotometric method has been successfully employed for both anodic and corrosion films on some metals.[37 - 40] Studies of optical properties of oxides have been reported in several papers.[29,31,39 - 42]

II - 2 - (3) Structure and Nature of Anodic Alumina Films.

Many workers[43 - 47] have examined anodic alumina films using optical, electron microscopic, and electron diffraction methods.

Thin barrier - type oxide films have been shown to be amorphous in nature,[46] and to replicate surface details of the metal.[46 - 49] Franklin[45] and Stirland et al.[46] have reported a cell structure for these films similar to that of porous films. Areas of crystalline $\bar{\gamma}$ - alumina have been found to develop as randomly distributed cylindrical columns, passing right through the amorphous layers at formation potentials exceeding 100 volts.[46] Pryor[48] has proposed the γ - alumina structure for anodic films (40 - 100 volts) formed in boric acid or ammonium tartrate solutions.

Hass[31] examined 10 - 150 volt films formed on evaporated aluminium mirrors in 3·0% tartaric acid solution (pH5 5 adjusted with ammonium hydroxide). He reported these films to be free from pores, and without any cell structure. A diffuse electron diffraction pattern was observed. Other studies[49] gave evidence of fine pores all over the surface.

The pore size in porous films has been shown to be dependent upon the forming electrolyte, and independent of voltage.[43 - 44]

The barrier - type film can contain a hydrated oxide, an anhydrous amorphous oxide and crystalline $\bar{\gamma}$ - alumina.[50 - 51] Variations in thickness of the oxide on a microscopic scale have been reported, together with holes and cracks which can be penetrated by electrolytes.[50 - 51] The barrier - type anodic alumina has been shown[35] to contain anions from the electrolyte as part of its structure.

Dorsey[52] has recently observed that the thin barrier layer beneath the porous oxide gives an infra - red absorption band with the alumina trihydrate region.

II - 3 Properties of Oxide Films and Metallic Corrosion.

II - 3 - (I) Introduction:

The oxide films, formed under different oxidizing conditions, have been divided into the following regions:

a) very thin films ($< 100\text{Å}$);
b) thin films (100 - 10,000Å);
c) thick films ($> 10{,}000\text{Å}$).

The thin film region may not be exceeded on some metals, even at relatively high temperatures.

Wagner's classical theory[16,19,26] is applied, within its limitations, to the oxidation of metals and alloys in the thick film region. Diffusion of ions through the oxide is the rate controlling process for oxidation.

Mott and Cabrera[16,18,26] have put forward a modified model for thin films, based on Mott's original theory of electron tunnelling for very thin films. Electrons tunnel in a quantum mechanical manner through very thin film, and produce oxygen ions which generate a strong electric field. The oxidation process is electric field controlled, which pulls out cations through the oxide.

Uhlig[26] proposed a theory in which the transfer of electrons is considered as the rate controlling process, rather than cation migration. He has suggested that the electronic work function of metals is the energy required for electron transfer.

II - 3 - (2) Conductivity of Oxide Films

Thin films exhibit both ionic and electronic conduction. Electronic conductivity has been considered as one of the important properties of the oxide which influences the corrosion rate directly, or indirectly.[7,24,26] The presence of traces of impurities in these oxides may bring about marked changes

in conduction.

The specific conductivity of oxidation products, ranges from 10^{-16} to 10^{2} ohm^{-1} cm^{-1} (approximately) depending upon the extent of participation of electrons in conduction.

Pryor et al ,[12,48,53,54] investigated the effect of various anions on the specific conductivity of anodic aluminium oxide. They have suggested that chromate ions are very strongly adsorbed on the surface of the oxide and produce a barrier against the entrance of the hydrogen and hydroxyl ions into the oxide. During immersion in sodium fluoride and chloride solutions, the anodic alumina films have been observed to show large increases in specific conductivity. This is not associated with thinning or corrosion enhancement.

Pryor and co-workers[12,48,53,54] have assumed that OH^{-}, Cl^{-} and F^{-} ions enter the oxide and exchange with oxygen ions of the oxide lattice forming n - type defects. These defects increase the conductivity of the film. They have also pointed out that the exchange is perhaps not uniform on a microscale, and occurs preferentially at structural discontinuities such as grain boundaries, dislocations and other internal surfaces in the oxide film. Under similar conditions $SO4^{--}$ ions do not appear to enter the oxide lattice of the thin surface oxide film significantly.

II - 3 - (3) The Electrolytic Nature of the Oxide:

It has been suggested that the oxide barrier layer acts as an electrolyte and a semiconductor.[24] It seems possible from such considerations that the electronic conductivity significantly affects ionic diffusion and the hydrogen pick - up. The partial reactions involved in metal oxidation are:

$$2M \rightarrow 2M^{++} + 4e^{-} \qquad \text{(II - 5)}$$

at the oxide-metal interface.

$$O_2 \longrightarrow 2O^{--} - 4e^- \quad \text{.....(II - 6)}$$

at the oxide-environment interface.

$$2M^{++} + 2O^{--} \longrightarrow 2MO \quad \text{.....(II - 7)}$$

ionic diffusion.

These reactions give an excess negative charge at the oxide - metal interface, and an excess positive charge at the gas - oxide interface. The electronic conductivity of the oxide will tend to diminish the charge difference across the barrier film and facilitate ionic diffusion through the oxide.

In the case of aqueous corrosion[7,24] the partial reactions may be written:

$$2H_2O \longrightarrow 2OH^- + 2H^+ \quad \text{.....(II - 8)}$$

in the solution.

$$2OH^- \longrightarrow 2O^{--} + 2H^+ \quad \text{.....(II - 9)}$$

at the oxide - solution interface.

$$2M \longrightarrow 2M^{++} + 4e^- \quad \text{.....(II - 10)}$$

at the oxide - metal interface.

$$2M^{++} + 2O^{--} \longrightarrow 2MO \quad \text{.....(II - 11)}$$

by diffusing species.

From consideration of these reactions a concentration gradient of H^+ ions seems likely which, together with the excess negative charge on the metal, produces a potential gradient. The protons can decrease the charge difference across the oxide by diffusing under the potential and activity gradients, or the electrons may diffuse and discharge the protons. The oxide behaviour, and the various possible reactions involved in aqueous corrosion, are depicted schematically in Fig.(1). There may be other possible reactions, e.g. reduction of oxygen at the solution - oxide interface. The total conductivity

of the film is given by the expression:

$$g_t = g_i + g_e \quad \text{.....(II - 12)}$$

where g_t = total conductivity.

g_i = electrolytic conductivity.

g_e = electronic conductivity.

II - 3 - (4) Semi - Conductivity of the Oxide:

The asymmetric electrical character of the oxide on a valve - metal suggests an asymmetric structure for the oxide layers. Indirectly, it has been shown[26,27,55] that thin oxides depart from stoichiometry and may contain excess cations and / or oxygen vacancies near the oxide - metal interface. The metal - rich layer behaves as an n - type semiconductor and the oxygen - rich layer as a p - type conductor. Van Geel et al.,[56] interpreted impedance measurements on aluminium oxide films in terms of a layer structure. An intrinsic oxide layer is suggested between an n - type conductor near the oxide - metal interface and a p - type conductor at the oxide - electrolyte interface. Similarly, Sasaki[57] represented oxide films on tantalum.

The variation in oxidation rates of metals results, in part, from the difference in the type of defects in their oxides. For example, Cu_2O in an environment of oxygen, shows a significant concentration of copper ion vacancies and positive (electron) holes, which allow for an enhanced diffusion of the copper ions and of electrons. While the Al_2O_3 lattice supports only a small concentration of lattice defects, hence it exhibits low diffusion

The defect structure of the oxide has a major influence upon its ionic diffusion characteristics, influencing the growth of the oxide and its subsequent reactions with the surrounding environment. Direct experimental data on the distribution of defects in thin films have been difficult to obtain, and there have been some assumed models of distribution of defects in the oxide.

Heckelsberg[58] and co-workers have determined the conductivity of both p - and n - type semiconducting oxides before and after hydrogen absorption. It has been shown that hydrogen, which acts as a donor impurity, increases the electronic conductivity of an n - type oxide and decreases that of a p - type oxide.

The harmful effects of the corrosion product hydrogen have been explained in terms of mechanical effects on the oxide or oxide - metal interface. More recently an explanation has been proposed[8 - 10,25,59] where hydrogen is treated as an alloying element. It is considered to be incorporated as H^+ or OH^- in the oxide, producing a change in the semiconductivity of the oxide. In order to maintain electrical neutrality electrons must enter from the metal. This results in a different rate of corrosion of the metal and enhanced hydrogen pick-up.

II - 3 - (5) Mechanical properties of the Oxide.

The nature of the stresses set up in oxide films on metals, depends upon the nature of diffusing species,[60] surface characteristics,[61] expitaxy and growth conditions.[62,63]

The volume ratio has been found in some cases to provide a qualitative estimate of stresses developed in oxides.

Alloying elements have been shown[8,64] to change the mechanical, and some physical properties of the oxide. Oxide films usually deviate from ideal bulk homogeneity under different regimes. For example, pores, cracks, and blisters have been reported[10,16,20] in these films, formed on various metals. The mechanical breakdown of a good protective oxide will lead to increased oxidation rates. This breakdown is believed to arise, in some cases, from failure due to stresses grown into the film.

II - 3 - (6) Diffusion and Migration Processes:

The phenomenon of diffusion through the oxide films is of fundamental significance in corrosion studies. The rate of oxidation of metals in any environment is dependent upon the kinetics of migration of the reacting species, assuming that a continuous layer of oxide is formed on the surface.

Diffusion of ions and electrons is further influenced by phase - boundary reactions, and the presence of chemical and potential gradients within the oxide film. Other significant factors include nucleation and crystal growth of the reaction product, and the thermodynamic stability and crystal structure of the oxidation layer and the metal.

The electrolytic nature of the oxide allows the diffusion and migration to occur, the extent of diffusion depending upon the ionic conductivity of the oxide. These processes are also influenced by the electronic conductivity of the oxide.

The data for diffusion of ions through the oxide are scarce. The parabolic rate law of oxidation of metals has been interpreted as arising from a diffusion controlled process. The flux of reacting species through the oxide layer (Jx gm/cm^2.sec.) has been related to the rate of weight gain (dw/dt_n gm./cm^2.sec.) by the following equation.

$$Jx = D \frac{dC}{dx} = \frac{dw}{dt_n} \text{ gm./cm}^2\text{.sec.} \quad \text{.....(II - 13)}$$

where D = coefficient of diffusion

x = oxide thickness

C = concentration of ions.

In order to maintain electrical neutrality within the oxide, usually one ion species and either electrons or electron holes are the diffusing species

Assuming that at equilibrium the concentration difference $(C_i - C_o)$ of reactant across the oxide layer is independent of its thickness (x)

$$dw = \frac{D(C_i - C_o)}{x} \, dt_m = \frac{D(C_i - C_o)}{Kw} \, dt_m \quad \text{.....(II - 14)}$$

x preceding weight gain.

Integrating gives:

$$w = \left(2\frac{D(C_i - C_o)}{K} \right)^{\frac{1}{2}} t_m^{\frac{1}{2}} \quad \text{.....(II - 15)}$$

where C_i is the reactant equilibrium concentration at metal - oxide interface

and C_o the concentration at oxide - atmosphere interface which depends upon oxygen pressure.

II - 3 - (7) Adsorption of Ions:

Pryor[65] has suggested that ions tend to adsorb on an aluminium electrode covered with a thin layer of continuous oxide, producing an electrostatic field. The electric field due to adsorbed anions, which depends on the anion diameter and its valency, enables aluminium ions to migrate across the oxide. The rate of transport of aluminium ions from the metal - oxide interface to the oxide - solution interface is considered to be an exponential function of the field strength and also dependent on the defect structure of the oxide. Cation adsorption, on the other hand, produces an electric field allowing transfer of electrons from the metal - oxide interface towards the oxide - solution interface.

Modi et al.[66] and O'Connor et al.[67] have shown that H^+, OH^- and CrO_4^{--} ions are strongly and specifically adsorbed on corundum. The hydrogen ions adsorbed on an oxide covered electrode will tend to accelerate the electron migration through the oxide lattice.

II - 3 - (8) Permeation of ions through seperated Oxide Films.

Burwell[68] first investigated permeation of an electrolyte through a membrane of separated porous alumina. He showed that potassium chloride and potassium nitrate penetrated the film at approximately equal rates. He suggested the presence of a comparatively impervious layer in the porous oxide films.

Mitchell and Solomon[69] studied the permeability of isolated 100 volt zirconia films to potassium nitrate. They have suggested on the basis of a higher observed activation energy for permeation through the oxide than through water, that the process is not simply diffusion through oxide pores.

II - 3 - (9) Impedance Characteristics of Oxides.

An oxide covered electrode can be considered analogous to a parallel plate condenser, with oxide as the dielectric and the metal and solution as plates. The film, however, is seldom a perfect insulator due to its defect structure.

A simple analogue consisting of a capacitor and a resistor in parallel, has been used to represent the oxide film, by many workers[8,25,71 - 72]. It is recognised that both the capacity and the resistance are frequency dependent. The equivalent impedance of the oxide is in series with the impedance of the Gouy - Chapman - Helmholtz double layer, in a solution. A.C. impedance measurements[8,29,73 - 75] have been applied to study both anodic and corrosion films. Frequency dispersion measurements help to detect pores and fissures in an insulating dielectric film.

In the case of an ideal capacitor R_p is infinite or R_s is zero, as the voltage and current would be out of phase by 90 . The phase angle (ϕ) in an actual dielectric capacitor deviates from 90°. This deviation ($90^\circ - \phi$) is called the "loss angle" δ. It can be shown that $\tan\delta = \omega C_s R_s = \frac{1}{\omega C_p R_p}$ and is known as the "loss tangent". Abnormally high frequency dependence of the capacity, and a higher tan δ , indicate flaws in the film.

Recently impedance measurements[71,75] have been applied to the study of the aqueous oxidation of such metals as Ti, U, Zr, V and Al and some of their alloys. It was observed that the impedance of these metal electrodes changes as a function of cathodic polarization and this was interpreted in terms of the entry of hydrogen during this polarization. The abnormally high capacities of electrodes of Ti, Nb, U and V, covered with an oxide film, observed by these workers, have been explained in terms of a chemical reaction:

(faradaic capacitance) involving a change of cation valency i.e.

$$M^{2+}O^{2-} + H^{+} + e^{-} \rightarrow M^{+}OH^{-} \quad \text{.....(II - 16)}$$

which contributes to the total capacity.

SECTION III

EXPERIMENTAL METHODS

III - 1 Introduction:

The experimental techniques are considered in the following order; preparation of the oxide films, determination of their thickness, optical, electron microscopic and electron diffraction studies, and investigation of electrical and permeation characteristics of the films.

III - 2 Preparation of the oxide films.

The characteristics of barrier type anodic films are influenced by a number of factors during growth, such as the nature of the electrolyte, its pH and temperature, electric field, substrate treament and the ultimate thickness of the film. Great efforts were made to optimize the growth conditions, which were carefully controlled during these studies.

III - 2 - (1) Materials.

Aluminium foil* (0.25 mm.thick) 99.99% pure and zirconium sheet† (0.30 mm.thick) 99.8% pure were used during this work. The impurities in zirconium were as follows (in p.p.m.):-

Hf	65 - 100
Fe	400 - 600
O_2	1000 - 1100
Sn	< 100
Others	< 50

‡upplied kindly by *Star Aluminium Co.Ltd., and
†Imperial Metal Industries Ltd., (U.K.)

III - 2 - (2) Specimens.

(a) Shape and size:

A standard size and shape of specimens was developed and retained for convenience of operation throughout the investigations. The specimens were cut, in one piece, from the metal foil or sheet in a shape of a "flag" 2 x 2 cm. with a "pole" (0.3 x 2 cm.). See Fig.2a.

(b) Degreasing:

The specimens were washed with methanol and acetone successively and allowed to dry in air at room temperature.

(c) Annealing:

The aluminium specimens were annealed at 350°C for sixty minutes in air, using a pyrex glass container. For the zirconium specimens a quartz sealed tube was used as a container and the specimens were annealed at 780°C for sixty minutes under vacuum initially better than 1×10^{-4} mm. Hg.

III - 2 - (3) Solutions used for surface preparations anodizing and isolation of oxide films.

A.R. grade reagents and distilled water were used in making the solutions for the respective metal to be treated and anodized. Unless stated otherwise the solutions were aqueous.

(a) Aluminium.

Solution I for (alkaline) etching: 100 g/l NaOH.
Solution II for washing after etching: 350 g/l HNO_3.
Solution III for (acid) etching: 5ml nitric acid (sp.gr.1.42), 2 ml hydrofluoric acid (40%) and 100 ml water.

Solution IV for electropolishing: 200 ml of perchloric acid (sp.gr. 1.48) mixed with 1 litre of absolute ethyl alcohol.
Solution V for electropolishing (chromic - phosphoric - sulphuric acids): 156 gm. of chromic acid anhydride, 617 ml. of orthophosphoric acid (sp.gr. 1.75) 134 ml. of concentrated sulphuric acid (sp.gr. 1.84) and 240 ml. of distilled water.

For anodizing aluminium the following solutions were used:-

Solution VI 30 g/l ammonium borate pH9.0± 0.1 (unless stated otherwise) adjusted carefully with ammonium hydroxide (sp.gr. 0.88).
Solution VII 30 g/l ammonium citrate pH 9.0± 0.1 adjusted with ammonium hydroxide (sp.gr. 0.88)
Solution VIII 30 g/l tartaric acid pH 5.5 adjusted with ammonium hydroxide (sp.gr. 0.88)

For stripping off alumina films.

Solution IX 150 g/l iodine in methanol (anhydrous).

(b) Zirconium.

Solution X for etching: 10 ml. of 40% hydrofluoric acid, 40 ml. concentrated nitric acid (sp.gr. 1.42) and 50 ml. of distilled water.
Solution XI for anodizing: saturated solution of ammonium borate pH 9.0± 0.1 adjusted with ammonium hydroxide (sp.gr. 0.88)
Solution XII for anodizing: 10 g/l KOH.
Solution XIII for anodizing: 0.2N Na_2CO_3

For stripping off zirconia films.
Solution XIV 120 g/l bromine in ethyl acetate.

III - 2 - (4) Surface preparations.

(a) For Aluminium

Etching: Two different chemical etching treaments were used. The specimens were etched in the sodium hydroxide solution (Solution I) for four minutes, dipped in the nitric acid solution (Solution II) for about 10 seconds and finally washed with distilled water. Some specimens were etched in Solution III for 30 - 60 seconds and washed with distilled water.

Electropolishing: Some specimens were electropolished in the perchloric acid - ethyl alcohol solution (Solution IV) for 2 minutes at $10^{\circ}C$ using a current density of 0.2 A/cm^2 at about 20 volts. The specimens were then washed with methanol and finally with water.

A number of specimens were electropolished in the chromic - phosphoric - sulphuric acids solution (Solution V) for two minutes at $80^{\circ}C$, employing a current density of 0.25 A/cm^2 at about 15 volts. These specimens were then washed with distilled water.

Electropolishing and etching: Some of the electropolished specimens were also etched in Solution I and subsequently washed with nitric acid, Solution II, and distilled water successively.

(b) For Zirconium:

Only chemical polishing was used. The specimens were dipped repeatedly in hydrofluoric - nitric acids etch (Solution X) and flushed with distilled water till a bright and unpitted surface was obtained.

III - 2 - (V) Anodization:

The "poles" of the specimens were initially anodized for insulation purposes to a potential about 50 volts greater than that intended for the main body of the specimens. These anodized "poles" of some specimens were further coated with Lacomite (Fig.$2a_1$) to ensure complete insulation during impedance studies of the oxide covered specimens. The "pole" ends were abraded to allow good electrical contact.

For oxide "window" formation a central portion on one side of the specimen was stopped off with Lacomit prior to anodization. See Fig.2b. A current - and voltage - stabilized d.c. power supply unit was used. The unit operated as a constant current generator below the preset voltage and changed over to the constant voltage mode automatically over an interval of 0.5% of the pre - set voltage limit.

The specimens were anodized at a specified current density to the required voltage. It was then possible either to switch off the current at the required voltage or allow the current to decay at constant voltage. This voltage was held constant either for a specified time or until a certain specified leakage current was reached. To obtain flat aluminium oxide films which were slightly under tension, a growth current density of 1.0 mA/cm^2 was used[76]. Considerable efforts were made to produce zirconia "windows" which were (a) free from pores and (b) flat slightly under tension. For these purposes different growth conditions current densities 0.1 - 10mA/cm^2 and forming electrolytes - solutions XI - XIII were employed. Pore free stripped - off oxide films were successfully obtained by using Solutions XI and XII and stripping Solution XIV at room temperature. It was not possible to obtain films which were

either stress free or under tensile stress. These isolated films tended to wrinkle and it appeared that the zirconium oxide was growing under compression.

Formation of oxide "windows".

The central stopped off portion of the specimen was scratched gently and very carefully after peeling off the Lacomit with a sharp blade. Fig.2(d)

(a) Alumina:

The anodized aluminium specimens were then immersed in the iodine - methanol solution (Solution IX) at 55°C for about 1 - 1½ hours to dissolve away the exposed metal in the centre, see Fig.3(a). The oxide "windows" so formed were washed thoroughly with methanol and allowed to dry in air at room temperature.

(b) Zirconia:

For anodized zirconium specimens the bromine - ethyl acetate (Solution XIV) solution was used at room temperature for an immersion time of about 12 - 14 hours. See Fig.3(b). The zirconium oxide "windows" were washed with ethyl acetate and methanol and allowed to dry at room temperature. A.R. grade anhydrous reagents were used for stripping these oxides and solutions were changed after isolation of about 10 specimens to avoid accumulation of moisture.

III - 3 Determination of film thickness and its optical properties

A number of methods may be used for measurement of films thickness e.g.

(a) Methods based on Faraday's Law.

(b) Gravimetric methods.

(c) A.C. Capacity methods.

(d) Optical methods.

The methods (a) (b) and (c) have certain limitations due to difficulty of determining precisely the parameters involved: such as true surface area, density and composition of the film, current efficiency of growth and dielectric constant of the film material. Moreover these methods become unapplicable during experiments with these films in after - growth investigation, especially when the film has been separated from the metal base.

III - 3 - (1) A.C. Capacity:

The inverse a.c. capacitance of the film is related to its thickness by the expressions

$$\frac{1}{c} = \frac{4\pi t}{\epsilon A} \quad \text{(in e.s.u.)} \quad \ldots\ldots\ldots\ldots\ldots\ldots\ldots\ldots \text{(III - 1a)}$$

$$= \frac{4\pi 9 \times 10^{11} t}{\epsilon A} \quad \text{(in farads)} \quad \ldots\ldots\ldots\ldots\ldots\ldots\ldots \text{(III - 1b)}$$

where

c = capacitance,

ϵ = dielectric constant of the oxide,

t = thickness of the oxide,

A = area

assuming the film to be a flawless insulating dielectric.

During present work the capacity measurements of film on the metal were calibrated against the spectrophotometric optical method described in the next section.

The capacitance was determined using a Wayne Kerr bridge (1592 cps) and a specially constructed rectangular shape (1.25 x 2.5 x 5 cm.) counter electrode made of stainless

steel gauze. The oxide covered electrode with the insulated "pole" (Fig.2a) was located inside the stainless steel rectangular electrode immersed in the electrolyte.

The capacitance of the oxide was recorded after five minutes from switching off growth current. In case of films which have been dried at room temperature while out of solution, a time of about sixty minutes was allowed for immersion prior to capacitance measurements.

III - 3 (2) Optical methods:

The spectrophotometric method is potentially one of the more useful of the non - destructive methods, provided the refractive index of the oxide, the net phase shift at the interfaces and the order of interference are known. This method was used and found most probably the quickest, most convenient and precise for determining a wide range of oxide thickness both on and off the metal base.

(a) Instruments:

Both Unicam S.P.700 and Perkin Elmer 450 instruments with wavelength range from 2000Å to 2.5μ were used during these measurements. Calibration was carried out using reflectance attachments at angles of incidence of 10° and 45° for reflection from stripped films or oxide films on the metal and transmission through stripped films at normal incidence. Three different modes of interference minima measurements were employed for each specimen during calibration experiments. These were:-

(a) reflection from oxide on the metal.

(b) reflection from stripped films.

(c) transmission through stripped films.

(b) Theory:

A schematic diagram in Fig.4. shows the optical path difference for a uniform transparent thin film for the three different configurations.

For Case 1, the condition for minimum reflectivity is given by the expression[77]:-

$$2\eta t \cos\phi' + f(\lambda) = \frac{(2m-1)\lambda}{2} \quad \text{.....(III - 2)}$$

where

t = thickness of film

ϕ' = angle of refraction

λ = wavelength of incident light

m = an integer, corresponding to the order of interference.

$f(\lambda)$ = a path difference due to net phase shift (θ).

For maximum reflectivity the above equation can be re-written

$$2\eta t \cos\phi' + f(\lambda) = m\lambda \quad \text{.....(III - 3)}$$

Putting $t = k_1 V$ in equation (III - 2), where V is the anodizing voltage (under specified growth conditions) and $k_1 = \text{Å}/V$ for the given anodizing conditions.

Therefore:-

$$4\eta k_1 V + \lambda_0 = (2m - 1)\lambda \quad \text{.....(III - 4)}$$

$$0 < \lambda_0 < \lambda$$

$\cos\phi' = 1$ at nearly normal incidence angle ($\sim 10^\circ$)

$$\alpha V + \lambda_0 = (2m - 1)\lambda \quad \text{.....(III - 5)}$$

where $\alpha = 4\eta k_1$ .....(III - 6)

For reflection, film stripped off (Case II)

$$\alpha V = 2(m - 1)\lambda \quad \text{.....(III - 7)}$$

because $\lambda_0 = \lambda$, the path difference corresponding to the net

phase shift on reflection from the air - oxide and oxide - air interfaces.

For transmission, film stripped - off (Case III)

$$\alpha V = (2m - 1)\lambda \quad \text{.............................(III - 8)}$$

because $\lambda_o = 0$

(c) Refractive index measurements:

The determination of the refractive index of the film was a requirement of the spectrophotometric method for estimation of the film thickness. Two methods were used for finding the refractive index of the oxide both employing isolated alumina films.

Becke method[29]: Fragments of films were immersed in mixtures of bromoform and α- bromo - naphthalene and examined under phase contrast. The composition of the liquid mixture was adjusted till the film fragment refractive index and that of the mixture of these liquids matched. The light source was the Hg 5460Å line.

Banter method[78]: Anodic alumina ~~oxide~~ windows were used during these measurements. Equations (III - 2 and 3) can be re-written:-

$$2\eta t \cos\phi' + \lambda_o = (2m - 1)\frac{\lambda}{2} \quad \text{..............(III - 9)}$$

(for minima)

$$2\eta t \cos\phi' + \lambda_o = m\lambda \quad \text{.......................(III - 10)}$$

(for maxima)

By putting $x = 2m$ or $(2m - 1)$ ....(III - 11)

and $\lambda_o = 0$ (Case III)

$$4\eta t \cos\phi' = x\lambda \quad \text{..............................(III - 12)}$$

At normal incidence ($\cos \phi' = 1$) the interference was determined for the alumina "window". By rotation of this oxide "window" the angle of incidence was increased, such, that at a certain angle of incidence (say ϕ°) the given order minima or maxima was shifted exactly to the position of its immediately adjacent maxima or minima at normal incidence.

$$\cos \phi' = \frac{\text{value of X at normal}}{\text{value of X at } \phi^\circ \text{ incidence}} \quad \text{.....(III - 13)}$$

(for that angle of incidence)

The refractive index was found out by applying Snell's Law

$$\frac{\sin \phi^\circ}{\sin \phi'} = \eta \quad \text{.....(III - 14)}$$

III - 4 Optical, electron microscopic and electron diffraction studies:

The transmission microscopy and electron diffraction studies were used to determine the homogeneity and nature of oxide films after growth and any changes involved during the experiments after their formation. The optical microscopic examination of the films was made on and off the metal base. Some films were examined by the scanning electron microscope. For this method of investigation a very thin layer of silver was deposited by evaporation (under vacuum) over the oxide to reduce the build up of static charge which reduced the definition obtainable during examination. The transmission electron microscopy and electron diffraction studies of these films were made on Hitachi HU - 11 electron microscope using an accelerating voltage of 100 KV.

Anodic alumina films upto 4200 Å in thickness were

examined. These films were formed on surfaces with different preparations. Thin films were examined directly while some thicker films were thinned down in the following solutions:-

(a) pH 9.7; buffer solution (0.2 N.$NaHCO_3$ + 0.2N.Na_2CO_3) at room temperature.

(b) 0.1M.K_2CrO_4 solution pH 13.0 (adjusted with KOH) at room temperature.

(c) chromic - phosphoric acids solution at 80°C (20 g. chromic acid and 35 ml. of 85% phosphoric acid, per litre of solution.)

Electron microscopic studies were also made on those films on which experiments were carried out after growth. This examination greatly helped in interpreting the results of these investigations.

III - 5 Electrical characteristics of the oxide on the metal:

The oxide films covered specimens shown in (Fig.2a) were immersed in different solutions of various pH values and containing a variety of ions. The impedance of the film was measured in situ using the Wayne Kerr bridge normally at 1592 cps. The special rectangular counter electrodes described in section (III - 3 - (3)) was employed. For impedance determinations at different frequencies an external signal generator and a detector were used and the bridge was disconnected from the a.c. power supply.

The solutions used contained combinations of the cations, K^+, Na^+, NH_4^+, and anions OH^-, CrO_4^{--}, CO_3^{--}, HCO_3^-, SO_4^{--}, Cl^-, in order to study their effect on the alumina films on the metal without involving any reactions with aluminium ions from the substrate.

III - 6 Measurement of the electrical characteristics of isolated oxide films:

III - 6 - (1) Apparatus:

The method developed is based on the technique used for measuring the conductance of electrolytes. The essential features of the technique are shown diagramatically in Fig.5, where circuits are given for use with direct and with alternating currents. E_1 and E_2 were the main electrodes in the cell AA which consisted of two symmetrical half cells. The standard calomel electrodes cs_1 and cs_2 were connected to each of the half cells with Luggin capillary probes F_1 and F_2. These sensing probes F_1 and F_2 approached as closely as possible (1 m.m.) the opposite surfaces of the film diaphragm when the cell was assembled for measurements.

A standard resistance was connected in series with the cell. The potential drop across the sensing probes F_1 and F_2 and across the standard resistor was measured continuously. A constant - current generator was used for passing direct current through the main electrodes, (E_1 and E_2). For A.C. measurements a low amplitude sine - wave source at low frequency ($\sim$ 50 cps) was employed. It was assumed that the current through the cell obeyed Ohm's Law.

III - 6 - (2) Procedure:

The experimental procedure is described below:-

(1) 99.9% purity aluminium sheet (5 x 5 cm by 0.15 cm thick) with a central hole (0.62 cm diameter) was placed between two silicone rubber washers of the same dimensions such that the holes were concentric Fig.6. These washers rested on a

vertical flange and the aluminium sheet made the assembly inflexible and rigid. The silicone rubber and pure aluminium were chosen to avoid contamination of the electrolytes. The oxide "window" was placed over these washers and another silicone rubber washer of the same dimensions was carefully positioned above it. Finally the oxide "sandwich" was held firmly in place by means of a second flange Fig.6. After a few hours the upper flange was removed and a careful visual examination was made with a magnifying glass to locate any wrinkling within the film. Those films which wrinkled during this operation were rejected. The assembly was ready for mounting into the cell.

(2) The oxide film assembled above (1) was held in between the flanges of the two half cells. These flanges were held tightly together by clamps. The silicone rubber washers were used without any grease and worked successfully without leakage.

(3) The two half cells were filled with the electrolyte carefully at approximately constant flow rates manually to avoid damage to the film arising from pressure differentials in opposite halves of the cell.

III - 7 Measurement of extent of permeation through isolated films by ions:

A cell was designed Fig.7. for measurement of rate of permeation of ions through the oxide film. It consisted of two half cells each provided with flanges to hold the oxide as a diaphragm in between, when these flanges were clamped together. The procedure for assembling the oxide diaphragm is

described briefly as in section(III - 6 -(2)). Two platinized platinum electrodes were fixed into one of the half cells for measurement of conductance of the conductivity water with which this half of the cell was filled; a semi - micro stirrer was used to ensure good mixing. Great care was taken during mounting the oxide diaphragm and filling the two half - cells with known equal volumes of the electrolyte and the conductivity water, separately, at approximately constant flow rates.

The change in conductance of the conductivity water was measured with the help of the Wayne - Kerr bridge (Universal bridge B221). There was not any need to replenish the electrolyte in the half cell. The cell constant of the half - cell which functioned as a conductivity cell was determined using 0.02N KCl solution.

Blank experiments were carried out with conductivity water in both half - cells with and without the oxide diaphragm extending over periods of six days.

Another method of mounting oxide films as diaphragms was tried. This time the oxide "window" (without "pole") was mounted with Araldite to the aluminium sheet washer making sure that it was completely water tight. This was finally held between two silicone rubber washers and mounted between the flanges of the cell as a diaphragm. The washer on the araldited side of the sheet had a larger (2 cm diameter) hole to avoid Araldite and thus enable it to rest on the aluminium sheet.

SECTION IV

RESULTS

IV - 1A Introduction.

The results are reported in two major groups as follows:

(a) Studies of growth characteristics of anodic films, their properties and thickness measurements, and microscopy (IV - 1 - 3)

(b) Studies of characterised alumina films in regard to their electrical properties, permeation characteristics in variety of solutions under different conditions, using as many techniques as possible. These results may be employed in an indirect mechanistic approach to the phenomenon of corrosion. Further work on zirconia was dropped due to shortage of time and these results (IV - 4 - 6) were obtained employing anodic alumina films formed in 30 g/l ammonium borate solution (pH 9.0, 20^{o}C) at 1.0 mA/cm^{2} and 10 minutes at voltage.

IV - 1 Anodizing Characteristics.

IV - 1 (1) Voltage vs time.

(a) Effect of different electrolytes:

Fig.8. shows the potential vs time plot for ammonium borate, tartrate and citrate solutions (pH 9.0) at 1.0 ± 0.02 mA/cm^2 and 20°C using both etched and electropolished aluminium specimens. The electrolytes were previously saturated with Al^{+++} ions by pre - anodizing several specimens in the solution. There is a tendency to non - linearity in the voltage - time plot at about 250 volts for ammonium tartrate and ammonium citrate solutions under these conditions. Evolution of oxygen caused this decrease in current efficiency and an earlier breakdown occurred in these solutions as compared to ammonium borate solution.

(b) Effect of surface preparation:

Fig.9. shows the voltage vs time graph for the formation of an anodic oxide film on annealed aluminium specimens, of different surface preparations. The same current density (1.0 ± 0.02 mA/cm^2), solution (30 g/l ammonium borate, pH 9.0) and temperature (20°C) were used in each case. The potential - time plot was linear upto the breakdown voltage. The film breakdown occurred for differently treated specimens in the order untreated (air - annealed), etched, and electropolished between 390 - 420 volts. Their reproducibility was good for electropolished specimens; however, reproduction of the same true surface area by etching was found to be difficult unless the etching conditions were carefully controlled.

(c) Effect of pH:

Measurements were made in ammonium borate solution of various pH values (8.1, 9.0 and 10.0), other conditions of oxide growth being the same. Fig.10. shows that the potential-time plot for pH 8.1 was linear for all different surface preparations, ~~while~~ for pH 10 the curve was irregular and showed an "induction" period. For pH 9.0 see Figs.8 - 9. for potential - time plot.

In 30 g/l tartaric acid solution (pH 5.5) the break-down of the film occurred at about 250 volts, which is earlier than in the same solution pH 9.0, under the same anodizing conditions.

IV - 1 - (2) Inverse capacity vs voltage.

(a) For anodized aluminium: Films were grown in ammonium borate solution (30 g/l, pH 9.0) at 1.0 mA/cm^2 and 20°C, using differently prepared specimens (air - annealed, etched and electropolished) to various ultimate voltages. For one series of specimens (a) the anodizing current was switched off immediately on attaining the required voltage, for a second series (b) the current was allowed to decay for 10 minutes at voltage. Capacitance and conductance in each case were measured at 1592 cps five minutes after the anodizing current was switched off. The capacitance values thus obtained were reproducible within $\pm$ 3.5%.

Fig.11. shows the inverse capacity vs voltage plots for series (a) and (b). Similar experiments were carried out in other electrolytes viz ammonium citrate and ammonium

tartrate solutions (pH 9.0) under the same growth conditions. The results were found to agree within ± 5% see Fig.12. Tests were repeated at various pH values (8.1, 9.0 and 10.0) in ammonium borate, (5.5, 8.0 and 9.0) in ammonium tartrate and (8.0 and 9.0) in ammonium citrate solutions. These pH changes did not seem to cause significant changes in the inverse capacity - voltage relationship of Fig.12.

The use of different growth current densities did not appear to effect the capacity values as long as the same leakage current density was attained.

(b) For anodized zirconium: Fig.15. shows the inverse capacity plotted as a function of voltage at (a) growth potential and (b) after 10 minutes current decay at voltage using saturated ammonium borate solution pH 9.0, at 4.0 mA/cm^2 and 20°C. The reproducibility was better than ± 3.5% for the above specified conditions.

IV - 1 - (3) Resistance vs growth voltage:

Fig.13. shows the resistance of the alumina films as a function of the anodizing voltage for different surface preparations and various forming electrolytes. The reproducibility was not very good, but the results were consistent with respect to the trends depicted. Points to be noted are as follows:-

(a) The resistance vs growth voltage plot is not linear.

(b) A pre - existing thermal film has considerable effect on the resistance of the anodic oxide formed.

(c) The resistance of an anodic layer formed on a surface

with a pre - existing thermal film or HF - HNO_3 etched (30 seconds) surface changed significantly with time, as compared with the resistance of films on differently prepared surfaces. The calculated values of tan δ $\left(\frac{1}{WC_pR_p}\right)$ for the films (other than those formed on thermally oxidized or HF - HNO_3 etched surfaces) are plotted as a function of voltage see Fig.14.

For anodic zirconia the measured values of Rp as a function of growth voltage for conditions (a) and (b) are given in Fig.15. These values did not change with time and were more reproducible than those obtained for alumina films.

IV - 2 Optical properties and the thickness measurement of oxide films.

IV - 2 - (1) Interference minima measurements:

Films were grown under carefully controlled conditions for calibration purposes. These conditions were (a) 30 g/l ammonium borate solution, (b) pH 9.0, (c) temperature 20°C, (d) current density 1.0mA/cm^2 and (e) 10 minutes at voltage. Fig.16. shows typical recorder traces of optical interference by a film for reflection before and after removal of the metal, and for transmission through the separated film. The film was grown on an NaOH- etched aluminium specimen. Fig.17. gives similar results for a film grown on untreated (air - annealed) aluminium.

The results obtained by reflection from a stripped oxide were in general the most precise and easiest to measure.

Interference measurements by reflection from oxides on the metal and transmission through stripped films could be made with greater precision with the Perkin Elmer 450 instrument than with the Unicam SP 700. It was possible, using the Perkin Elmer 450, to measure the thickness of films formed at less than 150 volts with a lower limit of about 75 volts. This was not possible with the Unicam SP700, because of the uniform linear wave - number scan.

Tables (1 - 5) list results from interference minima measurements for anodic oxide films formed on surfaces of different preparations. Reflection spectra from both surfaces of the stripped - off oxide films were similar, for films grown on prepared surfaces, but not for films formed on untreated specimens.

For anodic films formed on specimens with pre-existing thermal oxides (formed during annealing) the transmission trace (fig.17.) shows no marked interference minima, but reflection minima were measureable, Table 6. Several of these stripped oxide films were examined by reflection from both surfaces, and the minima obtained from the original oxide - metal surface showed an appreciable (3 - 6%) shift towards shorter wavelengths, Table.6.

The results are summarised Figs.18 - 20. in the form of graphs showing the relation between formation voltage and wavelength (micron) of interference minima positions for different modes of measurement on films formed under specified conditions.

(a) Voltage - thickness relationship:

On the basis of equations (III - 5 to 8), plots of

$(2m - 1)\lambda$ against voltage were obtained. These were straight lines, indicating a constant thickness/voltage ($\AA$ /V) ratio under these conditions of film growth. The results of inter-polation and extra - polation for all surface preparations are listed in Tables 7 - 9. Fig.21. shows a plot of $(2m - 1)\lambda$ against voltage at constant wavelength. The straight lines pass through or near 0 and λ for transmission and reflection respectively for stripped films, and between 0 and λ for reflection from oxides on the metal base. This behaviour is expected from equations (III - 5 to 8).

(b) Determination of alpha ($\alpha = 4\eta k_1$) Values:

The values of α were calculated for stripped films with the help of equations (III-7 and 8) and the results are given in Tables 7 - 8. Variation of α due to both film thickness and surface preparation are too small to justify detailed consideration. The aver ges of all values of α are plotted in Fig.22. with a curve of the form of the Sellmeir dis-persion equation fitted to the points:-

$$\alpha^2 = 4130 + \frac{4147}{1-\left(\frac{1.575}{\lambda^2 \times 10^{-6}}\right)} \quad \text{.....(IV - 1)}$$

(c) Estimation of λ_o for oxides on the metal base:

The values of α from Fig.22. and the data for reflection from the anodized metal were substituted into equation (III - 5) and values of λ_o were obtained. As the values of λ_o obtained represent the small difference between two large numbers, it is not surprising that these values showed a wide scatter.

However, the averages of λ_o are reasonably grouped around 650Å for all values of λ between 2000Å and 8000Å (Table.9.)

(d) Measurement of refractive index:

Table 10. lists the measured values of refractive index for anodic alumina films formed on differently prepared surfaces. Both Becke and Banter's* methods were employed, but the later method could not be applied to films formed on specimens with a pre - existing thermal film, because no well defined interference minima are observed by transmission through these films (Fig.17). The positions of minima at high angles of incidence were difficult to measure accurately.

Thicker films on electropolished aluminium gave reasonably measurable interference minima. These measurements were made in a similar way on the same area of a film at different angles of incidence. For accurate measurement of the angle of incidence relative to normal incidence on the transmission attachment measurements were carried out at equal inclinations on either side of the normal. Figs.23 - 24. show the position of minima (wave - number) against the cosine of the angle of incidence, and the comparision of values of refractive index by Becke and Banter's methods.

During these studies it was observed that the refractive

*The attachment for measuring the angle of incidence was designed by N.J.M.Wilkins(U.K. A.E.R.E.).

index of a "window" of oxide prepared about a year earlier and which had been stored in air at room temperature was significantly higher than that of recently prepared oxide, see Fig.25.

IV - 2 (2) Calculation of oxide thickness:

The values of oxide thickness (t) were obtained from data in Tables 1 - 5. using the theoretical value of α from equation (IV - 1) and taking $\lambda_o = 650\text{Å}$. The thickness of oxide was also calculated from the reflectivity data of the oxide covered metal and from the reflectivity and transmissivity data of a stripped oxide (Tables 1 - 5) using the appropriate equation from the following:-

(a) $t = \frac{(2m - 1)\lambda}{4\eta} - 650$ .....(IV - 2)
for reflection from the anodized metal.

(b) $t = \frac{2(m - 1)\lambda}{4\eta}$ .....(IV - 3)
for reflection from a stripped film and

(c) $t = \frac{(2m - 1)\lambda}{4\eta}$ .....(IV - 4)
for transmission through a stripped film.

The results agreed to within $\pm$ 1.5%.

The refractive index (η) values used are given in Table.9. Fig.22. shows the dispersion curve for the refractive index of alumina and is described by the equation:

$$\eta^2 = 1.330 + \frac{1.336}{1 - \frac{(1.575)}{\lambda^2 \times 10^{-6}}} \quad \text{.....(IV - 5)}$$

Wavelength of intensity minima for various orders of interference as a function of thickness are shown in Figs.26 - 29. These were obtained by various methods.

IV - 2. - (3) Variations in $\mathring{A}$ /V for different conditions.

Using the relation $\alpha = 4\eta k_1$, a value of k_1 = 14.0 $\mathring{A}$ /V was obtained, but it must be emphasized that the values of k_1 and hence α, are likely to vary with anodizing conditions and this value is only applicable to the conditions(1.0 mA/cm^2, 10 minutes at voltage in ammonium borate solution, pH9.0 at 20°C) used for these experimental results.

(a) Effect of a pre - existing thermal oxide film:

The optical properties of the anodic films formed on the surface of air - oxidized (during annealing) specimens are complicated. They showed significant absorption, see Fig.17. The refractive index value (1.62 $\pm$ 0.01 at wavelength 5460$\mathring{A}$) is lower than that for oxides grown on prepared surfaces. Assuming the applicability of equations (III - 5), (III - 7) and (III - 8) and using the apparently lower refractive index found at 5460$\mathring{A}$, the k_1 ($\mathring{A}$ /V) value is 6% smaller than for oxides grown on prepared surfaces.

(b) Effect of current decay time:

At constant voltage the ionic current decreases exponentially causing a consequent decrease in the rate of film growth, although growth still continues. Fig.30. shows a plot of oxide thickness vs formation potential (a) immediately

after growth voltage is reached (b) after 10 minutes at growth voltage. The corresponding k_1 values are 12.75 ± 0.25 Å /V and 14.0 ± 0.25 Å /V respectively. This is in agreement with the inverse capacity voltage plot in Fig.11. for the same conditions.

(c) Effect of pH:

Thickness measurements were made on films formed under similar conditions but at different pH values (8.1 and 10.0). The interference minima results for 30 g/l ammonium borate solutions (pH 8.1 and 10) are listed in Table 11. The results for pH 8.1. solution may be compared with data obtained in pH 9.0 solution (Tables 1-5) and show similar Å /V ratio. A greater number of minima for a given voltage were found in pH 10 solution. This indicates a thicker film.

(d) Effect of different current densities:

Various growth current densities (0.1 mA/cm^2) were employed in ammonium borate solution (pH 9.0). Fig.31. shows Å /V at growth voltage as a function of logi (apparent current density). The plot shows an unexpected deviation from linearity at high current densities. Accuracy of results at higher current densities was poor, possibly due to the manual arrangement for switching off the field and probably also to the heat envolved.

(e) Effect of various electrolytes:

Measurement of the thickness of oxide formed in ammonium citrate (pH 8.0 and 9.0) and ammonium tartrate (pH 5.5 and 9.0)

solutions was carried out for comparison with results already obtained in ammonium borate. Typical results of interference minima measurement on films formed in the above solutions (pH 9.0) and 1.0 mA/cm^2 current density and held 10 minutes at voltage, are listed in Table 12. Similar results were obtained for other pH values. The calculated values of $\mathring{A}$ /V ratio at growth voltage and after 10 minutes at growth voltage agreed to within $\pm$ 3.0% with those for films formed in ammonium borate solution (pH 9.0) under the same consitions.

IV - 2 - (4) Anodized zirconium:

Anodic zirconia films were formed at 4.0 mA/cm^2 in saturated ammonium borate (pH9.0) solution to various potentials (50, 100, 150, 200 and 250 volts) at (a) growth voltage and (b) after 10 minutes at growth voltage.

The transmission method did not give very accurate minima particularly for thicker films (250 volts). The results shown in Table 13. were obtained using the Unicam SP 700 instrument for the three different modes of measurements on films grown under (b) condition above. Films of less than 150 volts thickness could not be isolated. Other isolated films were symmetrical in their optical behaviour as indicated by reflection minima measurements from both surfaces of these films (Table 13). The thickness of these films was calculated using equations (IV - 2 to 4) and published data[40] for Δ_0 and η. Values of thickness calculated from the three methods agreed to better than $\pm$ 1.5%

The results of interference minima for anodized zirconium formed as (a) and (b) above were obtained, with the help of Perkin Elmer 450 instrument and the reflectance attachment (angle of incidence 45°). These are given in Table.14.

The value of $\cos \phi'$ was calculated (~~found to approach unity~~) from the equation:

$$\frac{\sin 45}{\sin \phi'} = \eta \quad \text{.................................(IV - 6)}$$

and the corresponding published[40] value of η.

The thickness of oxide film was calculated from the equation:

$$t = \frac{(2m - 1 \lambda - \lambda_0}{4 \eta \cos \phi'} \quad \text{.........................(IV - 2)}$$

using published values of λ_0 and values of η.

The higher order minima positions were not very accurate and gave slightly smaller (1.0%) thickness values than the lower order minima. Fig.32, shows thickness vs reflectivity minimum for anodized zirconium at an angle of incidence of 45°.

The values of k_1 (Å /V) were found to be 22.8 ± 3% and 24.8 ± 3% respectively for (a) at growth voltage and (b) after 10 minutes at growth voltage under these conditions, only upto 250 volts .

IV - 3 Optical, electron microscopic and electron diffraction studies.

IV - 3 - (1) Optical and scanning microscope examination:

An optical microscopic examination of films both on and off the metal did not reveal any significant information regarding the nature of the film. The rolling texture of the metal base was replicated by films formed on air - annealed surfaces, while etching characteristics were also shown for films on specimens which had been subsequently etched. Some inclusions appeared within these films. These were most pronounced for air - annealed specimens. Films formed on electropolished surfaces were more uniform than those formed on surfaces treated differently.

The scanning electron micrograph shown in Fig.33. supports the optical microscope results. The micrograph was obtained for a 300 volts film formed on an etched specimen with a thin layer of evaporated silver on the oxide. Higher magnification than x 1050 could not be attained because of electrostatic charge build - up.

IV - 3 - (2) Transmission electron microscopy:

(a) Films $\lesssim$ 1000 Å :

Figs.34. shows the transmission electron micrographs of an oxide film formed on an etched specimen. The patterns shown are not characteristic of the morphology of the oxide film, but reproduce the topological features of the substrate surface. Variations in the anodizing conditions did not seem

to influence these globular features. Above 200 volts these features were difficult to observe. Thin films formed on surfaces etched in HF - HNO_3 solution showed elongated patterns. The size and shape of these features seem to be influenced by the dissolution characteristics of the metal during etching. Arrangement of these features depends upon the scratches and the rolling texture of the metal as shown in Fig.35.

The transmission electron micrograph of a thin film formed on an electropolished specimen is shown in Fig.36. The hexagonal cell type features exhibited by the oxide are possibly due to the pre - existing film produced by the electropolished (chromic - phosphoric - sulphuric acids solution). A transmission electron micrograph of a thin anodic film formed on a specimen electropolished in a different solution (perchloric acid - ethyl alcohol) is illustrated in Fig.37. This shows pore type features all over the film. The brighter pores on the original grain boundary sites of the metal appear to pass right through the film while others do not. Films formed on electropolished and subsequently etched specimens showed the combined features of the pretreatments.

Fig.38. depicts a micrograph of a thin film formed on an air - annealed surface (350°C for 60 minutes).

There are two types of bright spots, possibly corresponding to (a) pores and (b) crystalline areas within the film. These pores are bigger than those for films on treated surfaces.

(b) Examination of films $> 1000\text{Å}$:

Thicker anodic films formed on electropolished (perchloric acid - ethyl alcohol) and etched surfaces showed spots more

transparent to the electron beam, illustrated in Figs.39 - 41, than the bulk of the film. Figs.42 - 43 show the bright spots which seem to appear within the film on sites which correspond to the original grain boundaries of the metal - substrate. Figs.44 -46 illustrate high magnification transmission micrographs for these spots, revealing a fine cellular structure with a network of dark radial streaks. Fig.47. shows one such single spot. The apparent features are the same for differently treated surfaces as shown in Figs.45 - 46. The bright spots were confirmed as inclusions, most of them continuous right through the amorphous film.

(c) Transmission electron diffaction patterns.

All thin films (< 1000 Å) gave diffuse electron diffraction patterns of the type shown in Fig.48. Thicker films were thinned down prior to examination. Selected area diffraction patterns were obtained for bright spots seen by microscopy. Parts of the film free from such bright spots gave diffuse patterns similar to those obtained for thinner films (Fig.48). The slected area diffraction patterns for the "inclusions" (bright spots) are shown in Figs.49 - 50. The complete pattern was difficult to obtain for relatively thicker films which were not greatly thinned. Fig.51. shows a general pattern obtained for a film which has been thinned down more than those films used above.

A diffraction pattern for thallous chloride was obtained for calibration purposes at 100 kV and using same microscope settings. The results of d spacings calculated for crystalline alumina are given in Table 15. The presence of $\bar{\gamma}$ - alumina can be confirmed by the two sharp rings seen in Figs. 49 - 50.

IV - 3 - (3) Preferential growth of crystallinity.

Fig.40. shows the crystalline inclusions as they were located within the film on sites corresponding to the original grain boundary sites of the metal surface. The initial fibrous texture shown in Fig.44. appears to change into a fine cellular structure, illustrated in Figs.45 - 46. with an increase in oxide thickness. These crystallites tend to spread along the grain boundary sites as seen in Figs.42 and 43. Figs.42 - 42A. show that the film on some grains has developed inclusions away from the grain boundaries of the substrate, while the oxide on other grains remained amorphous. The distribution of these inclusions of $\bar{\gamma}$ - alumina becomes random quite quickly in the case of an etched surface(Fig.41.) as compared to an electropolished surface (Figs.39 - 40).

Different surface conditions used, have shown different degrees of crystallinity occurring within the subsequent anodic layers. The tendency to crystallite growth has been observed to increase with different surface preparations in the following order:

electropolished and subsequent etch;
electropolish (perchloric acid - ethyl alcohol);
etch and air - anneal (no treatment).

This tendency for crystalline growth clearly depends upon the surface conditions and the first very thin pre - existing layer.

IV - 3 - (4) Development of pores by chemical dissolution in alkaline solutions:

Stripped films were immersed in alkaline solutions (a) pH 9.7 buffer (0.2N $NaHCO_3$ + 0.2N Na_2CO_3) and (b) 0.1M potassium chromate solution (pH 13 adjusted with KOH), so that dissolution occurred on both sides. An approximate estimate of thinning was obtained from optical interference minima measurements.

Fig.52. illistrates local dissolution of a film which was grown on an etched surface. Figs.53 and 54. depict the location of individual pores formed through the films. The lack of structure is noticeable in these bright pores. Fig.55. shows the pores developed in potassium chromate solution (pH 13.0) when a stripped film was immersed in this solution.

Some stripped films were immersed in chromic - phosphoric acids mixture at 80°C for about two minutes and washed in distilled water and allowed to dry prior to their examination. Fig.56. shows a 300 volts film formed on an etched surface when examined by transmission electron microscopy, after the above acids treament. About 25% of its original thickness had been lost as found by spectrophotometric measurements. A high magnification micrograph for the same is shown in Fig.57.

Fig.58. illustrates a transmission electron micrograph of a 200 volt film treated similarly as above. The film was originally formed on an etched surface in 30 g/l tartaric acid solution (pH 5.5) at 1.0 m A/cm^2. The circular bright spots are shown which are possibly different from crystalline inclusions observed for other films.

IV - 4 Effects of various electrolytes on the electrical characteristics and thickness of anodic alumina.

IV - 4 - (1) Anodizing solutions:

Some 300 volt anodized aluminium specimens (NaOH - etched), which were stored at room temperature for about four weeks, thickness having been determined spectrophotometrically, were re-immersed in anodizing solutions (ammonium borate pH 8.1 and 9.0). These solutions were saturated with aluminium ions by previously anodizing several specimens.

Fig.59. shows the plots of measured $\frac{1}{C_p}$ and Rp against time. The thickness of these films was determined by the spectrophotometric method at the end of these immersion tests and no significant thinning was observed. The observed decrease in $\frac{1}{C_p}$ and Rp may be associated with significant uptake of ions, possibly OH^-/H^+ from the solution during immersion. This was more pronounced in pH 9.0 than in pH 8.1 solution.

IV - 4 - (2) Ammonium chromate/sulphate and Potassium chromate/sulphate solutions.

pH range 5.5 - 10.5:

The specimens (electropolished in perchloric acid - ethyl alcohol) were anodized in a single batch under similar growth conditions for the following series of tests. Various initial thicknesses of films (188 - 300 volts) were employed, these being measured by the spectrophotometric method prior to immersion.

Series 1: Fig.60. shows the behaviour of anodized specimens (188 - 230 volts) immersed in 0.1M solutions of potassium chromate (pH 8.6), potassium sulphate (pH5.5 and 8.6), ammonium chromate (pH 7.6) and ammonium sulphate (pH 8.6).

During these tests no attempt was made to compensate for slight changes of pH which were significant for potassium salt solutions. However, the change in pH of the potassium sulphate solution (pH 8.6) influenced the results. The plot in Fig.60. also shows theoretical $\frac{1}{C_p}$ values calculated from the optical measurement of thickness of the film at the end of the test. The results are also summarized in Table.16. and suggest:

(a) no significant thinning of the alumina films in potassium sulphate solution (pH 5.5) and ammonium ~~sulphate~~ chromate solution (pH 7.6).

(b) thinning of the alumina films at higher pH values than those in (a) above, this was more pronounced in alkaline ammonium salts than in potassium salt solution.

(c) processes other than thinning ie. adsorption of OH^-/H^+ ions and/or the molecular ligand NH_3 were taking place thus bringing about significant decreases in $\frac{1}{C_p}$ and R_p values. Impedance changes cannot be accounted for merely by thinning of the films in these solutions. Some specimens (anodized to 200 - 300 volts) were immersed in chromate and sulphate solutions (pH range 5.5 - 7.6) for 24 hours and their thickness measured by spectrophotometry. These results shown in Fig.61 indicate no significant thinning in these solutions and confirm the observation (a) above:

Series 2: Fig.62. shows measurements of $\frac{1}{C_p}$ and R_p in ammonium chromate solution (pH 10.2), in ammonium sulphate solutions (pH 9.6 and 10.2); the pH being adjusted with NH_4OH and in potassium chromate solution (pH 10.2) the pH being carefully adjusted with KOH dilute solution.

After immersion these specimens were washed and dried at room temperature in air. Their thickness was determined

spectrophotometrically and converted into equivalent $\frac{1}{C_p}$ values, shown for each specimen in Fig.62. Four weeks later these specimens were re - immersed in the ammonium borate solution pH 9.0 and $\frac{1}{C_p}$ and R_p measured after 45 minutes when there was no significant change with time. The measured values are shown in Fig.62. and the results listed in Table.16. Rapid thinning was indicated in the solutions of ammonium salt solutions on the basis of measurement of $\frac{1}{C_p}$ in situ, while optically determined thickness values showed a considerably lower thinning rate. On the other hand measurement of $\frac{1}{C_p}$ after re-immersion showed a different rate intermediate to the above two results.

The decrease in R_p caused by immersion in ammonium salts solutions was more pronounced than that in potassium chromate solution. These results substantiate the observation (b) and (c) in Series 1. Similar tests were carried out in 0.1M potassium chromate and potassium sulphate solutions (pH 10.4 and 10.5 adjusted with ammonium hydroxide solution).

The results are summarized in Fig.63. and Table.16. These results were believed to confirm the possibility and ease of hydration of alumina and the adsorption of NH_3 ligands by alumina in alkaline ammonium salt solutions. It was also observed from these results that in solutions containing sulphate ions the above processes were more pronounced, than in those containing chromate ions.

IV - 4 - (3) 0.1M potassium chromate solutions.

pH range 7 - 11:

Fig.64. shows $\frac{1}{C_p}$ plotted against time for anodized aluminium specimens (300 volts) immersed in 0.1M potassium

chromate solutions (pH 7 - 11 adjusted carefully with KOH). Fig.65 shows the effect of pH on the R_p values of these films during immersion tests as a function of time.

Some specimens from solutions of pH values 9, 10, and 11 were then transferred into a fresh solution of 0.1M K_2CrO_4 (pH 9.0) and some into the anodizing solution (30 g/l ammonium borate, pH 9.0). Inverse capacity and R_p increased steadily with time for about 18 minutes after transfer for specimens originally immersed in solution of pH greater than 9. There was a tendency towards partial recovery of the $\frac{1}{C_p}$ and R_p values, obtained before immersion in the original solution. This effect was found to be dependent upon the pH and time of immersion in the original solution. These results are shown in Figs. 64 and 66.

After taking these specimens out of the solutions and washing and drying at room temperature, the thickness was determined by the optical interference method. The calculated values of inverse capacity equivalent to the above optical measurement of thickness for these specimens are indicated in Fig.64. and suggest less thinning than that observed by inverse capacity values during immersion and even after taking into consideration the recovery of capacity due to change in electrolyte after transfer to pH 9 solution.

These dried specimens were re-immersed after a few weeks in the anodizing solution pH 9.0 and capacity and conductivity were remeasured with time.

The measured values of C_p and R_p did not vary significantly after 60 minutes. The conductivity $(1/R_p)$ was not very different, but the capacity values were considerably changed. The results are also shown in Fig.64. The capacity values are indicated in Figs. 64 and 66. Assuming that the dielectric constant of these films

has not changed significantly, the thickness estimates were obtained from the capacity measurements after drying. These were still lower than those derived from optical determination. Calculated thickness loss from these results are given in Fig. 67 and also listed in Table.16. These results suggest (a) that entry of OH^-/ H^+ into the oxide is not completely stopped by chromate ions (b) that the recovery of $\frac{1}{C_p}$ shown above after transferring the specimen to the lower pH solution is significant and may be caused by establishment of an equilibrium between the alumina film and the electrolyte involving OH^-/H^+ amd other ions. (c) that the difference in the $\frac{1}{C_p}$ values after recovery due to change of electrolyte and after drying and re-immersion was greatly significant and important. (d) that pores are indicated by the different values of thickness obtained by $\frac{1}{C_p}$ values and optical measurement of thickness after immersion.

IV - 4 - (4) 0.1M KCl + 0.1M K_2CrO_4 solutions.

pH range 7 - 11:

Similar tests as in (IV - 4 - (3) above were repeated in 0.1MKCl + 0.1MK_2CrO_4 solutions (pH 7 - 11) using 300 volts anodized aluminium specimens (electropolished perchloric acid - ethyl alcohol) similar to previous sections IV - 4 - (2) and (3) pH of these solutions was adjusted with KOH. Inverse capacity and R_p values measured during immersion against time are plotted in Fig.68. These changes in impedance are more pronounced than those found in 0.1M K_2CrO_4 solutions of corresponding pH values. This figure shows markedly large decrease in resistance during the initial 1 hour. Measurements of $\frac{1}{C_p}$ and R_p values after transferring from immersion solution into ammonium borate solution (pH 9.0) were made. It was found that steady recovery

of $\frac{1}{C_p}$ and R_p required 20 minutes. These values are plotted in Fig.68. The specimens were removed, washed and allowed to dry at room temperature. The optical measurement of thickness was carried out and loss of thickness calculated assuming that the optical characteristics were not significantly changed. After four weeks $\frac{1}{C_p}$ and R_p values were re-measured in ammonium borate solution pH9 andthese are plotted in Fig.68. Results are summarised in Table.16. These results supported the observations made in earlier sections (IV - 4 - 1-3) and suggested the enhanced effect of Cl^- in these solutions.

Fig.69. shows the optical measurements of the thickness of anodized aluminium (100, 150, 200 and 300 volts) immersed upto five days in 0.1M and 1.0M potassium chloride solutions. No change in thickness was obtained, although visual and optical microscopic examination indicated local attack.

IV - 4 - (5) 0.2Na HCO_3 + 0.2N Na_2CO_3:

Buffer solution pH 9.7

Fig.70. shows measurement of $\frac{1}{C_p}$ and R_p during immersion in carbonate - bicarbonate buffer at various repeat frequencies (1 Kc, 5 Kc and 10 Kc). The $\frac{1}{C_p}$ values vary only slightly over this frequency range. On the other hand R_p values become considerably lower as the frequency is increased. Although overall reproducibility of both $\frac{1}{C_p}$ and R_p is not high, the trends appear to be highly reproducible. The optical measurement of thickness after drying and remeasurement of $\frac{1}{C_p}$ and R_p (1592 cps) in ammonium borate solution (pH 9.0) were made. These results are also shown in Fig.70. These measurements clearly indicate thinning, hydration and pore formation processes occurring during immersion.

IV - 4 - (6) Effect of dissolved aluminium ions on the thinning of oxide films:

Fragments of separated alumina films and anodized aluminium were introduced into pH 9.7 buffer solution (0.2N $NaHCO_3$+0.2N Na_2CO_3) and 0.1M K_2CrO_4 solution. These solutions were allowed to dissolve the oxide for 48 hours. The pH of the buffer was not significantly changed and the resulting pH 8.8 was measured for potassium chromate solution. Inverse capacity, R_p and spectrophotometric thickness measurements of 300 volts anodized aluminium specimens made in the above solutions are shown in Figs.71 - 72. Results are also shown in the same figures of similar measurements made in solutions which had not been previously treated with alumina. Comparison of these two sets of results clearly indicates the influence of aluminium ions on thinning of alumina films.

Thinning behaviour of films on and off the metal base in 0.1M potassium chromate solution with added alumina (pH 8.8) and pH 9.7 buffer solution with and without dissolved alumina flakes is shown in Fig.73. as observed by optical measurement of thickness. These results confirm the observation made above. There was no significant thinning observed in pH 8.8 solution as it was previously saturated with aluminium ions. Thinning rates for films on and off the metal were different, because thinning for strip-off films was occuring on their two surfaces. Rate of thinning for stripped films as shown in Fig.73 decreased with time due to significant increase of dissolved aluminium ions in the solution.

IV - 5 - Electrical characteristics of stripped films in various electrolytes:

The results described overleaf show the effect of the following

on the electrical resistance of alumina films stripped from the metal base:-

(a) Field: the nature (a. c. or dc.) and strength of the field:
(b) Electrolyte: type of ions and pH of the solution;
(c) time of immersion and
(d) thickness of the film.

Alumina films employed were all grown on etched specimens in ammonium borate solution (30 g/l, pH 9.0) at 1.0 mA/cm^2. The current was allowed to decay for 10 minutes at voltage. Considerable efforts were made to reproduce the absolute resistivity of the stripped film in an electrolyte, but this was not always achieved in practice. The results, however, show certain trends which are of interest. Most of these measurements were repeated at least three times to ensure the reliability of the results.

Fig.74. shows the resistance of stripped films (200 and 300 volts) mounted in the cell, as a function of time and employing 0.25M sodium sulphate solutions (pH 5.5, 7.0 and 10.7). These measurements were made by both a.c. and d.c. methods. The following observations were made:-

(1) the a.c. resistance of the stripped oxide is very much lower (about two orders of magnitude) than that of a film on a metal base. For comparison see Fig.13 and 74.
(2) the a.c. resistance of the film does not change in pH 5.5 with time.
(3) the d.c. field causes a considerable decrease in the film resistance and this effect is greatest in the highest pH solution (10.7)

The results in buffer solution pH 9.7 are given in Fig.75.

These results support observations (1) and (3) and also suggest that (4) the a.c resistance of the film changes significantly with time in a similar fashion to that of a film on the metal Fig.70.

Fig.76. shows the effect of the film thickness on the initial resistance. The resistance was measured by d.c. method in pH 9.7 buffer solution. During these d.c. method measurements, a current density of 3.3 mA/cm^2 (considering the area of the film) was employed. It was also observed that the higher current densities lowered the resistance of these films very rapidly.

It has been shown in earlier measurements that the thickness of these isolated films does not change in pH 5.5 and 7.0 during immersion in same solutions, see Fig.61. Similar earlier film thinning observations made in Fig.73. suggest insignificant (about 2% loss) thickness loss during 60 minutes immersion in pH 9.7 buffer solution. Some films used in these measurements were removed for optical measurement of thickness, which confirmed the above observations.

No appreciable thickness loss was believed to have occurred in pH 10.7 solution in 30 minutes. On the basis of these observations, the initial film thickness and the appropriate data in Figs.74 - 75 were used to calculate the specific resistivity of these isolated films, which is shown in Fig.77. For comparison the resistivity of film on the metal as a function of voltage was obtained from earlier measurements, which is hown in Fig.78. The specific resistivity of isolated films is very low as compared to films on the metal (anodized to the same voltage under the same conditions) using a.c. technique. The d.c. field further decreases the resistivity considerably.

IV - 6 Extent of permeation of ions through isolated alumina films:

The cell constant of the half cell Fig.7. which was employed as a conductivity cell was found out to be 0.47 using 0.02N potassium chloride solution.

Blank experiments showed a slight increase of conductance of conductivity water, with oxide films as diaphragms and conductivity water in both half cells. This occurred during initial period of 3 - 4 hours. It was believed to be due to unavoidable contamination of the film assembly. After this the conductance remained constant and that was followed by a slight decrease. This may be possibly due to adsorption of ions by the alumina film. Films formed (300 volts) in NaOH etched and electropolished (perchloric acid - ethyl alcohol) specimens were used.

Fig.79. shows the change with time of both the conductance and corresponding calculated ionic concentration (in terms of K^+ and Cl^- ions) of conductivity water caused by permeation of ions through the oxide diaphragms. During these experiments 1.0M KCl solution was used.

These results show a period of about 48 hours, during which the behaviour was similar to that observed for the blank experiments. This behaviour was fairly reproducible for different films, illustrating that no permeation of ions was taking place through the oxide into the conductivity half - cell.

After this stage the slow permeation of ions occurred into the conductivity water which changed its conductance, which was corrected for the area of the film acting as a diaphragm. Various film behaviour at this stage was not highly reproducible. Finally an enhanced permeation rate resulted as shown in Fig.79. Some films used above were removed, washed and examined by electron - microscope. After washing there was some local thinning indicated

Fig.80 shows clearly holes developed during these permeation experiments after mounting the film as a diaphragm for seven days. The over all thickness of the films was not significantly changed as indicated by earlier results reported in Fig.69. and shown by approximate spectrophotometric results of some of these removed films, after about four days permeation tests. These films after removal and washing also showed local attack by optical microscopic examination, which was not uniformily distributed over the film area. This was believed to be the cause of variation in the overall permeation rate of ions through the oxide film.

Figs.81. and 82. show the holes produced in a diaphragm of an oxide film which was mounted for the permeation test and after six days a d.c. field was applied across the film in situ. This was done by placing two platinum electrodes on either side of the diaphragm in both half cells. A constant current of 1.0mA was passed for 10 minutes which resulted in a change of 20 micromhos in the conductance of the conductivity water. (The area of the diaphragm was 0.25 sq.cm.) This suggested that d.c. field produced considerable effect on the permeation characteristic of the film, and caused holes in it.

SECTION V

DISCUSSION

V . 1

(a) Introduction:

An examination of the literature has shown that anodic film formation on metals is a process of considerable complexity. An attempt has been made in the present work to investigate the influence of several variables on the growth of anodic films on aluminium and their characteristics after formation. The results have been summarised to show the importance of the following factors to the process:

(a) Impurities in the metal,

(b) Surface treament of the metal substrate,

(c) The formation current density,

(d) Composition of the electrolyte.

The discussion will therefore, for the sake of clarity, be divided into four parts dealing with these variables in turn.

(b) Experimental Techniques:

Interpretation of data on the properties of anodic films on aluminium are significantly influenced by the experimenter's choice of technique. Thus, evidence[50 - 51] for the existance of "holes" in anodic alumina by electron microscopic examination of films stripped in aqueous mercuric chloride may be debated on the grounds that Cl^- and Hg^{++} ions can preferentially attack defects within the oxide. It is well known that Cl^- ions can cause local attack. Pryor and co-workers[53 - 54] have, on the basis of capacity measurements, proposed uniform thinning of γ- alumina films in chromate solutions, but have been unable to confirm their results by the use of ancilliary techniques. Combination of various techniques in the present study has suggested, hydration of the oxide, pore formation in addition to the thinning effect.

It is suggested that useful results and interpretations are in general obtained only when several different methods of examination are employed simultaneously, This becomes clear when considering the limitations for capacity measurement for determining absolute film thickness of anodic alumina. Porosity in the oxide may lead to misleading values. Moreover, the wide variation in published values of the dielectric constant also adds to the difficulty. Capacity measurements are therefore useful in this connection only when the dielectric constant is known accurately and when a flaw - free film is being employed. The use of optical measurements of the thickness of film in conjuction with capacity measurements tends to eliminate many of these problems, and it is possible to distinguish between actual changes in thickness and processes involving hydration and pore formation.

Electron miscroscopy has been employed in the present investigation for additional confirmation of the presence of flaws and local defects, which may be caused by chemical reactions during film growth, and after growth studies. Structural changes, also important for the characterization of these films, have been studied by electron diffraction.

V - 2 Effect of impurities present in the metal:

The material used for present investigation was 99.99% pure aluminium foil and results obtained regarding the nature of film agree with those of other workers for super-purity aluminium. The impurities like Fe and Si about 1% are known[79] to exert a direct effect on the defects in the thin passive oxide film on commercial aluminium. Some remarks may be made about the

possible influence of 0.01% impurities. The type of pores shown in Fig.37. located on the sites corresponding to the original grain boundaries of the metal, in thin oxide films, could be dependent upon the impurities, which are more likely to be present as precipitates at these localities. Some defects within thin oxide films were noticed as follows. It was observed that oxide covered aluminium specimens anodized to $\lesssim$75 volts (using different surface preparations) suffered local attack beneath the oxide during immersion in the stripping, bath at 55°C for 1 - 1½ hours. This was not observed for thicker films $>$75 volts. This again suggests the possibility of defects which provide site for local attack, which may be associated with substrate impurities and various inhomogeneities. The surface treament and the electrolyte and the forming solution may also affect the behaviour of surface impurities and occlusions. Our study of films was biased towards thicker films greater than 100 volts, where there was no direct evidence of pores and gross defects under the conditions used.

V - 3 Effect of surface - preparation and the characteristic pre-existing film:

The alumina film characteristics observed during these investigations have been found to be influenced by the surface preparations normally employed. Abraded, metallographically polished and buffed specimen are not usually used. The method of preparation of a metallic surface often affects the anodic and corrosion behaviour of most metals. Roughness of the surface is known to cause considerable effect in electrochemical studies due to its greater catalysing power. A surface cannot be

adequately described by the roughness value alone. These surface state characteristics have been recognised by Jacquet[80] and supported by others[81]. These are (a) geometrical, (b) chemical and (c) structural characteristics.

Untreated air-annealed surfaces complicated the nature of oxide films. On the other hand etching, electropolishing and electropolish with subsequent etching also influenced the subsequent anodic layers. The two different chemical etches or electropolishing baths produced differently behaving films in certain respects. Therefore, all the surface state characteristics of the substrate must be accurately defined for studying the anodic behaviour of metals. Similar remarks have been made for the studies of corrosion of metals by Berge[81].

Thin anodic films formed on these prepared surfaces are normal replicas of the metal surface, as shown by the microscopic examination of these films on and off the metal base. The substrate geometrical features could be seen by the transmission micrographs of thin films shown in Figs.33 - 37. These are characteristic of the pretreament. Chemical etch has been described by Young[29] to produce some "orange peel" effect on the substrate which may be noticeable at low magnification. This may be comparable to globular features shown in Fig.34. at high magnification. Electropolished specimens are considered to be flat and may have very thin film in some cases left by the specific treament. Fig.36 shows the hexagonal pattern for the anodic film formed an electropolished specimen, which is a characteristic of the initial film formed by the chromic - phosphoric - sulphuric acids electropolishing bath. Films on electropolished and subsequently etched specimens showed combined features of the pretreatments.

The value of dv/dt_m according to the equation (II - 3) is directly proportioned to the ionic current density, which builds up the oxide. The results in Figs.8 - 9. indicate variation in dv/dt_m values (about 5 - 8%) for a given electrolyte using different surface preparations. It may be argued that these variations give an estimate of roughness factor for the geometrical area, assuming that electropolishing permits the true area to approach the geometrical area. The irregular behaviour of the untreated (air - annealed) surfaces shown in Figs.9 - 10 is believed to be an extreme case of the effect of a pre - existing film, which is an approximately 60 Å thick thermal oxide. The electron micrograph in Fig.38. illustrates flaws which may be contributing to the above behaviour.

Fig.37. shows pores <150 Å much smaller than those observed for film formed on an air - annealed (untreated) surface, see Fig.38. These pores are located at the grain boundary sites of the metal, which may be dependent upon the chemical and structural inhomogeneities of these sites. Pores were difficult to observe in films formed on specimens electropolished in chromic - phosphoric - sulphuric acids bath, because of the hexagonal pattern which obscures other features.

Growth of $\bar{\gamma}$ - alumina crystalline inclusions was found to vary significantly with surface preparation, the growth conditions being the same. Films on untreated (air - annealed) surface showed such inclusions much earlier, Fig.38, than films on other surface preparations. This may be due to the presence of nuclei within the initial film which causes the recrystallisation of the amorphous anodic oxide. The nature of the initial pre-existing film as well as the surface asperities and inhomogeneities may be expected to influence the internal stresses within the

subsequent anodic layers. Recrystallisation of the amorphous oxide may be the result of internal stress relief, with increasing thickness. This maybe considered as another factor leading to the earlier growth of crystallites and for causing the formation of more crystallites on an etched surface (Fig.40) than on an electropolished one (Fig.39). This explanation may also be applied to the appearance of crystallites on an electropolished specimen on sites corresponding to the original grain boundaries of the metal surface. There may be other supporting factors influencing the growth of crystallinity e.g. degree of hydration and the field.

The effect of impurities and the composition of the initial thin film was also very marked on the other characteristics of the subsequent anodic films. The increase of capacitance with time after removal of growth potential has been mentioned in Section IV - 1 - (2). This was observed to be significant for films formed on untreated specimens and HF - HNO_3 etched surfaces. The conductivity ($1/R_p$) was also higher and increased with time. These phenomena are possibly associated with the presence of flaws in these films caused by initial surface oxide. Moreover F^- ion impurities may not have been removed completely during the washing of specimens after etching in HF - HNO_3 solution. This may produce n - type current carriers within the anodic films. These factors may lead to conditions where hydration of the oxide is perhaps easier. Harkness and Young[29] have explained similar capacitance increases for anodized aluminium specimens etched in HF solution in terms of possible hydration of the oxide with time.

Higher $1/R_p$ values shown in Fig.13. for these films may be considered briefly as follows. The measured resistance of an oxide film is normally controlled by the outer layer which is

known[53 - 54] to be a p - type semi - conductor. This layer may be influenced by the impurities like F^- ions and the observed microscopic flaws for these type of films and the consequent hydration during formation and also after growth. These films showed pronounced inclusions when observed under the microscope during refractive index measurements. These were of lower refractive index than the bulk of the films, and may consist of hydrated oxide (amorphous?) as opposed to anhydrous bulk oxide. Such inclusions were less pronounced for films on an NaOH etched surface and negligible for films on electropolished surfaces.

The optical behaviour of films formed on air - annealed surfaces was found to be complicated. Reflectivity minima measurements on stripped films give different results for their two surfaces Table 6. This could be due to significant absorption on that surface of the film which includes the initial air - formed oxide. The absence of any measurable minima by transmission Fig.17. may be due to scattering within the film possibly caused by inclusions associated with the initial thermal oxide. Results obtained by reflection from the original outer interface of these stripped films and from films still on the metal are shown in Figs.18 and 19. respectively. These indicate a shift of minima positions towards shorter wavelengths. It is difficult to decide conclusively which of the following factors or their combinations are producing the displacement of minima but the first two seem most probable.

(a) change in thickness of film.
(b) change in refractive index.
(c) change in phase shift.

Determination of other physical constants such as the density of these films would provide useful information regarding the thickness effect (a). For these films a lower refractive index value was observed and is shown in Fig.22. This could perhaps be attributed to hydration of the films. Banter's method for determining refractive index is not applicable to these films because of appreciable optical absorption and poor transmission interference characteristics Fig.17. However, the Becke method has potentialities for measuring the refractive index of similar absorbing films formed by oxidation and corrosion of metals. For obtaining accurate thickness measurements of films formed by anodic or thermal oxidation, or during corrosion, precise data on the optical properties of these oxides must be obtained.

The apparent lower $\mathring{A}$ /v (6%) value given in section IV - 2 - (3), of these films on air - annealed surface could not be justified unless there is sufficient data for such physical properties as density and chemical composition. Inverse capacity values measured for films on air - annealed surfaces agreed to within $\pm$ 5% of the values observed for films formed on prepared surfaces (NaOH etched or electropolished). The dielectric constant value was calculated as 9.2 $\pm$ 5% (at 1592 cps) from the appropriate data and equation (III - 1 b) as compared to 9.8 $\pm$ 0.35 for the other films.

V - 4 Effect of growth current density:

Results obtained from various conditions of growth current showed:

(a) a slight variation of about 4% in dv/dt_i values for a constant current density and a given surface preparation (Fig.8) using different solutions.
(b) a linear voltage - thickness relationship for films grown on all prepared surfaces at constant current density or to a known leakage current density in ammonium borate, ammonium citrate and ammonium tartrate solutions of different pH values. A constant $\mathring{A}$ /V ratio for all the pH values of these solutions except pH 10. (Section IV - 2)
(c) a change of about 10% in $\mathring{A}$ / V values resulting from a change of an order of magnitude in growth current densities below 1 mA/cm^2 (Fig.31).
(d) small increase in the film thickness which continues at constant voltage while the current is decaying exponentially. (Section IV - 2)

Variations in dv/dt_i values are indicative of change in the current efficiency for growth (equation II - 3). However, the variation of 4% shown in Fig.8. appeared to have no significant effect on the $\mathring{A}$ /V values of film grown in ammonium borate, citrate and tartrate solutions. $\mathring{A}$ /V was calculated as 12.75 at $1mA/cm^2$ current density.

Current efficiency values were calculated by substituting in equations (II - 3) the appropriate data shown in Figs.8 - 10 and other obtained. A value of 3.1 g/cm^3 was chosen for the density of the oxide and the values of current efficiency are

listed in Table 17. The inefficient part of the current may be ascribed to one or both of the following factors:

(a) evolution of oxygen at the oxide surface,

(b) inability of some aluminium ions to take part in film formation i.e. dissolution.

It is well known[29] that a plot of logi against Å /V should be a straight line. However, Fig.31. shows a deviation from linearity at current densities between $1mA/cm^2$ to $10mA/cm^2$. This deviation of about 4 - 5% for high current densities may be due partly to heat evolved in the reaction and partly to delay in switching off the current which can cause significant error at high growth rates. Neufeld[64] has observed a similar effect and has shown a steady increase in Å /V values at current densities greater than $10mA/cm^2$.

Van Geel and Schalen[34] have obtained by a gravimetric method two different Å /V values of 13.9 and 12.7 for oxide grown to an unspecified low leakage current on respectively a chemically - cleaned specimen and a specimen with an intact air - formed film. However, they obtained a value of 12.9 Å /V for these films by an optical method. They suggested that chemical cleaning caused an increase of 7% in the surface area and selected 12.7 Å /V as the best value of Å /V for the two treatments.

Hass[31] anodized evaporated aluminium mirrors in 3% tartaric acid pH (5.5) at constant voltage using a resistor for limiting the initial current. An optical method indicated 13.0 Å /V after 2 minutes anodizing at voltage and 5% increase in Å /V after 15 minutes (no leakage current density given) with a further increase of 1% per hour. He has calculated a current

efficiency of 80% in this electrolyte. The present results are in agreement with those of Hass. However, Plumb[35] has observed an Å /V value 13.8 ± 0.3 in the above electrolyte and reported that the Å /V value was independent of time. Bernard and Cook[36] have also observed different values of Å/V 11.3 - 14.4 for current densities 1.0mA to 0.1mA, although in non - aqueous solution.

These variations in Å /V values which have been reported by several workers may in general be considered to result from one or more of the following factors:

(a) unjustified assumptions regarding values of refractive index, dielectric constant and density of the films.

(b) variations in the determined values of the above parameters due to non - uniform methods of formation and conditions of growth.

(c) incomplete definitions of the limiting thickness, which, for example, have been shown to vary with leakage current density.

However, Å /V can be a useful parameter when considered with these limitations.

Capacitance measurements are useful primarily for relative thickness estimates on characterized barrier - type oxides as the wide variations in the dielectric constant values reported in the literature limit their usefulness in calculating absolute thickness. A value of 9.8 ± 0.35 (at 1592 cps) was obtained for the dielectric constant of barrier - type alumina films formed in ammonium borate solutions (pH 8.1 and 9.0). This value did not seem to change significantly for films grown in ammonium citrate and ammonium tartrate solutions. The value agrees with that obtained by Harkness and Young[29]. However, the

situation becomes more complicated when growth leakage current densities are not correctly defined. A significant change in current efficiency during growth at constant current should affect thickness/voltage ratios and hence $\frac{1}{CV}$ values. This has been seen for anodized zirconium Fig.15, at 250 volts and above. Some preliminary observations on voltage - time relationships indicate a decrease in current efficiency above 250 volts. For anodic zirconia formed in saturated ammonium borate (pH 9.0) solution the dielectric constant was calculated as 25.0 ± 1.0. This agrees with that obtained by Young[29] who has reported 24.7 as the dielectric constant for zirconia.

It has been shown in Section IV - 3 - (2) that for thicker films the amorphous oxide has a tendency to transform into $\bar{\gamma}$ - alumina structure. This tendency for crystalline growth has been observed to depend upon the surface conditions and the very thin pre - existing layer as discussed in Section V - 3. Fig.44, shows the initial structure of the crystallites which changes into fine cellular structure shown in Figs.46 and 47. This maybe associated with the continued application of field as the film is growing. Crystallisation may produce well defined grain boundaries and other discontinuities, like dislocations within the oxide. It is believed that the dark radial streaks shown in Figs.45 - 47 may possibly be some discontinuities in the crystalline $\bar{\gamma}$ - alumina. Different current density may influence the growth of these crystallites and their discontinuities. The film did not rupture during crystallization. However, Vermilyea[82] has shown rupture of the amorphous tantalum oxide due to field crystallisation.

V - 5 Effect of composition of the electrolyte:

V - 5 - (1) Growth characteristics.

The results in Table.17, suggest that solutions of the ammonium salts of boric, citric and tartaric acids, give maximum current efficiency for oxide growth at pH values between 8 - 9. This pH range has a useful combination of favourable features for these solutions (a) a good buffering capacity and (b) lower solubility of aluminium oxide than at higher pH values. Plumb [35] has suggested that the solvent action of the electrolyte during anodic oxidation depends upon the buffering capacity of electrolyte. The inability of some aluminium ions to form oxide is influenced by the nature of anions in the electrolyte.

The anomalous behaviour of ammonium borate solution pH 10.0 (Section IV - 1) was most probably due to the formation of a porous - type overlying film and a barrier type film underneath, caused by high dissolution and hydration effects of OH^- ions on the oxide. The possible enhanced formation of pores at constant voltage during 10 minutes decay time, did not permit a decrease in current which in this case remained very large. The pore formation was probably similar to that observed in ammonium borate solution (pH 9.7) at 50°C by Neufeld [64]. It is a well established fact that electrolytes which dissolve aluminium oxide will form a porous film overlying a barrier - type layer. Dorsey [52] has observed this type of oxide formation at high temperatures, in tartaric acid solution. The optical interference measurements have indicated a greater thickness for the films formed in pH 10 solution. The films showed faint interference colours.

Dorsey has suggested that the effect occurs by the initial transformation of the barrier layer surface to a reactive hydrous

alumina layer which is then converted into a porous overlying layer.

The resistance vs voltage Fig.13, for films on prepared surfaces shows two ranges, a range of low resistance upto approximately 120 volts and a linear range of higher resistance above this value. It is possible that lower resisting range is associated with pores in the thin films as shown in Fig.37. Electron microscopy has shown that the pores tend to disappear with increasing thickness of the film. Previously in Section V - 3 it was suggested that the measured resistance of the oxide film is controlled by the thin outer layer which is known[55] to be a p - type semi-conductor. This layer is possibly sensitive to film crystallinity and composition and is hence difficult to reproduce for films formed under varying conditions and enviroments. This may account for the scatter in R_p values shown in Fig.13.

V - 5 -(2) Studies of alumina films after growth:

Corrosion of aluminium has been suggested to depend upon the protective film which must remain continuous and unbroken and resist transport of ions to react with the metal. The action of ions on alumina produced by anodic or air - oxidation has, therefore, been studied by many workers[13 - 14,48,53 - 54]. The present work has employed relatively thicker films than those used by Pryor et. al.[48,53 - 54] and others[14,73]. This choice was made due to the following reasons:-

(a) to avoid the possibility of pores and defects which are more likely to be present in thinner films as shown by microscopy of these films. However, thicker films contained more

crystalline inclusions within the film strata, than are found in thin films.

(b) optical interference technique of thickness determination limited the lower thickness of a film to be measured accurately.

(c) comparative examination of films both on and off the metal was possible by using these relatively thicker and thus mechanically stronger films.

(d) to ensure that aluminium ions from the metal surface were not involved in reactions during these studies.

Examination of results obtained during the present work and those obtained by others[48,53 - 54] suggests that aluminium oxide when immersed in a solution tends to adsorb ions on its surface from its enviroment. Possibly an equilibrium is attained with the ions in solution, depending upon the pH, nature of ions, temperature and structure of the oxide. For example dried anodized specimens when re-immersed in the anodizing solution Fig.59, reproduce the original capacity after about sixty minutes. It is believed that some ions are incorporated into the oxide lattice possibly in solution under these conditions. The observation of electron diffraction patterns, however, showed no change in the structure of the oxide.

The steady change observed in the electrical properties of the oxide during immersion tests (Section IV - 4) maybe due to the transport of ions into oxide under the concentration, gradient towards oxide - metal interface. This is proposed because the changes cannot be explained by thinning of the films in various solutions. It is well accepted that small ions like F^-, Cl^-, Br^-, I^- and OH^- have high penetration power. Pryor et.al.[48,53,54] have suggested an exchange reaction mechanism involving the

penetrating ions and the O^{-2} ions of the oxide lattice. However, another possibility may be the entry of an equivalent number of positively charged ions along with the penetrating anions for example a proton - the smallest ion. This will not upset the charge balance and does not change the original crystal structure of the oxide. For example OH^- ion uptake may be considered as

$$Al_2O_3 + OH^- + H^+ \longrightarrow 2\ AlO(OH) \quad \ldots\ldots\ldots\ldots\ldots\ldots (V - 1)$$

which is a thermodynamically favourable process at 25°C with ΔG =-1.54kcal/g mol of Al_2O_3 [83]. However, it is believed that initial OH^- adsorption suggested above is the slowest step and dependent on OH^- ions concentration.

Similarly Cl^- ions penetration may be as follows:

$$Al_2O_3 + Cl^- + H^+ \longrightarrow AlOCl + AlO(OH) \quad \ldots\ldots\ldots (V - 2)$$

Further transport of these ions within the oxide may be visualized by consideration of the oxide as an electrolyte and a semi - conductor[24]. There is general support to the view that protons can easily migrate from one O^{-2} ion to the neighbouring one.

Aluminium oxide being amphoteric in character dissolves readily in acids and alkalis and its solubility is minimum in the pH range of about 6 - 7. Therefore, in solutions with pH values other than those above, thinning of the oxide film would be expected in addition to hydration and penetration of ions. Uniformity of hydration and penetration of ions may be difficult to visualize due to different behaviour of the amorphous and crystalline parts of the oxide. Several papers[29] have reported that amorphous part of the oxide dissolves readily in chromic - phosphoric acids solution. On the other hand

γ - alumina (crystalline) part is insoluble in the acids mixture. Fig.56, shows that amorphous part of the oxide dissolved in preference to the $\bar{\gamma}$ - alumina crystalline spots. However, after thinning of the alumina film in alkaline solutions, the electron microscopy indicated formation of pores at the crystalline spots. This suggests preferential dissolution of the crystalline oxide at these spots which may have arisen due to enhanced adsorption of ions occurring locally.

Increased adsorption at these crystallite sites may also be associated with the discontinuities within the oxide, such as grain boundaries, discussed in Section V - 4. Pure alumina is known as an insulating dielectric. However, the penetrated ions are believed to change its electrical conductivity. Pryor et. al.[48,53,54] have suggested a change in the defect structure of the oxide due to Cl^- and F^- ions entry into the oxide, which act as n - type current carriers.

Hydration:

The observed decrease in measured $\frac{1}{C_p}$ and R_p values of the oxide without involving any significant thinning during immersion in borate (pH 8.1 and 9.0), sulphate and chromate (pH 5.5 - 7) solutions is believed to be associated with the uptake of ions OH^- and or H^+ (Section IV - 4). This probably modifies the outer p - type layer. After significant entry of these ions the oxide may be represented by a double electrical analogue

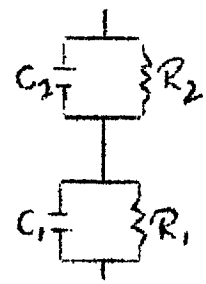

(where $R_1 \gg R_2$) as against originally assumed analogue of a R_p and a C_p in parallel.

The results of measurement of resistance of stripped films in different solutions (Section IV - 5) support the fact that uptake of ions by alumina lowers its resistance. The initially lower resistance (about two orders of magnitude) of these stripped films as compared with that of films on the metal is possibly due to unavoidable traces of moisture, which allow I^- ions to enter the original p - type outer layer. This p - type region of the oxide is small as compared to the total thickness of the oxide. This I^- ion penetration is believed to vary with the history of the stripping bath, temperature and time of immersion. Therefore, a wide scatter of results was observed. However, these results provide useful information regarding the effect of ions on the resistance of the oxide. Fig.74, shows no change in the a.c. resistance of the film in a sulphate solution (pH 5.5) during the time of measurement. The results suggest that sulphate ions do not enter the oxide and that there was no significant uptake of OH^- or H^+ during this short time. Whereas d.c. field allows significant uptake of ions by the oxide and consequent decrease in the resistance of the film. However, at higher pH value (10.7) it is shown in the same Fig.74, that there is substantial decrease in the resistance of the film when compared to that at pH 5.5 or 7. Pryor et.al. have shown that SO_4^{--} ions are not incorporated in the aluminium oxide film.

For the buffer solution pH 9.7 the change of resistance with time shown in Fig.75, may also be associated with the entry of OH^- or H^+ ions from the solution into the oxide. It is obvious from these results that ion penetration and transport are easier under applied d.c. field.

Cl^- ions:

A considerably significant effect of Cl^- ions on the resistance of the oxide has been observed as shown in Fig.68. This effect is more pronounced during immersion times of less than 100 minutes. This suggests that contamination of the oxide by possible entry of Cl^- ions is very rapid. This substantial decrease in R_p values in chloride solutions (0.1M KCl + 0.1M K_2CrO_4) is not significantly affected by pH of the solution. It is believed that the entry of Cl^- ions occurs preferentially at the crystalline spots. In neutral chloride solutions no significant change in overall thickness of the oxide was observed, Fig. 68. The film may be represented by an electrical analogue.

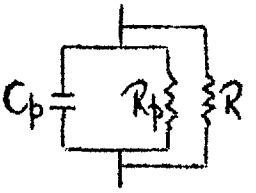

The preferentially attacked crystallites are represented by R, a very low resistive path.

The permeation tests described in Section IV - 6, using 1.0M potassium chloride solution showed the following facts:

(a) ions permeate through the oxide diaphragm after about 48 hours and ultimately a high permeation rate is observed Fig.79. Burwell et.al.[68] showed a much higher permeation rate for porous - type films and using a different stripping method and also completely anodized foils.

(b) developments of holes at the crystalline spots within the Oxide Fig.80, which produce enhanced rates of permeation shown by part (c) of the plot in Fig.79. The films showed wide scatter due to non - uniform distribution and size of pores or holes.

These observations may be taken to support the idea of preferential attack at the crystalline spots where subsequently holes were formed. Moreover, well defined crystalline discontinuities may facilitate enhanced penetration locally. This explains the electrical behaviour of the oxide. However, Pryor et.al.[48,53-54] have assumed exchange of Cl^- and F^- ions with oxygen ions in the oxide lattice uniformly distributed over the oxide surface on a macro - scale. The present results which suggest a preferential uptake of Cl^- and OH^-/H^+ ions, support a different point of view. Further evidence of local attack was indicated by the "disfiguring" of the oxide locally during immersion in chloride solutions for optical thickness measurements. These measurements showed no change in the overall thickness of the oxide.Fig.69. Moreover, the application of a d.c. field across the oxide diaphragm showed local damage of the film at spots originally associated with preferential attack, as shown in Figs.81 - 82. Any aqueous stripping solution, like mercuric chloride will be expected to cause significant changes in the electrical properties and possibly in the homogeneity of the film.

Penetration of ions, thinning and pore formation:

The present measurements of R_p and C_p and the optical measurement of thickness of oxide films (Section IV - 4) in various solutions with pH values greater than 7, indicate uptake of OH^-/H^+ and/or Cl^- and OH^-/H^+ and NH_3 ligands in addition to thinning of the oxide. Pores have been inferred from the data of thickness losses in various solutions Table.16, and

confirmed microscopically Figs.52 - 55. However, Pryor et.al. (48, 53 - 54) have explained the increase of the capacitance of the anodized aluminium in chromate solution pH (7.1 - 9) as uniform thinning. They have suggested that chromate ions possibly inhibit the entry of OH^- ions into the oxide. This is perhaps not completely true. It is believed as a result of the present work that a hydration process occurs throughout the film and/or in certain local areas in addition to expected thinning. However, it has been observed that thinning and impedance changes for anodized aluminium were more pronounced than in solutions other than chromate solutions. Figs.62 - 63. Thus CrO_4^{--} ions possibly hinder the enterance of OH^- ions into the film. Modi et.al.(66) and O'Connor et.al.(67) have shown that H^+, OH^- and CrO_4^{--} ions are strongly and specifically adsorbed on corundum. Thinning hydration and pore formation are more pronounced in very alkaline solutions. The results in Fig.64, show clearly the effect of pH on the $\frac{1}{C_p}$ and R_p values during immersion in the 0.1M K_2CrO_4 solutions. This change in $\frac{1}{C_p}$ values measured in pH $>$ 7 solutions, indicates the combined effect of thinning hydration and pore formation. The steady recovery $\frac{1}{C_p}$ and R_p after transfer to pH 9 solution for specimens originally immersed in solutions of pH greater than 9 is shown in Figs. 64 and 66. This suggests the re-establishment of the equilibrium at the oxide surface for adsorbed OH^-/H^+ ions and possible partial dehydration of the oxide. After drying these specimens the inverse capacitance values when remeasured in ammonium borate showed a greater recovery as shown in Figs.64 and 66. This recovery is believed to be due to further dehydration of the film, and may involve some filling and healing of pores due to sealing characteristics of alumina. However, pores are

definitely indicated by the difference between optical measurement of thickness and the equivalent calculated estimate of thickness from remeasured $\frac{1}{C_p}$ after drying shown in Table.16. The pores were confirmed by examination of stripped films by electron microscopy see Fig.55. These pores are shown to be associated with the crystalline sites and may not be uniformly distributed all over the film because these crystallites depend upon surface preparation (Figs.39 - 40), and grain structure of the substrate (Fig.42). Some crystallites do not penetrate right through the film.

The decrease of $\frac{1}{C_p}$ and R_p values in alkaline ammonium chromate/sulphate which is greater than that in potassuim chromate/sulphate solutions shown in Figs.62 - 63, suggest the uptake of molecular ligand NH_3 with OH^-/H^+ ions by the alumina. This effect was not observed in ammonium salt solution of pH less than 8, as NH_4^+ ions exist below this pH and no NH_3 ligands. It has been suggested earlier in this section that adsorption of ions may depend upon various factors such as nature of the ions present, pH of the solution and structure characteristics of the film. However, the complexing reactions involving various ligands will depend upon the stability constants of the complex molecule, both in the solid phase and in solution. It is believed that adsorption and penetration of NH_3 ligands would not affect the crystal structure of the oxide. It is further suggested that chromate ions possibly hinder this reaction as indicated by the change in $\frac{1}{C_p}$ and R_p in chromate solutions which is smaller than that in sulphate solutions Figs.62 - 63.

Thinning behaviour of the alumina films are shown to depend upon the concentration of aluminium ions already present in the solution, Figs.71 - 73. Enhanced thinning has been observed in

the presence of Cl^- ions as shown by the data given in Table. 16. It has been shown that both sodium chloride and sodium carbonate increase the solubility of hydrargillite (Al_2O_3 $3H_2O$) in dilute solutions of sodium hydroxide (6 - 13% Na_2O)[84].

SECTION VI

SUMMARY

VI Summary

The following gives the summary of the major observations made during the present work.

1) Current efficiency for oxide growth:

(a) The current efficiency was about 5 - 8% lower for oxide growth on NaOH etched surfaces than on electropolished specimens under the same conditions.

(b) A maximum current efficiency was observed for oxide formation in ammonium borates, citrate and tartrate solutions between pH 8 - 9 for a given surface preparation. There was a decrease in current efficiency in ammonium citrate and tartrate solutions above 250 volts, resulting in oxygen evolution. A similar observation was made for anodic zirconia formation in saturated ammonium borate solution pH 9.0 above 250 volts.

2) Capacity and resistance measurements:

(a) Change in the pH of the oxide forming electrolytes(ammonium borate, citrate and tartrate solutions) did not affect significantly the linear capacity-voltage relationship so long as the same current density (at constant current formation) or same leakage current density (at constant voltage growth) were employed. On the other hand the resistance-voltage plot was not linear and showed two regions (a) a low resistivity region up to about 120 volts and (b) a high resistivity region above 120 volts for oxide films formed in these electrolytes.

(b) Films formed on surfaces air-annealed or etched in HF - HNO_3 showed lower resistance than films formed on differently

prepared surfaces. The measured capacitance and conductance values of these films showed significant increase with time after switching off the current.

(c) A stripped film showed a lower resistance (about two orders of magnitude) than that of a similar film on the metal. The resistance was found to decrease during immersion in alkaline solutions. Application of a d.c. field across the stripped oxide film caused a considerable decrease in the resistance of the anodic alumina film.

3) Optical properties and thickness measurement of oxide films:

(a) A linear voltage-thickness relationship was observed for oxide films grown in different electrolyte under the specified conditions.

(b) The refractive index for anodic alumina films formed on prepared surfaces was found to be 1.655 ± 0.01 at 5460 Å. A value of 1.620 ± 0.01 at the same wavelength was found for films formed on air-annealed (untreated) surfaces. A film stored at room temperature for twelve months showed higher refractive index than that of a freshly formed film.

(c) No significant change in Å /V ratio due to electrolyte changes was observed for anodic alumina film grown in ammonium borate, citrate and tartrate solution (except pH10) provided the same growth current density or the same leakage current density were employed. The thickness of the oxide, however, increased significantly during decay of current density at voltage.

(d) Three different methods of obtaining optical interference minima were employed for films both on and off the metal base for finding their thickness. The results of these different

measurements agreed to better than $\pm$ 1.5% .

(e) Stripped anodic alumina films formed on air-annealed specimens showed different interference spectra on opposite surfaces. A lower value of $\mathring{A}$ /V (about 6%) was inferred for these films as compared to that of the films formed on prepared surfaces under the same conditions. These films showed appreciable optical absorption resulting in transmission spectra with less marked maxima and minima from which the oxide thickness was not determinable.

(f) The alumina films formed in ammonium borate solution pH 10 were found to be thicker than those produced in solutions of pH less than 10, using the same growth conditions.

(g) A change of about 10% in $\mathring{A}$ /V value was obtained for a change of an order of magnitude in current density.

4) Electron microscopic and electron diffraction examination:

(a) Thin stripped films behaved as normal replicas of the substrate surface and showed features characteristic of the surface treatment.

(b) These thin films formed on prepared surfaces showed pores which were much smaller than 150$\mathring{A}$. However, films formed on air-annealed specimens showed relatively bigger pores and crystallites. There was no direct evidence of pores in films greater than 1400 $\mathring{A}$ (100V)

(b) Crystallites of γ - alumina were observed within the amorphous oxide films thicker than 1000$\mathring{A}$. The occurrence of these crystallites was dependent upon surface preparation and on the ultimate thickness of the oxide. For films formed on electropolished specimens (perchloric acid-ethyl alcohol) these

crystallites were found to be located on sites corresponding to the original grain boundaries of the metal. As the film thickness increased oxide film on some grains showed these crystallites, while film on others remained completely amorphous. Some of these crystallites were not right through the oxide films.
(c) Pores were observed to form when thicker oxide films were thinned down in alkaline solutions. These were located at the crystalline spots of the oxide.

5) Effect of composition of electrolyte on anodic alumina during immersion:

(a) $\frac{1}{C_p}$ and R_p of anodized aluminium specimens were found to decrease during immersion in different solutions. The decrease was dependent upon the pH and on the nature of the anions present in the solution. At a given pH greater than 8 the change was more pronounced in ammonium salt solutions than in solutions of potassium salts. There was greater change observed in the value of R_p and $\frac{1}{C_p}$ in chloride solutions and this was not significantly dependent upon pH of the solution. The optical measurements of thickness for these specimens showed considerably less thinning rate than that indicated by $\frac{1}{C_p}$ value measured during immersion in various solutions of pH greater than 7. It was observed that uniform thinning of film alone could not account for these changes in $\frac{1}{C_p}$ and R_p values.
(b) Thinning of the alumina film was found to be dependent upon the pH of the solution and the concentration of aluminium ions already present in the solution. There was significantly enhanced thinning of alumina films in alkaline chloride solutions. No overall thinning of the alumina film was observed in neutral chloride solutions.

6) Permeability of stripped alumina films to potassium chloride:

No permeation of ions was observed through the oxide diaphragm during the initial 48 hours. A slow rate of permeation was shown after this time, which later changed into an enhanced rate. Holes were found to have developed in the oxide film. D.c. polarization produced bigger holes through the oxide diaphragm and caused considerable damage to the film.

SECTION VII

CONCLUSIONS

Conclusions:

The following conclusions have been drawn from the results obtained during this work.

1) Surface preparation and the initial pre-existing film influence the nature of subsequent anodic film. All the surface state characteristics must be accurately defined for studying anodic behaviour of metals.

2) Current efficiency for aluminium oxide growth depends upon the buffering capacity of the electrolyte and its dissolution effect upon the oxide.

3) The optical interference technique offers an accurate, most convenient and non-destructive method of measuring the thickness of the oxide film both on and off the metal base. However, the optical properties of the film must be precisely known.

4) **The chemical reactions involved** in stripping films of oxide from aluminium using iodine in methanol and from zirconium using bromine in ethyl acetate do not significantly alter the optical properties or the thickness of these films. However, aqueous stripping solutions like $HgCl_2$ will significantly affect the electrical resistance of the alumina films and possibly their homogeneity.

5) Oxide films with precisely controlled thickness can be produced on aluminium specimens in electrolyte such as ammonium borate, citrate and tartrate solutions under specified growth conditions.

However, as expected from the equation for conduction in condition of high electric field intensity the thickness of the film alters with the current density for growth.

6) It is suggested that useful results and interpretations are most easily obtainable when several different methods of examination are employed simultaneously.

7) (a) It is believed that anodic alumina films take-up ions as a solid solution into the lattice without changing the structure of the oxide. Some of these species are F^-, Cl^-, Br^-, I^-, OH^- and H^+ ions, and NH_3 ligands.
(b) At crystalline inclusions within the oxide, the adsorption of ions and hence their uptake is probably more pronounced. Halogen ions penetrate rapidly at these sites and produce considerable decrease in the resistance of the oxide locally. This effect of halogen ions is not dependent upon pH of the solution.
(c) Strongly adsorbed chromate ions tend to hinder the uptake of OH^- and/or H^+ ions or NH_3 ligands by the oxide from the solution
(d) In alkaline solutions thinning occurs in addition to hydration and pore formation in various electrolytes. Pores were located preferentially at the crystalline spots within the amorphous bulk oxide.
(e) Thinning behaviour of alumina is dependent upon the pH of the solution, concentration of aluminium ions and any complexing ligands present in the solution. Presence of Cl^- ions increases the solubility of alumina in alkaline solutions.
(f) It is suggested that Cl^- ions permeate through the isolated films forming pores locally at crystalline spots.

(g) The uptake of ions by the alumina, lowers the electrical resistance. D.c. field enhances the permeability of alumina to ions.

ACKNOWLEDGEMENTS.

It gives the author a real pleasure to acknowledge the advice and assistance of his supervisor Dr.J.S.Ll.Leach, throughout this work. The author is greatly indebted to Mr.N.J.M.Wilkins for his help and interest in the spectrophotometry of oxide films part of which was carried out in his laboratory. The contribution made by the United Kingdom Atomic Energy Authority in financially supporting the work at Imperial College and in providing experimental facilities in the Metallurgy Division; Harwell for some of the optical measurements is gratefully acknowledged. The help of Dr.J.E.Castle(C.E.R.L.) Leatherhead for the scanning electron microscope examination of the oxide film is sincerely acknowledged. The author wishes to thank his colleagues at department of metallurgy, for their helpful discussion and criticism especially Dr.S.R.J.Saunders, Dr.A.Y. Nehru, Mr.A.J.Breen, Miss Beryl Follows and also Mr.F.Applewhite and Mr.W.W.Bishop for their technical assistance.

The financial support for maintenance by Messrs.Star Textile Mills Ltd.,(Karachi) through the Pakistan Council of Scientific and Industrial Research, a travel grant from the Commonwealth University Interchange Scheme and also study-leave by the Panjab University are gratefully acknowledged. The author expresses his thanks to Professor J.G.Ball for laboratory facilities and to Professor K.Salahuddin and Professor M.S.H.Siddiqui for their encouragement.

The author feels extremely gratefull to his wife and children who have been separated for three years and his eldest brother Mr.G.Ali Khan for his supervision of the author's family. The author thanks all those who have contributed towards his work and encouragement of his efforts.

BIBLIOGRAPHY

1. D.H.Bradhurst and J.S.Ll.Leach, Trans.Brit.Ceram.Soc.62,793 (1963)

2. J.S.Ll.Leach and P.Neufeld, Proc.Brit.Ceram.Soc,6, 49 (1966)

3. D.A.Vermilyea, J.Electrochem.Soc.,110, 345 (1963)

4. D.L.Douglass, Corrosion Science,5, 255 (1965)

5. D.L.Douglass and J.van Landuyt, Acta Metallurgia, 13, 1069 (1965)

6. W.E.Tragert, AEC Euratom Conf.Aq.Corrosion Reactor Materials, Brussels, TID - 7587, 121 (1958)

7. J.E.Draley and W.E.Ruther, J.Electrochem.Soc.104 329, (1957)

8. J.S.Ll.Leach and A.Y.Nehru, Corrosion of Reactor Materials, 1, 59, I.A.E.A. Vienna (1962)

9. J.S.Ll.Leach and A.Y.Nehru, J.Electrochem.Soc.,111, 781 (1964)

10. A.J.Breen, G.D.Fawkes, H.S.Isaacs, J.S.Ll.Leach and A.Y.Nehru, 3rd International Congress on Metallic Corrosion, Moscow, May (1966)

11. A.A.Elsayed, M.Sc.Thesis, University of London (1966)

12. J.N.Wanklyn, C.F.Britton, D.R.Silvester and N.J.M.Wilkins, J.Electrochem.Soc.,110, 856 (1963)

13. A.F.Beck, M.A.Heine, D.S.Keir, D.van Rooyen and M.J.Pryor, Corrosion Science,2, 133 (1962)

14. K.F.Lorking and J.E.O.Mayne, J.Appl.Chem.,11, 170 (1961)

15. N.B.Pilling and R.E.Bedworth, J.Inst.Metals, 29, 529 (1923)

16. O.Kubaschewski and B.E.Hopkins,"Oxidation of Metals and Alloys" Butterworth's, London (1953)

17. U.R.Evans, "Metallic Corrosion, Passivity and Protection", Arnold, London (1937)

18. H.H.Uhlig, "Corrosion and Corrosion Control", John Wiley, New York (1962)

19. K.Hauffe, "Oxidation of Metals", Plenum Press, New York (1965)

20. U.R.Evans, "Corrosion and Oxidation of Metals" Arnold, London (1960)

21. K.Thomas and M.W.Roberts, J.App.Phys.,32, 70 (1961)

22. R.K.Hart, Trans Faraday Soc.,53, 1020 (1957)

23. P.E.Doherty and R.S.Davis, J.App.Phy.,34, 619 (1963).

24. J.S.Ll.Leach, International Conference on Properties of Reactor Materials and the Effects of Radiation Damage, Butterworths London (1962)

25. J.S.Ll.Leach, J.Inst.Metals,88, 24 (1959)

26. A.U.Seybolt, Advances in Physics,Vol.XII, No.45 (1963)

27. W.D.Kingery, "Introduction to Ceramics" John Wiley, New York (1960)

28. H.A.Johansen, G.B.Adams Jr., P.V.Rysselberghe, J.Electrochem. Soc.,104, 339 (1957)

29. L.Young, "Anodic Oxide Films", Academic Press London (1961)

30. L.Young, Trans.Faraday Soc.,50, 841 (1957)

31. G.Hass, J.Opt.Soc.Amer.,39, 532 (1949)

32. K.Nagass,Mem.Inst.Sci.Ind.Res.Osaka University,10,66 (1953)

33. H.Hennig, Z.Physik,144, 296 (1956)

34. W.ch.van Geel and B.J.J.Schelen, Philips Res.Repts,12 240 (1957)

35. R.C.Plumb, J.Electrochem.Soc.,105, 498 (1958)

36. W.J.Bernard and W.Cook, ibid,106, 643 (1959)

37. L.Young, Proc.roy,Soc.,A244,41 (1958)

38. A.B.Winterbottom, Appendix to U.R.Evans "Metallic Corrosion, Passivity and Protection"Arnold, London (1946)

39. N.J.M.Wilkins, J.Electrochem.Soc.,109, 10,998 (1962)

40. N.J.M.Wilkins, Corrosion Science,4, 17 (1964)

41. W.P.Ellis, J.Chem.Phys.,39,5,1172 (1963)

42. W.P.Ellis, J.Opt.Soc.Amer.,53, 613 (1963)

43. F.Keller, M.S.Hunter and D.L.Robinson, J.Electrochem.Soc., 100, 411 (1953)

44. F.Keller, M.S.Hunter and D.L.Robinson, ibid,101, 335 (1954)

45. R.W.Franklin, Nature, 180 1470 (1957)

46. D.J.Stirland and R.W.Bicknell,J.Electrochem.Soc.,106, 481 (1959)

47. D.J.Stirland and R.W.Bicknell, ibid, 110, 262 (1963)

48. J.J.McMullen and M.J.Pryor, "Proc.First International Congress on Metallic Corrosion" Butterworths, London (1961)

49. Maria Gy.Hollo, ibid (1961)

50. R.W.Franklin, The Proc.Institution of Elect.Engineers, Part B Supplement Nos.21 - 22, 412 (1962)

51. R.W.Franklin, ibid, 525 (1962)

52. G.A.Dorsey Jr., J.Electrochem.Soc.,113, 284 (1966)

53. M.A.Heine and M.J.Pryor, ibid, 110, 1205 (1963)

54. M.A.Heine and M.J.Pryor, ibid, 112, 24 (1965)

55. M.A.Heine and P.R.Sperry, J.Electrochem.Soc.,112, 359 (1965)

56. W.ch.van Geel and J.W.A.Scholte, Philips Res.Repts.,6, 54 (1951)

57. Y.Sasaki, J.Phys.Chem.Solid,13, 177 (1960)

58. L.F.Heckelsberg, G.C.Bailey and A.Clarke, J.Amer.Chem.Soc., 77, 1373 (1955)

59. G.D.Fawkes, M.Sc.Thesis, London University (1962)

60. J.A.Davies, B.Domeij, J.P.S.Pringle and F.Brown, J.Electrochem.Soc.,112, 675 (1965)

61. D.A.Vermilyea, ibid,110, 345 (1963)

62. D.H.Bradhurst and J.S.Ll.Leach - to be published

63. A.J.Breen, Private Communication (1966)

64. P.Neufeld, Private Communication (1966)

65. M.J.Pryor, Z.Elektrochem.,62, 782 (1958)

66. J.J.Modi and D.W.Fuerstenean, J.Phys.Chem.,61, 640 (1957)

67. D.J.O'Connor, P.G.Johansen and A.S.Buchanan, Trans.Faraday Soc.,52, 229 (1956)

68. R.L.Burwell Jr., and T.P.May, J.Electrochem.Soc., 94, 195 (1948)

69. A.H.Mitchell and R.E.Solomon, ibid, 112, 361 (1965)

70. G.Okamoto, M.Nagayama and Y.Mitani, Trans.Electrochem. Soc., Japan,24, 69 (1956)

71. H.S.Isaacs and J.S.Ll.Leach, J.Electrochem.Soc.,110, 680 (1963)

72. S.R.J.Saunders, Ph.D.Thesis, London University (1964)

73. K.F.Lorking, J.Appl.Chem.,10, 449 (1960)

74. J.N.Wanklyn, Nature, 177, 849 (1956)

75. J.S.Ll.Leach. Private Communication (1966)

76. D.M.Bradhurst and J.S.Ll.Leach, J.Electrochem.Soc.,110, 1289 (1963)

77. A.Charlesby and J.J.Polling,Proc.Roy.Soc.,A227, 434 (1955)

78. J.C.Banter, J.Electrochem.Soc.,112, 388 (1965)

79. W. Hübner and G.Wranglen,"Scandinavian Corrosion Congress", Helsinki (1964)

80. P.A.Jacquet, Metallurgical Rev.Vol.1,Part 2, 157 (1956)

81. J.Ph.Berge, 3rd International Congress on Metallic Corrosion, Moscow, May (1966)

82. D.A.Vermilyea, J.Electrochem.Soc.,102, 207 (1955)

83. E.Deltombe and M.Pourbaix, Corrosion,14, 498 (1958)

84. A.N.Lyapunov A.G.Khodakova and Z.G.Galkina, T.Svetn. Metal, 37 (3), 48 (1964)

TABLE 1

WAVELENGTHS (μm) OF MINIMA PRODUCED BY ANODIC ALUMINIUM OXIDE FILMS

(ALUMINIUM ETCHED - SODIUM HYDROXIDE)

392 Volts			342 Volts			300 Volts		
R(m)*	T_r≠	R(s)=	R(m)	T_r	R(s)	R(m)	T_r	R(s)
1.196	1.181	1.778	1.055	0.990	1.525	0.884	?	1.349
0.715	0.678	0.885	0.622	0.608	0.767	0.551	0.557	0.673
0.516	0.509	0.590	0.449	0.443	0.513	0.402	0.394	0.456
0.409	0.399	0.450	0.360	0.352	0.392	0.320	0.313	0.351
0.340	0.332	0.365	0.297	0.292	0.318	0.267	0.261	0.285
0.291	0.286	0.308	0.257	0.253	0.270	0.232	0.228	0.244
0.257	0.252	0.269	0.227	0.224	0.237		0.205	0.215
0.231	0.228	0.240		0.204	0.213			
	0.208	0.218						
		0.202						

260 Volts			200 Volts			160 Volts		
R(m)	T_r	R(s)	R(m)	T_r	R(s)	R(m)	T_r	R(s)
0.812	0.770	1.191	0.662	0.604	0.930	0.521	0.493	0.745
0.492	0.483	0.590	0.396	0.385	0.474	0.325	0.308	0.382
0.361	0.346	0.401	0.291	0.278	0.323	0.242	0.228	0.263
0.285	0.275	0.307	0.235	0.225	0.250			0.209
0.241	0.234	0.252			0.208			
	0.205	0.218						

*R(m) = reflection from anodised aluminium surface.

≠T_r = transmission through oxide.

=R(s) = reflection from oxide removed from the metal.

TABLE 2

WAVELENGTHS (μ) OF MINIMA PRODUCED BY ANODIC ALUMINIUM OXIDE FILMS

(ALUMINIUM ELECTROPOLISHED PERCHLORIC ACID - ETHYL ALCOHOL)

342 Volts			300 Volts			250 Volts		
R(m)	T_r	R(s)	R(m)	T_r	R(s)	R(m)	T_r	R(s)
	1.064	1.563	0.884		1.388	0.791	0.763	1.147
0.625	0.611	0.775	0.575	0.556	0.696	0.480	0.466	0.568
0.457	0.450	0.521	0.410	0.401	0.468	0.346	0.332	0.387
0.362	0.363	0.397	0.326	0.320	0.356	0.274	0.267	0.296
0.299	0.298	0.322	0.271	0.266	0.289	0.232	0.225	0.244
0.257	0.256	0.273	0.235	0.232	0.247	0.203		0.210
0.228	0.227	0.239		0.207	0.218			
	0.206	0.215						

200 Volts			150 Volts		
R(m)	T_r	R(s)	R(m)	T_r	R(s)
0.653	0.614	0.935	0.505	0.476	0.703
0.393	0.387	0.475	0.307	0.294	0.362
0.289	0.283	0.323	0.226	0.219	0.250
0.233	0.225	0.250			0.200
0.200		0.209			

TABLE 3

WAVELENGTHS (μ) OF MINIMA PRODUCED BY ANODIC ALUMINIUM OXIDE FILMS

(ALUMINIUM ELECTROPOLISHED PERCHLORIC ACID - ETHYL ALCOHOL AND ETCHED SODIUM HYDROXIDE.)

342 Volts			300 Volts			250 Volts		
R(m)	T_r	R(s)	R(m)	T_r	R(s)	R(m)	T_r	R(s)
?	1.056	1.538	0.882	?	1.376	0.796	0.764	1.144
0.636	0.604	0.767	0.568	0.550	0.685	0.481	0.471	0.575
0.465	0.447	0.516	0.410	0.397	0.463	0.348	0.333	0.393
0.364	0.355	0.393	0.325	0.319	0.353	0.276	0.270	0.300
0.303	0.293	0.320	0.270	0.265	0.287	0.233	0.229	0.247
0.261	0.253	0.270	0.235	0.230	0.245	0.204	0.201	0.213
0.232	0.225	0.237		0.206	0.217			
	0.204	0.213						

200 Volts			150 Volts		
R(m)	T_r	R(s)	R(m)	T_r	R(s)
0.650	0.614	0.939	0.498	0.465	0.687
0.394	0.388	0.475	0.300	0.290	0.355
0.289	0.282	0.323	0.224	0.216	0.245
0.233	0.226	0.250			0.197
0.199		0.209			

TABLE 4

WAVELENGTHS (μ) OF MINIMA PRODUCED BY ANODIC ALUMINIUM OXIDE FILMS

(ALUMINIUM ELECTROPOLISHED PHOSPHORIC/CHROMIC/ SULPHURIC ACIDS

342 Volts			300 Volts			250 Volts		
R(m)	T_r	R(s)	R(m)	T_r	R(s)	R(m)	T_r	R(s)
?	1.060	1.537	0.882	0.885	1.370	0.772	0.763	1.162
0.615	0.610	0.759	0.568	0.558	0.684	0.473	0.465	0.575
0.453	0.443	0.512	0.407	0.399	0.460	0.344	0.333	0.391
0.358	0.350	0.389	0.323	0.318	0.352	0.273	0.268	0.298
0.298	0.291	0.316	0.269	0.265	0.286	0.230	0.226	0.245
0.255	0.252	0.268	0.233	0.230	0.244	0.202	0.199	0.212
0.226	0.223	0.235	0.209	0.206	0.216			
	0.203	0.212						

200 Volts		
R(m)	T_r	R(s)
0.633	0.613	0.918
0.388	0.384	0.466
0.285	0.276	0.318
0.229	0.223	0.246
0.197		0.206

TABLE 5

WAVELENGTHS (μ) OF MINIMA PRODUCED BY ANODIC ALUMINIUM OXIDE FILMS

(ALUMINIUM ELECTROPOLISHED PHOSPHORIC/CHROMIC/ SULPHURIC ACIDS/AND ETCHED - SODIUM HYDROXIDE)

342 Volts			300 Volts			250 Volts		
R(m)	T_r	R(s)	R(m)	T_r	R(s)	R(m)	T_r	R(s)
?	1.058	1.527	0.890	?	1.370	0.790	0.760	1.176
0.616	0.612	0.758	0.566	0.553	0.680	0.486	0.472	0.585
0.454	0.442	0.512	0.407	0.396	0.459	0.346	0.344	0.398
0.358	0.351	0.389	0.322	0.316	0.351	0.277	0.274	0.300
0.296	0.291	0.317	0.268	0.264	0.286	0.233	0.230	0.249
0.256	0.251	0.268	0.233	0.229	0.245	0.205	0.202	0.214
0.227	0.222	0.235	0.208	0.205				
0.202	0.212							

200 Volts		
R(m)	T_r	R(s)
0.651	0.613	0.931
0.398	0.385	0.471
0.291	0.280	0.321
0.232	0.225	0.248
0.199		0.208

TABLE 6

WAVELENTH (μ) OF MINIMA PRODUCED BY ANODIC OXIDE FILM FORMED ON AIR - OXIDISED ALUMINIUM.

392 Volts			342 Volts			300 Volts		260 Volts		200 Volts	
R(m)	$R(s)^1$	$R(s)^2$	R(m)	$R(s)^1$	$R(s)^2$	R(m)	$R(s)^1$	R(m)	$R(s)^1$	R(m)	$R(s)^1$
1.227	1.882	1.835	1.054	1.575	1.566	0.871	1.386	0.817	1.210	0.602	0.859
0.702	0.880	0.856	0.595	0.730	0.712	0.515	0.636	0.463	0.563	0.353	0.428
0.501	0.576	0.540	0.426	0.467	0.443	0.377	0.410	0.341	0.386	0.259	0.286
0.388	0.429	0.426	0.331	0.366		0.291	0.322	0.266	0.289		
0.317	0.334	0.332	0.273	0.290		0.242	0.256	0.220	0.232		
0.271	0.285	0.282	0.235								
	0.249										

R(m) reflection from anodized aluminium surface

$R(s)^1$ reflection from oxide removed from the metal - "air" side

$R(s)^2$ reflection from oxide removed from the metal - "metal" side

TABLE 7

VALUES OF α FOR STRIPPED ALUMINIUM OXIDE (FROM REFLECTION MINIMA).

		NaOH etched		$HClO_4$ electro-polished		$HClO_4$ electo-polished and etched		H_2CrO_4 H_3PO_4 H_2SO_4 electro-polished		H_2CrO_4 H_3PO_4 H_2SO_4 electro-polished and etched	
λ	m	V	α	V	α	V	α	V	α	V	α
2000	5	151	106	150	106.7	153	104.6				
	6	189.5	105.5			188	106.4	192	104.2	192	104.2
2100	5	161	104.4	160	105	162	103.7				
	6	202.5	103.7	202	104	201.5	104.2	204.5	102.7	202.5	103.7
	7	248	101.6	250	100.8	246	102.4	246.5	102.2	244.5	103.1
2200	5	170.5	103.2	170	103.5	171.5	102.6				
	6	216	101.9	216	101.9	215	102.3	217.5	101.2	215	102.3
	7	263	100.4	264	100.0	262	100.8	262	100.8	260	101.5
2300	5	180.5	102.0	180	102.2	181	101.7				
	6	230	100.0	230	100.0	228	100.8	231	99.6	227.5	101.1
	7	278	99.3	277.5	99.5	277	99.6	278	99.3	276	100.0
2400	4	144.5	99.7	143	100.7						
	5	190.5	100.8	190	101.1	191	100.5				
	6	244	98.4	244.5	98.2	242	99.2	244	98.4	239.5	100.2
	7	293.5	98.1	291	99.0	292.5	98.5	294	98.0	293	98.3
2500	4	151.5	99.0	150	100.0	153.5	97.7				
	5	200	100.0	200	100.0	200	100.0	203.5	98.3	201.5	99.3
	6	257.5	97.1	258.5	96.7	254.5	98.2	256	97.7	252	99.2
	7	309	97.1	305	98.4	308	97.4	309.5	97.0	309	97.1
2700	4	165	98.2	164	98.8	166	97.6				
	5	221	97.7	221	97.7	220	98.2	223	96.9	221.5	97.5
	6	281	96.1	279	96.8	279.5	96.6	280	96.4	278.5	97.0
	7	342	94.7	337	96.1	342	94.7	345	94.0	346	93.6
2900	4	178	97.8	177.5	98.0	178.5	97.5				
	5	242	95.9	243.5	95.3	240	96.7	242.5	95.7	241	96.3
	6	306	94.8	302	96.0	304.5	95.2	306.5	94.6	305.5	95.0
	7	369	94.3								
3100	4	191.5	97.1	191.5	97.1	191.5	97.1	194	95.9		
	5	262.5	94.5	261.5	94.8	260	95.4	262	94.7	260	95.4
	6	331.5	93.5	327.5	94.7	330	94.0	333	93.1	332.5	93.2
	7	395.5									

TABLE 7 CONT'D.

		NaOH etched		$HClO_4$ electro-polished		$HClO_4$ electro-polished and etched		H_2CrO_4 H_3PO_4 H_2SO_4 electro-polished		H_2CrO_4 H_3PO_4 H_2SO_4 electro-polished and etched	
λ	m	V	α	V	α	V	α	V	α	V	α
3300	4	205	96.6	205.5	96.4	204.5	96.8	207.5	95.4	206	96.1
	5	281	94.0	278.5	94.8	279.5	94.5	280.5	94.1	280	94.3
	6	355.5	92.8	353	93.5	356	92.7				
3500	3	146	95.9			148	94.6				
	4	221	95.0	221	95.0	219	95.9	221.5	94.8	219	95.9
	5	299	93.7	296	94.6	298.5	93.8	299	93.7	299	93.7
	6	376	93.1								
3700	3	155	95.5	153.5	96.4	156.5	94.6				
	4	236.5	93.9	237	93.7	233.5	95.1	235.5	94.3	232	95.7
	5	319.5	92.7	315	94.0	318.5	93.0	320	92.5	320.5	92.4
	6	397.5	93.1								
3900	3	163.5	95.4	162.5	96.0	164	95.1				
	4	252	92.9	252	92.9	248	94.4	249.5	93.8	245.5	95.3
	5	340	91.8	335	93.1	339	92.0	342	91.2	343	91.0
4100	3	172	95.4	171.5	95.6	173	94.8				
	4	267	92.1	266	92.5	262.5	93.7	264	93.2	259	95.0
	5	358	91.6	355	92.4	359	91.4	362	90.6		
4500	3	189.5	95.0	189	95.2	189.5	95.0	192.5	93.5	190.5	94.5
	4	295.5	91.4	289.5	93.3	290.5	93.0	293	92.2	293	92.2
	5	392	91.8								
5000	3	213.5	93.7	213.5	93.7	212.5	94.1	211	94.8	212.5	94.1
	4	332.5	90.2	325.5	92.2	329.5	91.1	332.5	90.2	332.5	90.2
5500	3	239	92.1	240.5	91.5	238.5	92.2	238.5	92.2	235	93.6
	4	366	90.2								
6000	3	264.5	90.7	262.5	91.4	261.5	91.8	262	91.6	258	93.0
	4	398.5	90.3								
7000	2	150.5	93.0	149.5	93.7	154	90.9				
	3	312	89.7					309	90.6	311	90.0
8000	2	172	93.0	171	93.6	172	93.0				
	3	356	90.0								
9000	2	193.5	93.0	192.5	93.5	192	93.8				
	3	398	90.5								
10,000	2	216	92.6								

TABLE 8

VALUES OF α (FROM TRANSMISSION MINIMA) OF STRIPPED ALUMINIUM OXIDE

		NaOH etched		$HClO_4$ electro-polished		$HClO_4$ electro-polished and etched		H_2CrO_4 H_3PO_4 H_2SO_4 electro-polished		H_2CrO_4 H_3PO_4 H_2SO_4 electro-polished and etched	
λ	m	V	α	V	α	V	α	V	α	V	α
2000	4										
	5										
	6										
	7	251	103.6			249	104.4	250.5	103.8	247	105.3
	8	289	103.8								
2100	4	146	100.7	143.5	102.4	145.5	101.0				
	5	182	103.8	182.5	103.6	182	103.8				
	6	225.5	102.4								
	7	268.5	101.7			266	102.6	267.5	102.1	265	103.0
	8	311	101.3								
2200	4	154	100.0	151	102.0	153	100.7				
	5	194	102.1	194.5	101.8	193.5	102.3	197	100.5	194	102.1
	6	240	100.8	243.5	99.4			241.5	100.2		
	7	286	100.0			284	100.7	283.5	100.9	283.5	100.9
	8	333.5	98.5								
2300	4	162	99.4	159	101.3	160.5	100.3				
	5	206	100.5	206.5	100.2	205.5	100.7	208	99.5	204.5	101.2
	6	254	99.6	256	98.8	252	100.4	254.5	99.4	250	101.2
	7	302.5	98.9			300	99.7	300	99.7	301.5	99.2
2400	4	170	98.8	167	100.6	168	100.0				
	5	218	99.1	218.5	98.9	216	100.0	219	98.6	214.5	100.7
	6	269	98.1	268.5	98.3	266	99.3	267.5	98.7	266	99.3
	7	320	97.5					319.5	97.7	320.5	97.4
2500	4	178	98.3	174.5	100.3	175.5	99.7				
	5	230	97.8	230.5	97.6	227.5	98.9	230.5	97.6	225	100.0
	6	283	97.2	280.5	98.0	280	98.2	281	97.9	280.5	98.0
	7	337	96.4					338.5	95.6	340	95.6
2700	4	194	97.4	190	99.5	191	99.0	194.5	97.4	192.5	98.2
	5	254	95.7	254	95.7	250	97.2	252	96.4	246	98.8
	6	312	95.2	305.5	97.2	307.5	96.6	308.5	96.3	308.5	96.3
	7	367.5	95.5								

TABLE 8 CONT'D.

		NaOH etched		$HClO_4$ electro-polished		$HClO_4$ electro-polished and etched		H_2CrO_4 H_3PO_4 H_2SO_4 electro-polished		H_2CrO_4 H_3PO_4 H_2SO_4 electro-polished and etched	
λ	m	V	α	V	α	V	α	V	α	V	α
2900	3			150	96.7	148	98				
	4	210	96.7	208	97.6	208	97.6	212	95.8	208	97.6
	5	276	94.6	272	96.0	271	96.3	272	96.0	269	97.0
	6	339	94.1	332	96.1	337.5	94.7	340	93.8	340	93.8
3100	3	161	96.3	159	97.5	160	96.9				
	4	228	95.2	227	95.6	228	95.2	230	94.4	224	96.9
	5	297	94.0	290.5	96.0	291.5	95.7	292	95.6	294	94.9
	6	364.5	93.6								
3300	3	171.5	96.2	169.5	97.3	170.5	96.8				
	4	245.5	94.1	247.5	93.3	246.5	93.7	246.5	94.1	239	96.7
	5	318.5	93.3	310	95.8	313	94.9	316	94.0	317	93.7
	6	390	93.1								
3500	3	182	96.2	180.5	97	181	96.7				
	4	263	93.2	263.5	93.0	263.5	93.0	262.5	93.3	256	95.0
	5	340	92.7	330	95.5	336.5	93.6	342.5	92.0	340.5	92.5
	6										
3700	3	192	96.4	191	96.9	191	96.9	191.5	96.6	191	96.9
	4	280	92.5	278	93.2	279	92.8	278	93.2	275	94.2
	5	361.5	89.5								
3900	3	202.5	96.3	201.5	96.8	201.5	96.8	203	96.1	202.5	96.3
	4	297	92.0	291	93.8	295	92.6	293	93.2	294.5	92.7
	5	382.5	91.8								
4100	3	215	95.4	214.5	95.6	213.5	96.0	215.5	95.1	213.5	96.0
	4	314	91.4	308	93.2	311	92.3	310	92.6	313	91.7
	5	409	91.3								
4500	2			140	96.4						
	3	240	93.8	241	93.4	237.5	94.7	241	93.4	238	94.5
	4	348	90.5	342.5	92.0	345	91.3	348.5	90.4	349	90.3
5000	2	162.5	92.3	159	94.3	161.5	92.9				
	3	269	93.0	269	93.0	268.5	93.1	269	93.0	268	93.3
	4	385.5	90.8								
5500	2	180.5	91.4	177	93.2	182	90.7				
	3	296	92.8	296.5	92.8	300	91.7	298.5	92.1	296	93.0
6000	2	198.5	90.7	195	92.3	195.5	92.1	196	91.8	196	91.8
	3	335.5	89.4	334	89.8	338.5	88.6	334	89.8	333.5	90.0
7000	2	234.5	89.6	229	91.7	229	91.7	229.5	91.5	230	91.3
	3	407									

TABLE 9

VALUES OF PHASE SHIFT (λ_o) AND REFRACTIVE INDEX (η) FOR REFLECTION FROM ANODIZED ALUMINIUM SURFACES.

			NaOH etched	$HClO_4$ electro-polished	$HClO_4$ electro-polished and etched	H_2CrO_4 H_3PO_4 H_2SO_4 electro-polished	H_2CrO_4 H_3PO_4 H_2SO_4 electro-polished and etched	Average λ_o	
λ	α	m	V	V	V	V	V	λ_o	η
2000	104.9	6		200	201	204.5	202.5	640	1.882
		7		246	244				
2100	102.5	6		216	216	219.5	216.5	696	1.839
		7		261.5	260.5	263	259.5		
2200	101.4	4	142.5	145	146.5			634	1.819
		5	182						
		6		231.5	231	235	231		
		7	280.5	277	276.5	279	277		
2300	100.2	4	151	153	154.5				1.798
		5	194	196	19	201	197.5	690	
		6	243	246.5	245.5	250	245		
		7	297.5	293	292.5	295	294.5		
2400	99.3	4	159	161	162				1.782
		5	206	208.5	208	212.5	208.5	609	
		6	258.5	260	260.5	263	260		
		7	314	310	309	312.5	312		
2500	98.4	4	167	169	170				1.766
		5	218	221	219.5	223.5	219.5	523	
		6	274.5	273	274	276	274.5		
		7	331.5	329	326	332.5	331.5		
2700	97.0	4	183	184.5	185				1.741
		5	242	245	243	246.5	242	626	
		6	304.5	299	300	301	302.5		
		7	361.5						
2900	96.1	4	199	200.5	200.5	204	199.5		1.725
		5	265.5	265.5	265	266	265	582	
		6	334.0	329.5	326	330.5	332.5		

TABLE 9 CONT'D

			NaOH etched	$HClO_4$ electro-polished	$HClO_4$ electro-polished and etched	H_2CrO_4 H_3PO_4 H_2SO_4 electro-polished	H_2CrO_4 H_3PO_4 H_2SO_4 electro-polished and etched	Average	
λ	α	m	V	V	V	V	V	λ_o	η
3100	95.4	3	151.5	151.5	155				1.712
		4	216	218.5	218.5	221	218	778	
		5	288	285	285	286.5	286.5		
3300	94.9	3	163	163.5	165.5				1.703
		4	233.5	236	237	238	236	675	
		5	310	305	306	308.5	309		
3500	94.5	3	174	175	176				1.696
		4	251	253	252	255	253.5	560	
		5	331.5	329	327.5	332	332		
3700	94.1	3	185.5	186.5	187				1.689
		4	268.5	269	268	270.5	269.5	657	
		5	352.5						
3900	93.8	3	196.5	198	197.5	201	195.5		1.683
		4	288	284.5	184	286.5	286	664	
		5	373.5						
4100	93.6	3	208.5	210	209	214.5	206.5		1.680
		4	307.5	300	300	302.5	302.5	570	
		5	394.5						
4500	92.9	3	233.5	233	232.5	238	229.5	509	1.667
		4	342.5	334	331	339.5	338		
5000	92.5	2	153.5	148.5	151				1.660
		3	265	261	261.5	264.5	259	742	
		4	380						
5500	92.2	2	168	165.5	167				1.655
		3	299.5	287	290	290.5	290	815	
6000	92.0	2	182.5	182.5	183.5		182		1.651
		3	329.5	321	321	328.5	328.5	552	
7000	91.8	2	215	217	217	224	218	766	1.648
		3	384						
8000	91.6	2	255	251.5	252.5	262.5	255	615	1.644

TABLE 10

DETERMINED VALUES OF REFRACTIVE INDEX (η) OF ANODIC ALUMINA FILMS

Description of Film	Becke Method	Banters Method
Films formed on Prepared Surfaces		
(a) Fresh	1.655+0.01 (5460 Å)	1.70+0.02 (3960Å) 1.765+0.035 (2610Å)
(b) Aged		1.76+0.02 (5220Å) 1.75+0.02 (3960Å) 1.765+0.025 (3515Å)
Films formed on untreated air - oxidized surface		
Fresh	1.62+0.01 (5460 °A)	

TABLE 11

WAVELENGTH (μ) OF MINIMA PRODUCED BY ANODIZED ALUMINIUM (ALUMINIUM ELECTROPOLISHED - PERCHLORIC ACID - ETHYL ALCOHOL)

	200 V R(m)	220 V R(m)	250V R(m)	270V R(m)	300V R(m)
30 g/l Ammonium Borate pH 8.1	0.385	0.426	-	-	-
	0.282	0.309	0.346	-	-
	0.230	0.249	0.273	0.294	0.321
		0.210	0.232	0.247	0.267
			0.203	0.215	0.232
					0.208

	200 V R(m)	220 V R(m)	250 V R(m)	270 V R(m)	300 V R(m)
30 g/l Ammonium Borate pH 10	0.633	-	1.064	-	-
	0.458	-	0.630	-	0.826
	0.361	-	0.450	0.505	0.585
	0.299	0.331	0.355	0.395	0.461
	0.259	0.283	0.293	0.327	0.380
	0.230	0.225	0.253	0.280	0.326
	0.209	0.206	0.211	0.247	0.285
			0.203	0.222	0.256
				0.204	0.232
					0.215
					0.201

TABLE 12

WAVELENGTHS (μ) OF MINIMA PRODUCED BY ANODIZED ALUMINIUM (ANGLE OF INCIDENCE $\sim 45^{\circ}$)
(ALUMINIUM ELECTROPOLISHED - PERCHLORIC ACID - ETHYL ALCOHOL)

	150 V R(m)	180 V R(m)	200 V R(m)	220 V R(m)	250 V R(m)
30 g/l	0.288	0.331	0.360	0.396	0.432
Ammonium	0.217	0.244	0.267	0.293	0.322
Citrate	-	0.206	0.218	0.235	0.260
pH 9					0.221

	150 V R(m)	180 V R(m)	200 V R(m)	220 V R(m)	250 V R(m)
30 g/l	0.289	0.332	0.365	0.394	0.433
Ammonium	0.218	0.244	0.271	0.291	0.323
Tartrate	-	0.207	0.221	0.235	0.260
pH 9					0.221

TABLE 13

WAVELENGTHS (μ) OF REFLECTIVITY AND TRANSMISSIVITY MINIMA FOR ANODISED ZIRCONIUM AND CORRESPONDING FILM THICKNESSES.

	250 Volts.				200 Volts.			150 Volts.	
	R(m)	T_r	R(s)[1]	R(s)[2]	R(m)	T_r	R(s)	R(m)	R(s)
	1.743	-	-	-	1.440	1.325	1.033	1.100	1.573
	1.037	-	1.263	1.254	0.842	0.775	1.013	0.654	0.786
	0.731	0.720	0.830	0.823	0.611	0.592	0.676	0.475	0.533
	0.573	0.571	0.627	0.624	0.481	0.472	0.514	0.377	0.410
	0.468	0.465	0.510	0.496	0.400	-	0.418	0.316	0.334
	-	-	0.431	-	0.345	-	0.352	0.276	0.289
	-	-	-	-	0.302	-	0.311	0.252	0.258
Film thickness (Å)	6090	6160	6150	6080	4970	4920	4960	3730	3835

TABLE 14

Wavelengths (μ) of minima produced by anodic zirconium oxide (4.0 mA/cm^2 saturated ammonium borate pH 9.0).

(A) 10 minutes at growth voltage
(B) at growth voltage

(A)

50 volts	100 volts	150 volts	200 volts	250 volts	300 volts
-	0.453	0.627	-	-	-
0.278	0.334	0.458	0.579	-	-
0.232	0.274	0.365	0.456	0.580	0.680
-	0.243	0.316	0.376	0.486	0.558
-	-	0.273	0.325	0.425	0.475
-	-	0.249	0.290	-	0.414

(B)

50 volts	100 volts	150 volts	200 volts
-	-	0.597	-
0.350	0.413	0.437	0.540
0.259	0.307	0.344	0.425
0.219	0.257	0.292	0.353
-	0.234	0.258	0.307
-	-	0.242	0.275
-	-	-	0.253

Reflectance attachment for 45 angle of incidence was used.

TABLE 15

Indexed spacings and intensities of $\bar{\gamma}$ - alumina produced anodically.

Measured spacings and estimated intensities			Indexed spacings and intensities reported in literature.(46)					
(hkl)	Intensity	d_{hkl} (Å)	Intensity	d_{hkl} (Å)		Intensity	d_{hkl} (Å)	
(111)	F	2.273	VVF	2.287		F	2.281	
(200)	VS	1.972	S	1.980		VS	1.975	
(220)	VS	1.397	VS	1.399		VS	1.397	
(311)	F	1.181	VF	1.193		NOT	OBSERVED	
(222)	M	1.130	M	1.143		M	1.140	
(400)	M	0.974	F	0.990		MS	0.988	
(331)		N O T	O B S E R V E D					
(420)	M	0.887	M	0.885		MS	0.883	
(422)	M	?	S	0.805		S	0.806	

Measured radii for diffraction rings and using Tl Cl for calibration under the same microscope settings.

$\bar{\gamma}$ - Alumina		Tl Cl	
(hkl)	Radius (cm)	(hkl)	Radius (cm)
(111)	0.9895	(100)	0.5865
(200)	1.141	(110)	0.8235
(220)	1.610	(111)	1.050
(311)	1.905	(200)	1.1715
(222)	2.004	(210)	1.298
(400)	2.311	(211)	1.421
(420)	2.535		
422	?		

TABLE 16.

Thickness lost during immersion in various electrolytes at various pH values against time.

0.1M Solution (pH)	Time minutes	t_i Å	t_c Å	t_r Å	t_o Å
$(NH_4)_2CrO_4$					
7.6	1460	Nil	-	-	Nil
10.2	54	218	-	516	310
$(NH_4)_2SO_4$					
8.6	250	840	-	-	42
9.6	200	1512	-	924	756
10.2	50	2100	-	728	644
K_2SO_4					
5.5	1440	Nil	-	-	Nil
8.6	1500	292	-	-	70
$K_2SO_4+NH_4OH$					
10.4	95	1942	-	868	728
10.5	53	1344	-	588	490
$K_2CrO_4+NH_4OH$					
10.4	60	726	-	476	350
10.5	46	672	-	306	280
K_2CrO_4					
10.2	141	546	-	406	300
7	1750	54	-	Nil	Nil
8	1750	700	-	616	450
9	1615	1320	1260	1120	980
10	208	904	840	712	588
10	350	1904	1740	1302	1148
11	100	1904	1580	1000	910
8.6	1445	966	-	-	812

TABLE 16 CONT'D

0.1M Solution (pH)	Time minutes	t_i Å	t_c Å	t_r Å	t_o Å
11	102	1890	1680	1232	1148
K_2CrO_4+KCl					
7	1400	84	-	Nil	Nil
8	1350	868	-	616	250
9	1500	1540	1400	1190	945
10	210	1904	1764	1456	975
11	55	1946	1652	868	700

Thickness lost

(t_i = thickness equivalent to $\frac{1}{C_p}$ during immersion
(in situ.
(t_c = thickness equivalent to $\frac{1}{C_p}$ by changing to
(pH 9.0
(t_r = thickness equivalent to $\frac{1}{C_p}$ after drying
(and re-immersion.
(t_o = thickness by optical measurement.

TABLE 17

Current efficiency calculated for different electrolytes.

Ammonium borate solution (1.0 mA/cm^2)

	pH 8.1.	pH 9.0.	pH 10.
Electropolished Chromic-phosphoric -sulphuric acids	-	95.0%	anomalous behaviour of dv/dt_m
Electropolished perchloric acid-ethyl alcohol	94.0%	94.0%	
Etched (NaOH)	85.5%	86.0%	
Unetched	The dv/dt_m behaviour was complicated		

Ammonium citrate solution (1.0mA/cm^2) up to 250 volts.

	pH 9.0
Electropolished perchloric acid - ethyl alcohol	91.0%
Etched (NaOH)	85.0%

Ammonium tartrate solution (1.0mA/cm^2) up to 250 volts

	pH 5.5	pH 9.0
Electropolished perchloric acid-ethyl alcohol	81.0%	92.0%
Etched (NaOH)	-	85.0%

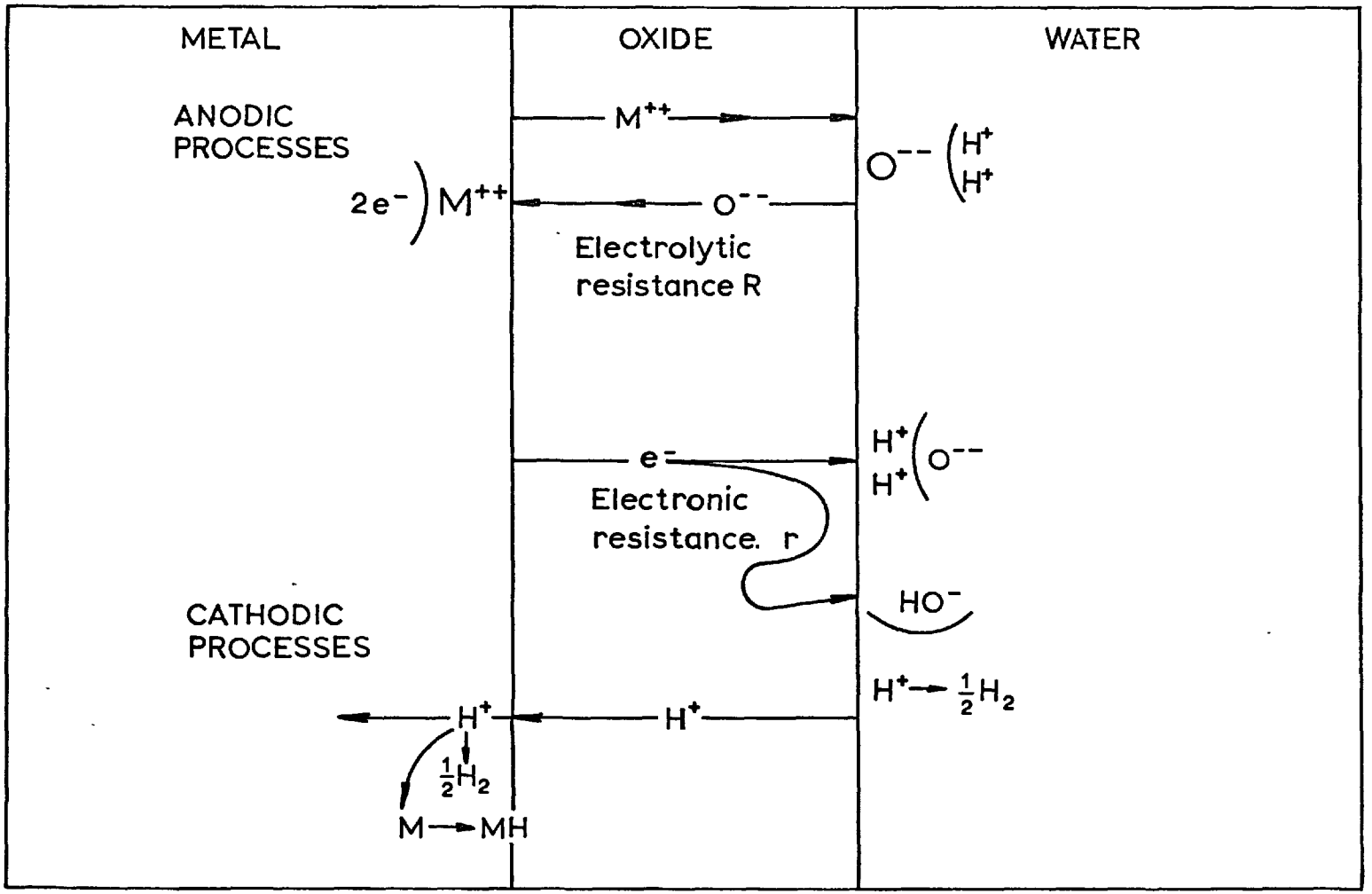

Fig.1. Schematic representation of corrosion processes (after Draley et al.)

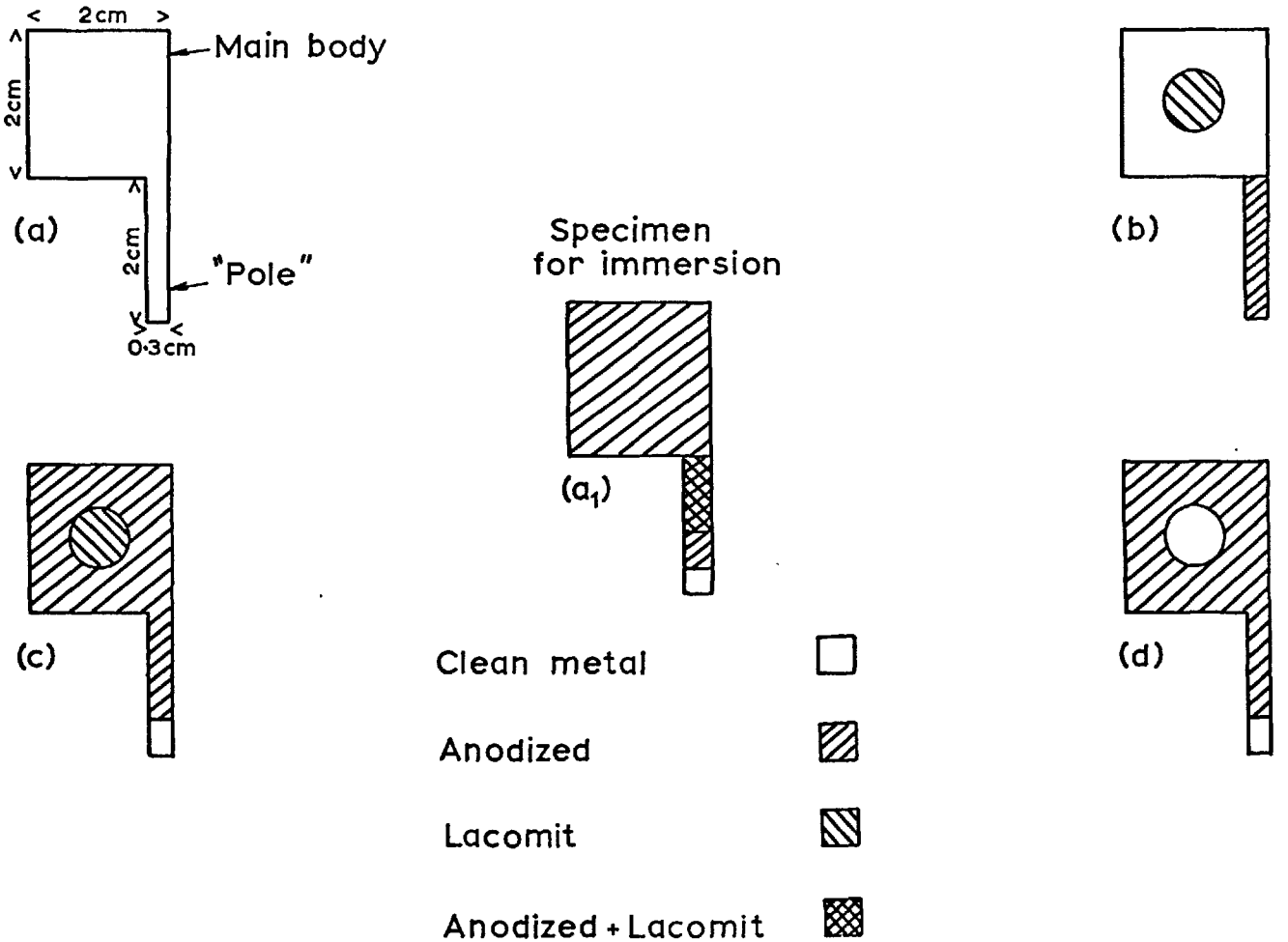

Fig.2. Specimen preparation

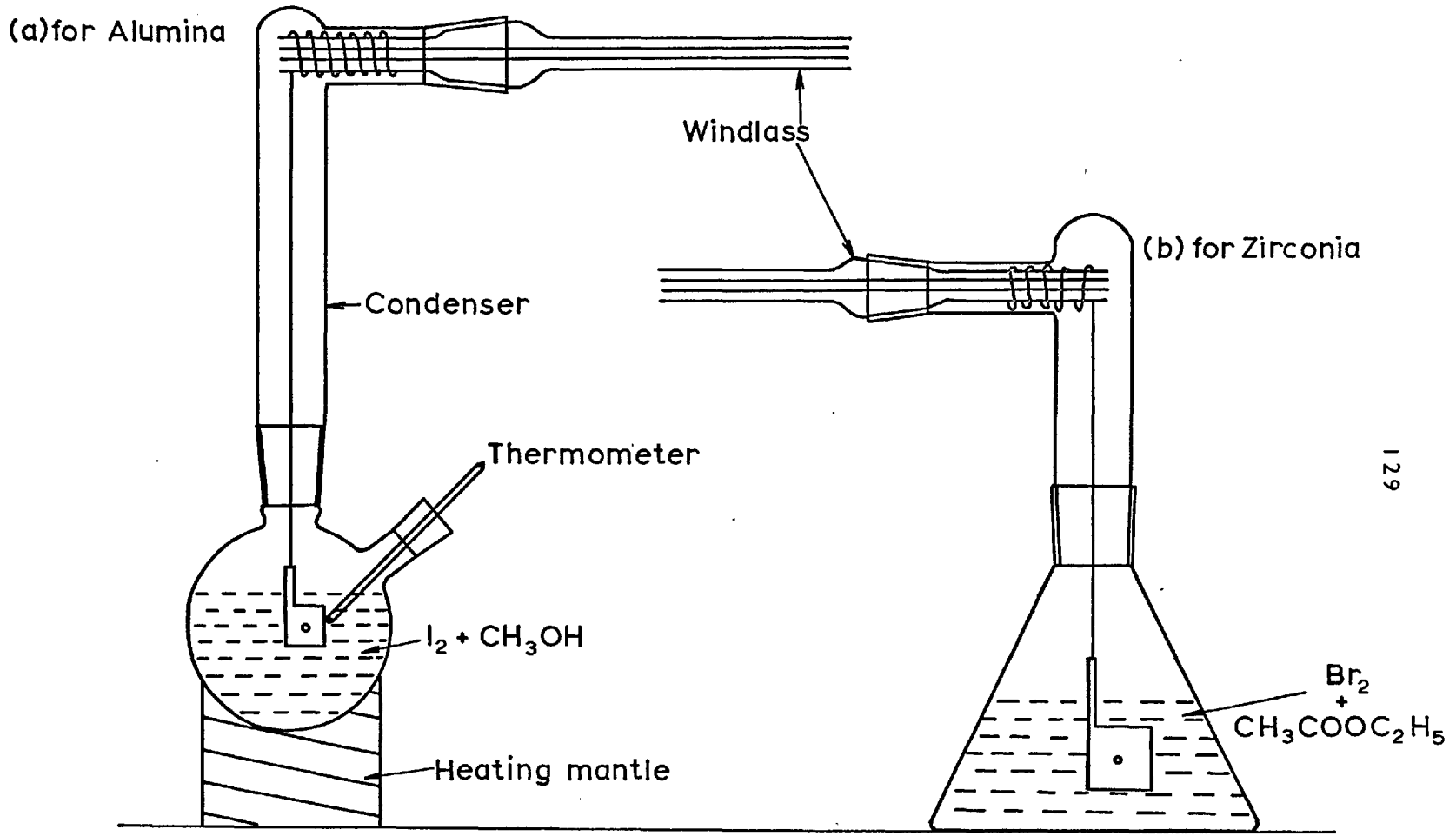

Fig.3. Stripping apparatus

CASE 1

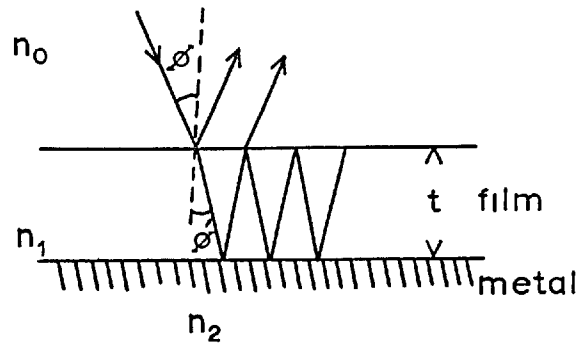

STRIPPED OFF FILMS

CASE 2

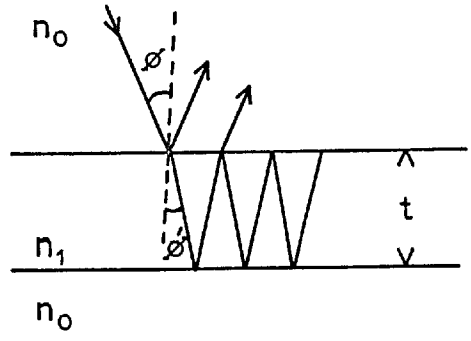

CASE 3

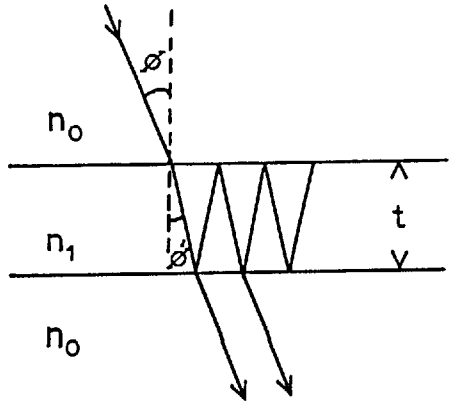

Fig. 4. Optical interference for transparent films

FIG.5. SCHEMATIC DIAGRAMS FOR MEASURING ELECTROLYTIC RESISTANCE OF OXIDE FILMS BY ALTERNATING AND DIRECT CURRENT METHODS.

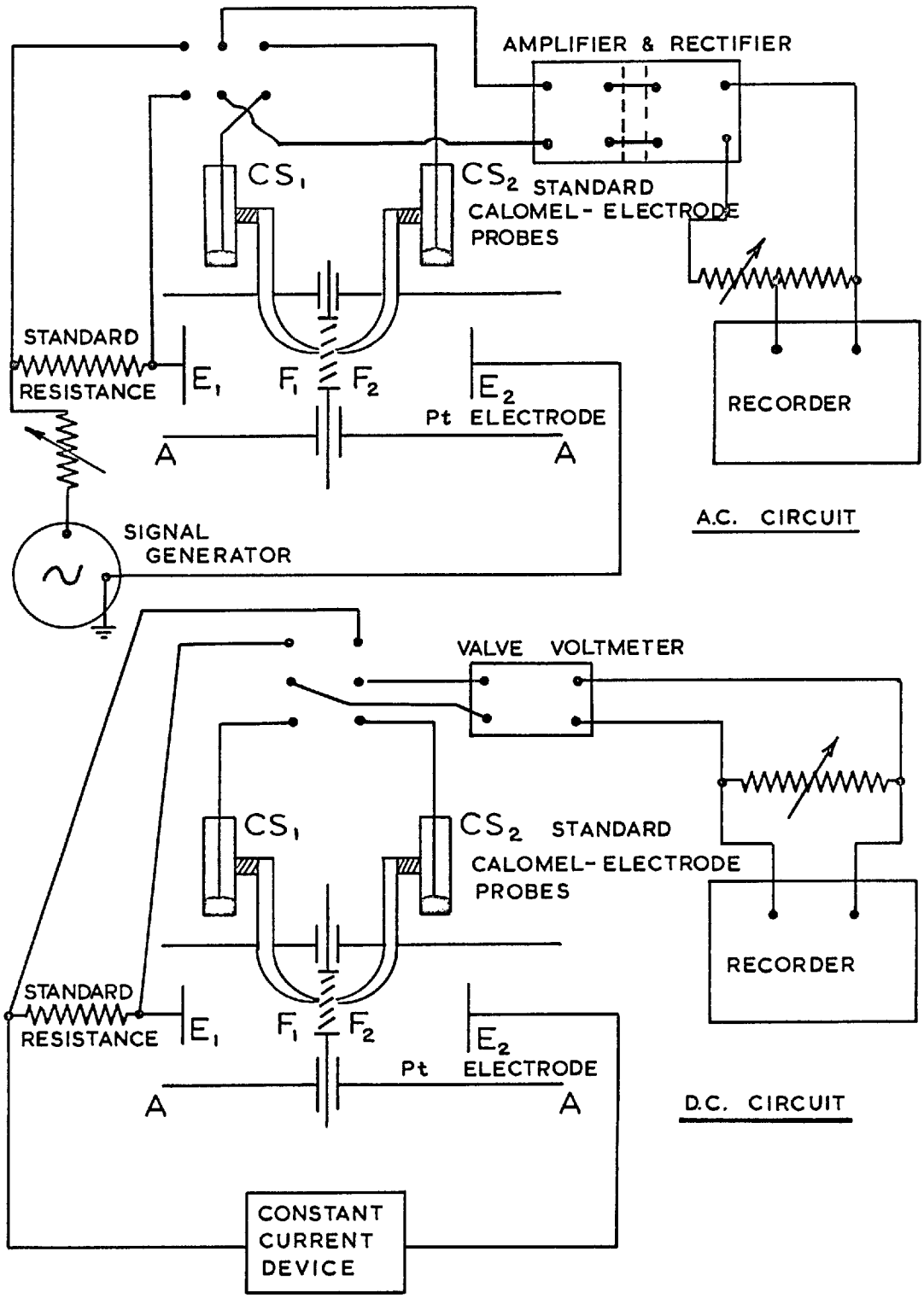

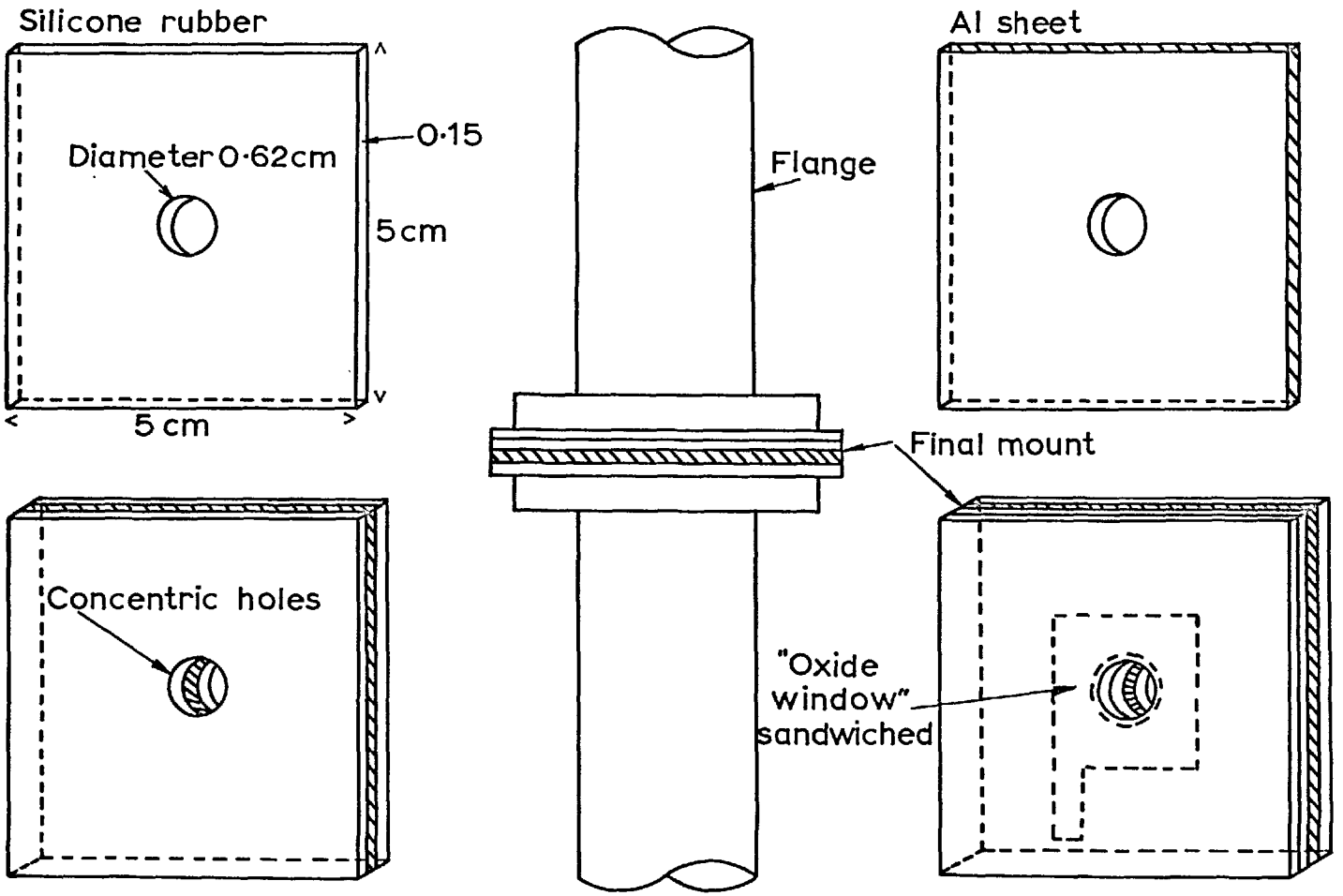

Fig.6. Mounting arrangement of oxide film

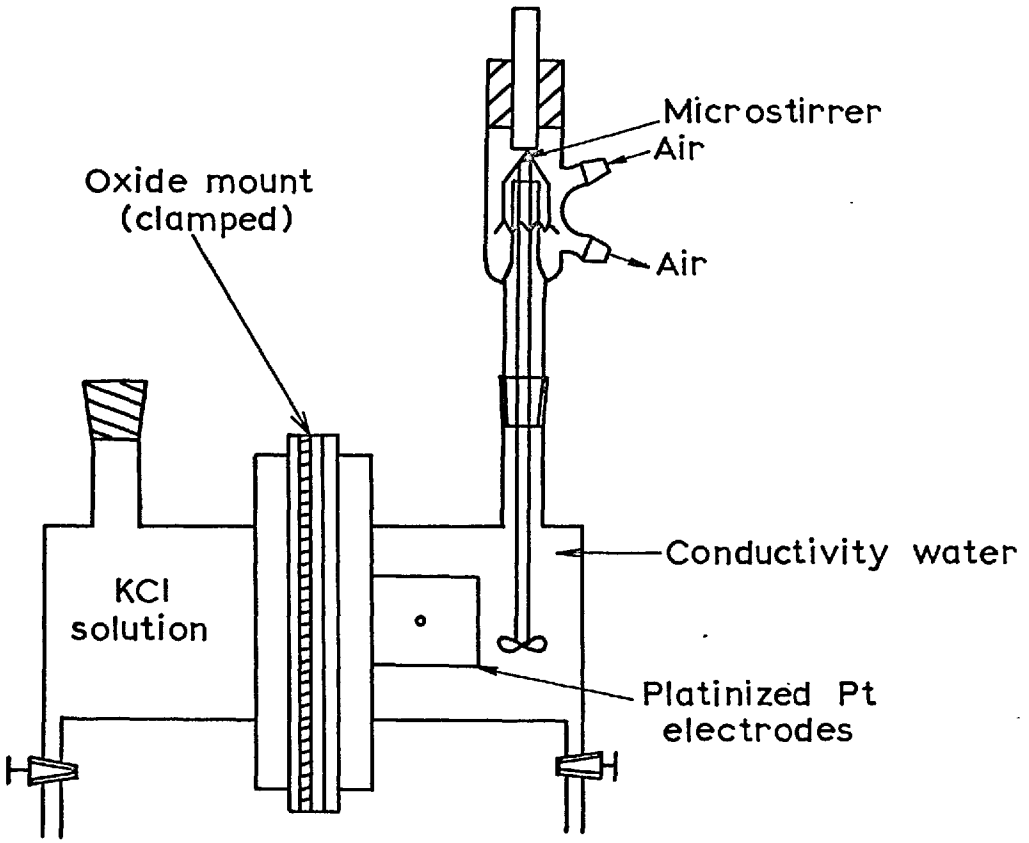

Fig. 7. Cell for the study of permeation through an oxide film

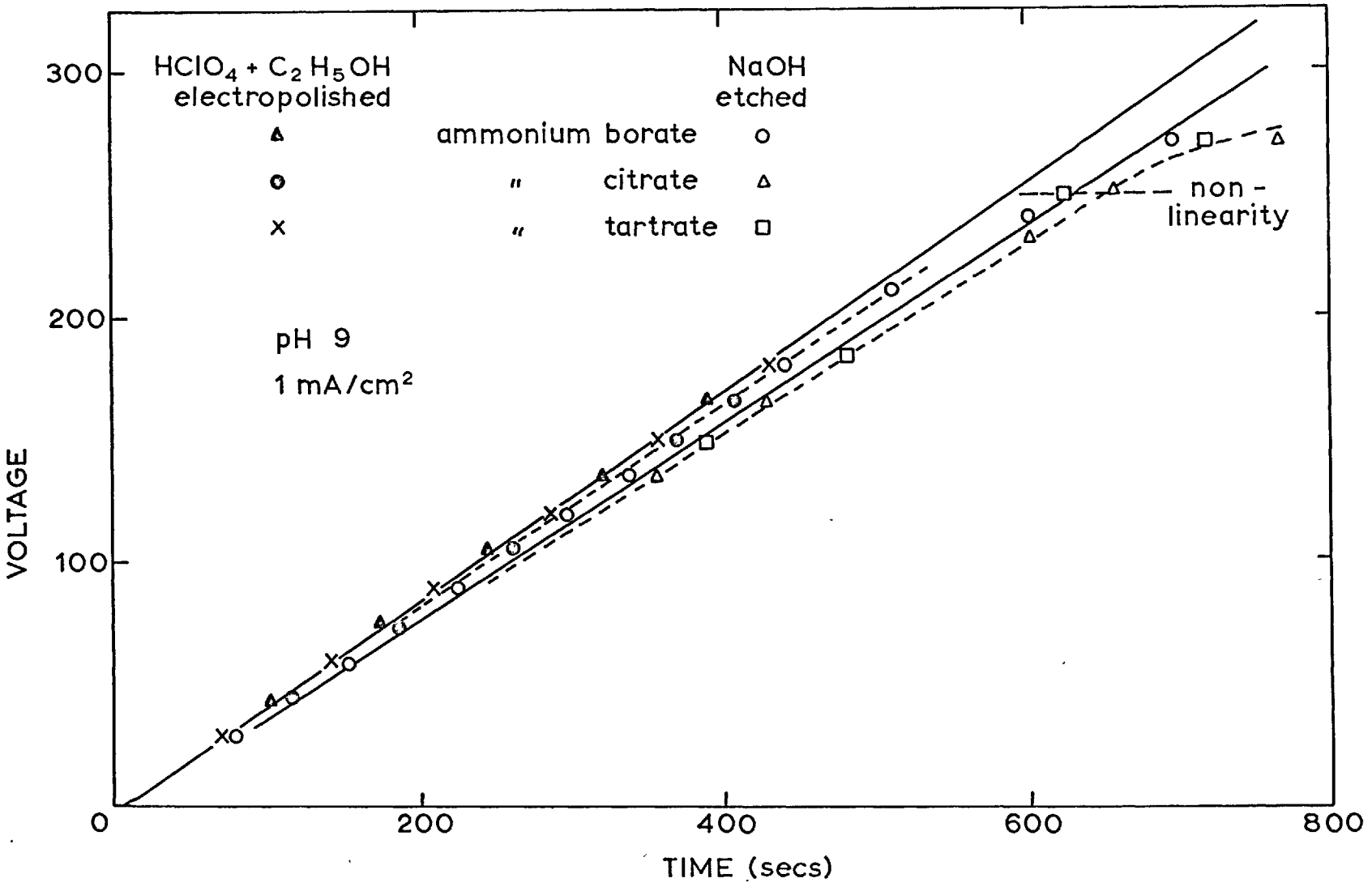

Fig. 8. Voltage versus time for anodizing Al

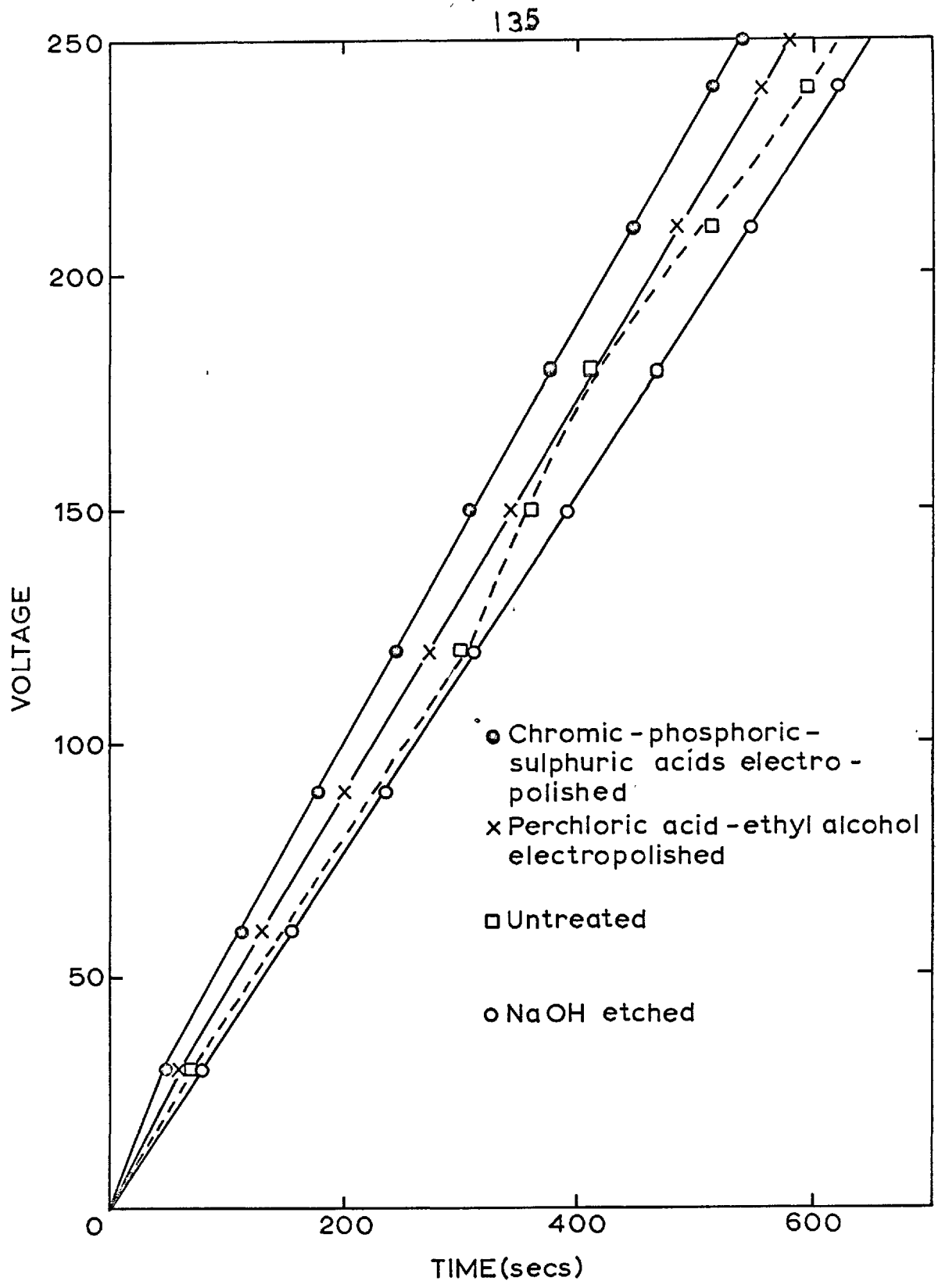

Fig.9. Voltage versus time (30g/l ammonium borate pH 9) 1 mA/cm^2

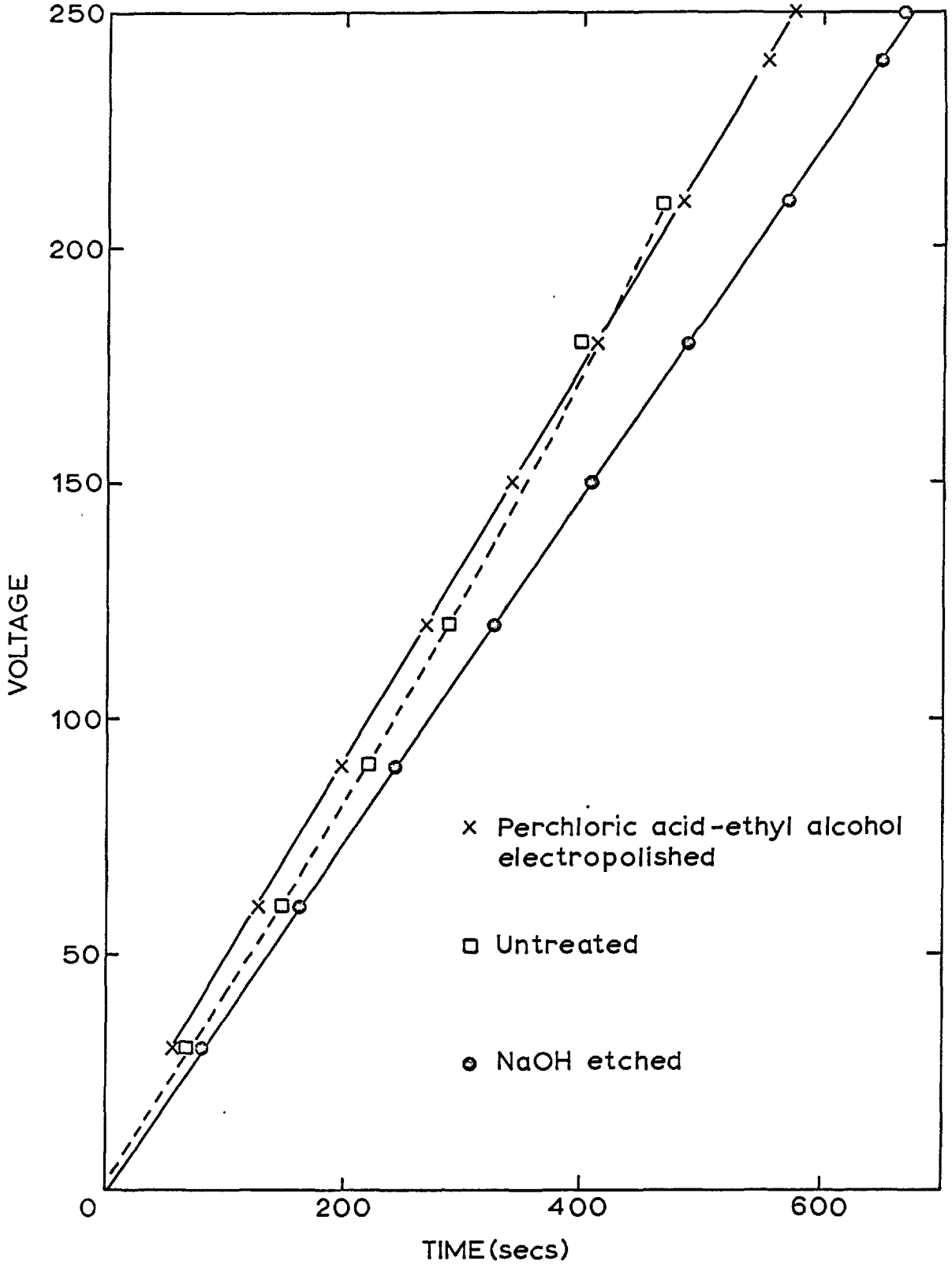

Fig.10. Voltage versus time (30 g/l ammonium borate pH 8·1) 1 mA/cm²

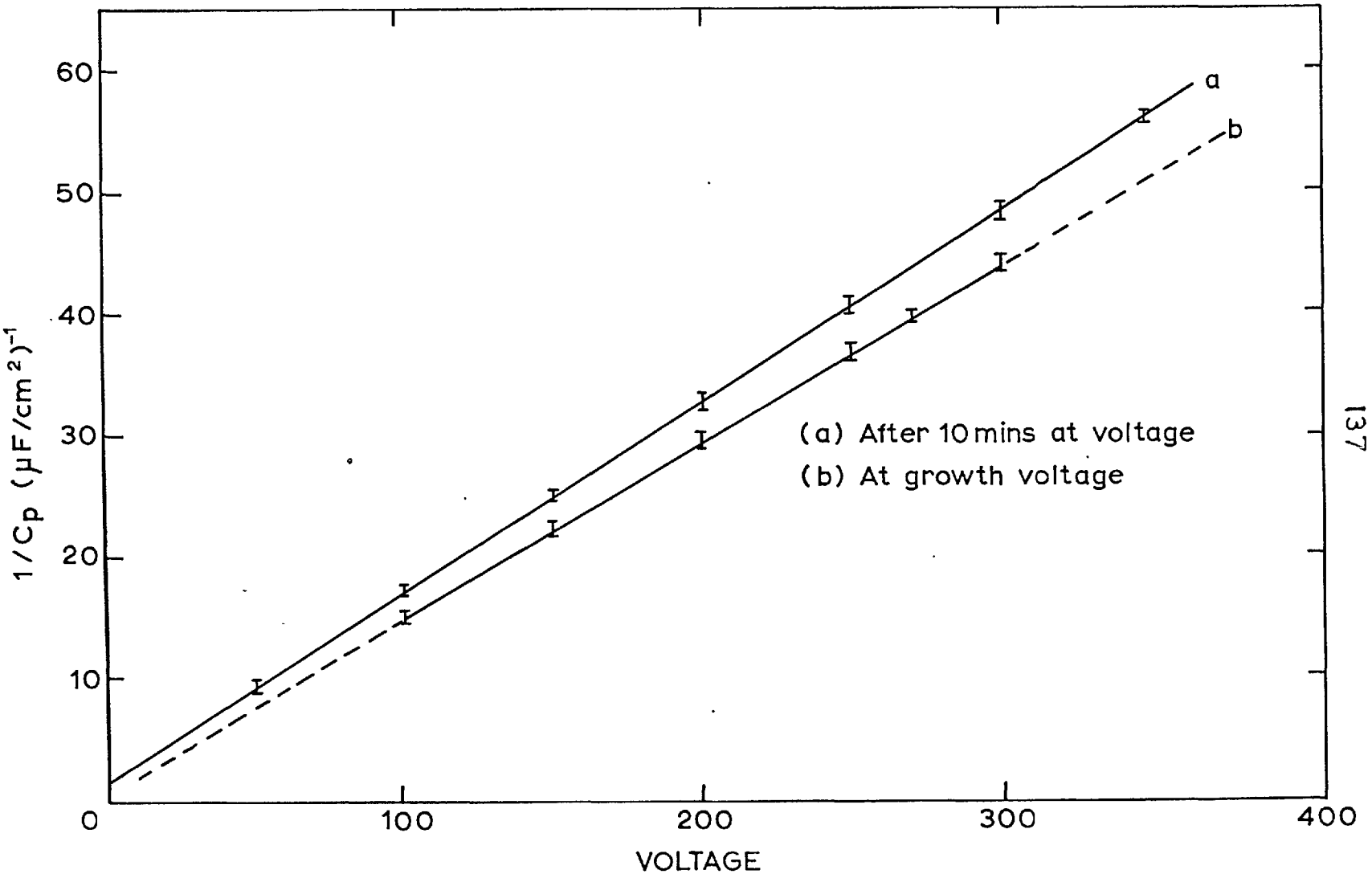

Fig.11. Inverse capacity versus anodizing voltage (1 mA/cm²) using various surface preparations (30g/l ammonium borate pH 9)

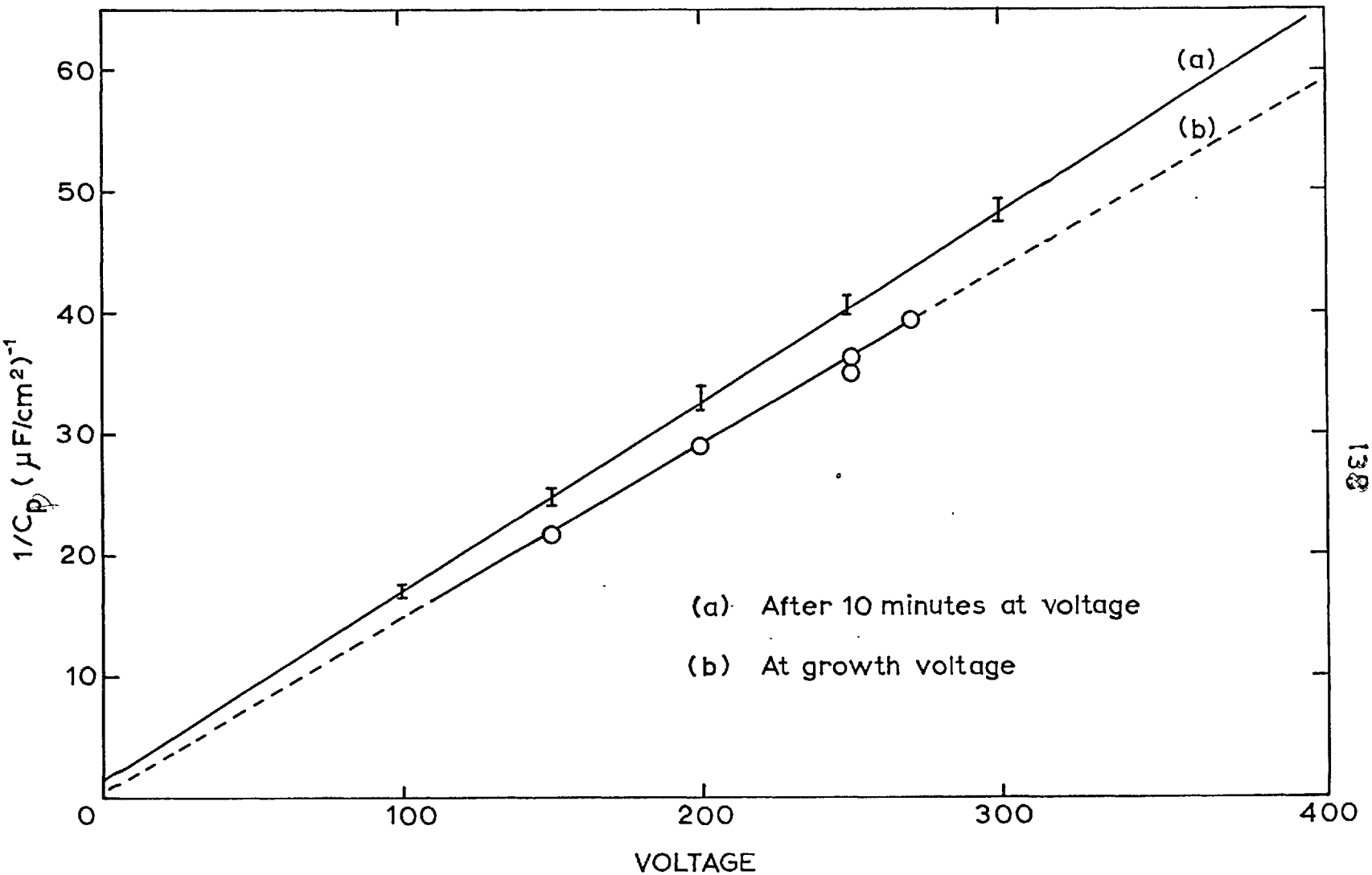

Fig.12. Inverse capacity versus anodizing voltage (1mA /cm^2) for Al using various surface preparations and different solutions.

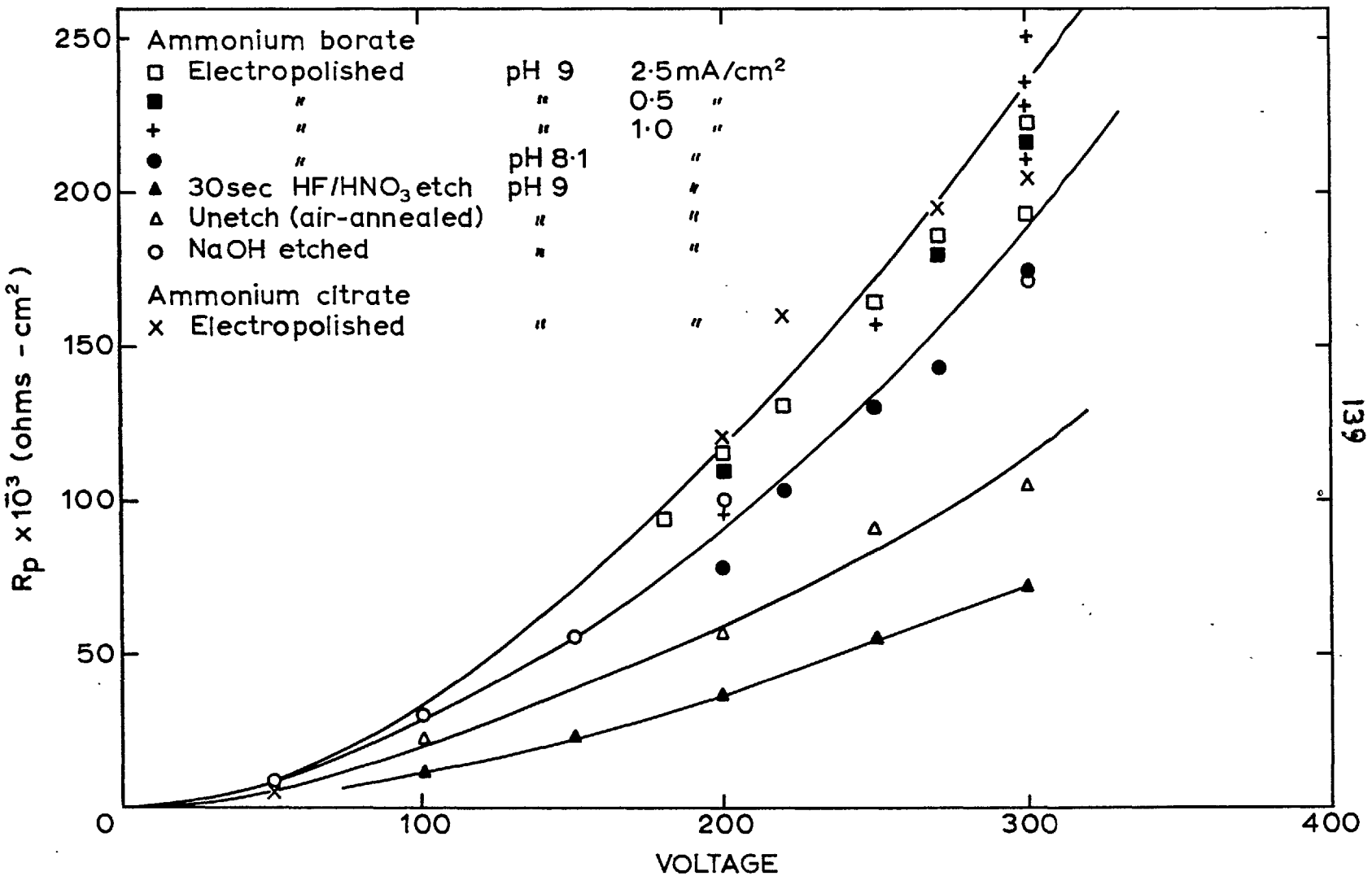

Fig.13. Resistance versus anodizing voltage for Al.

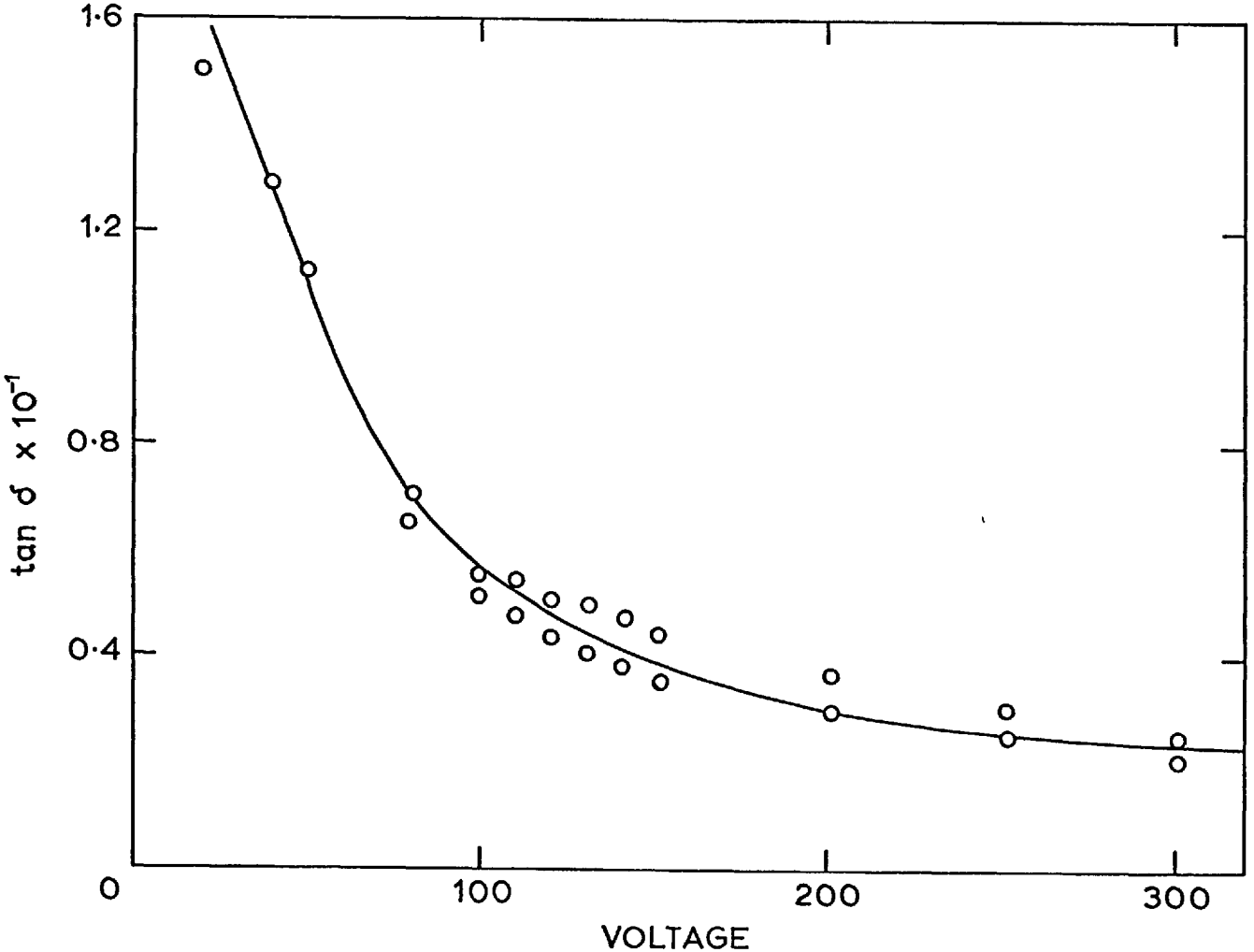

Fig 14 Calculated tan δ versus voltage for anodic alumina

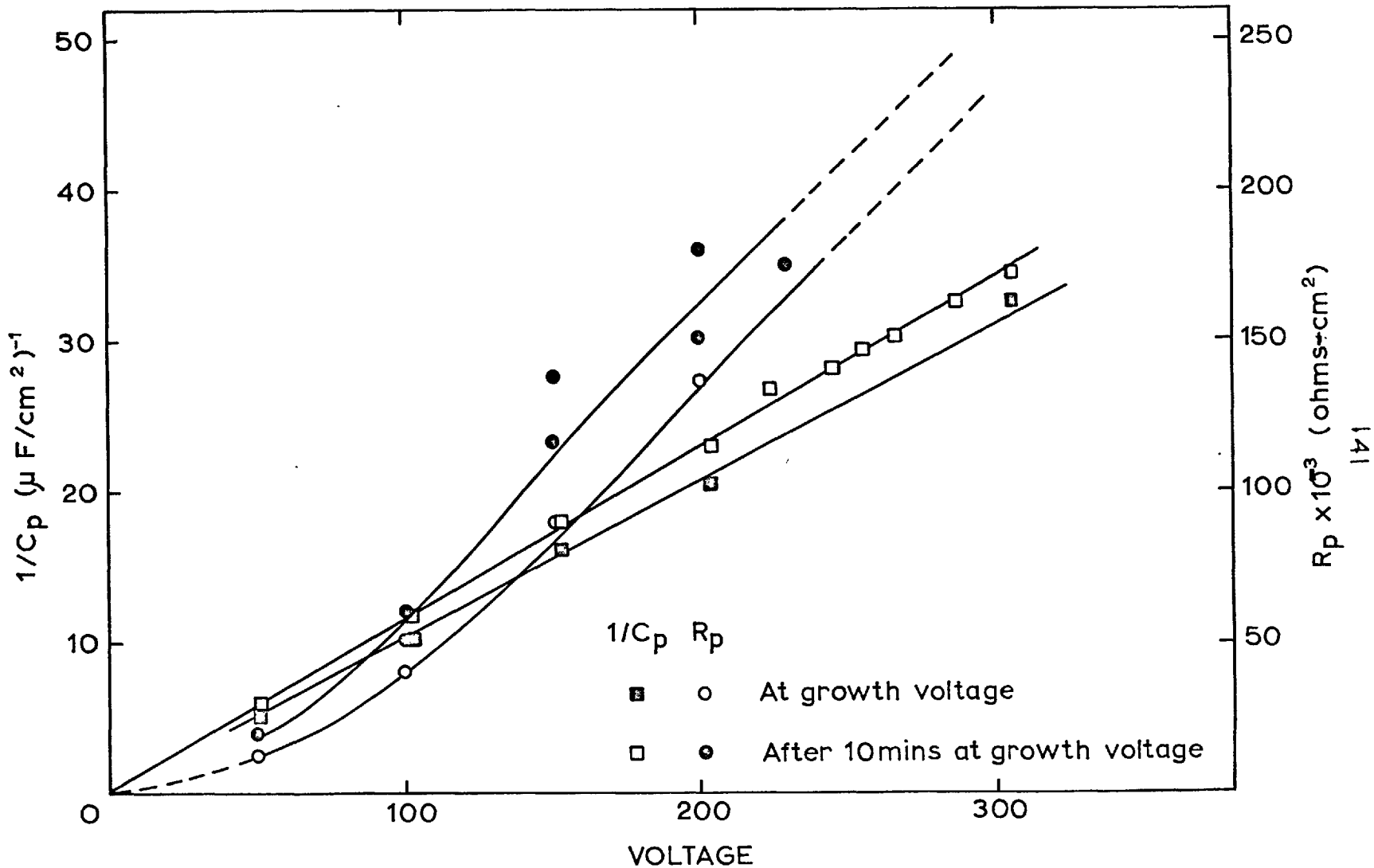

Fig.15. Inverse capacity and resistance versus anodizing voltage (4 mA/cm²) for Zr (saturated ammonium borate pH 9)

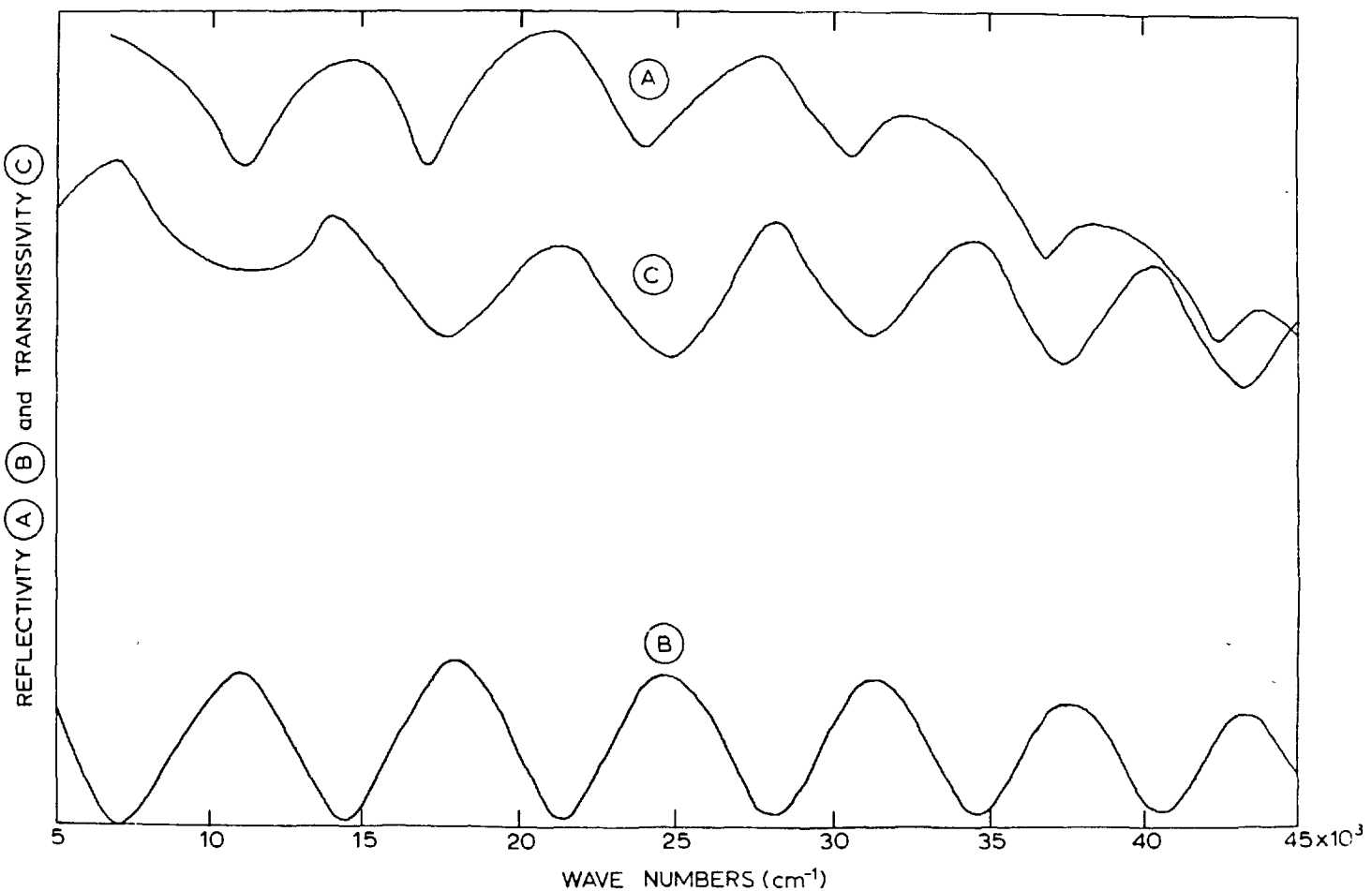

Fig 16 Reflectivity of anodized Al (A) and reflectivity (B) and transmissivity (C) of anodic Al oxide (300v film, etched Al)

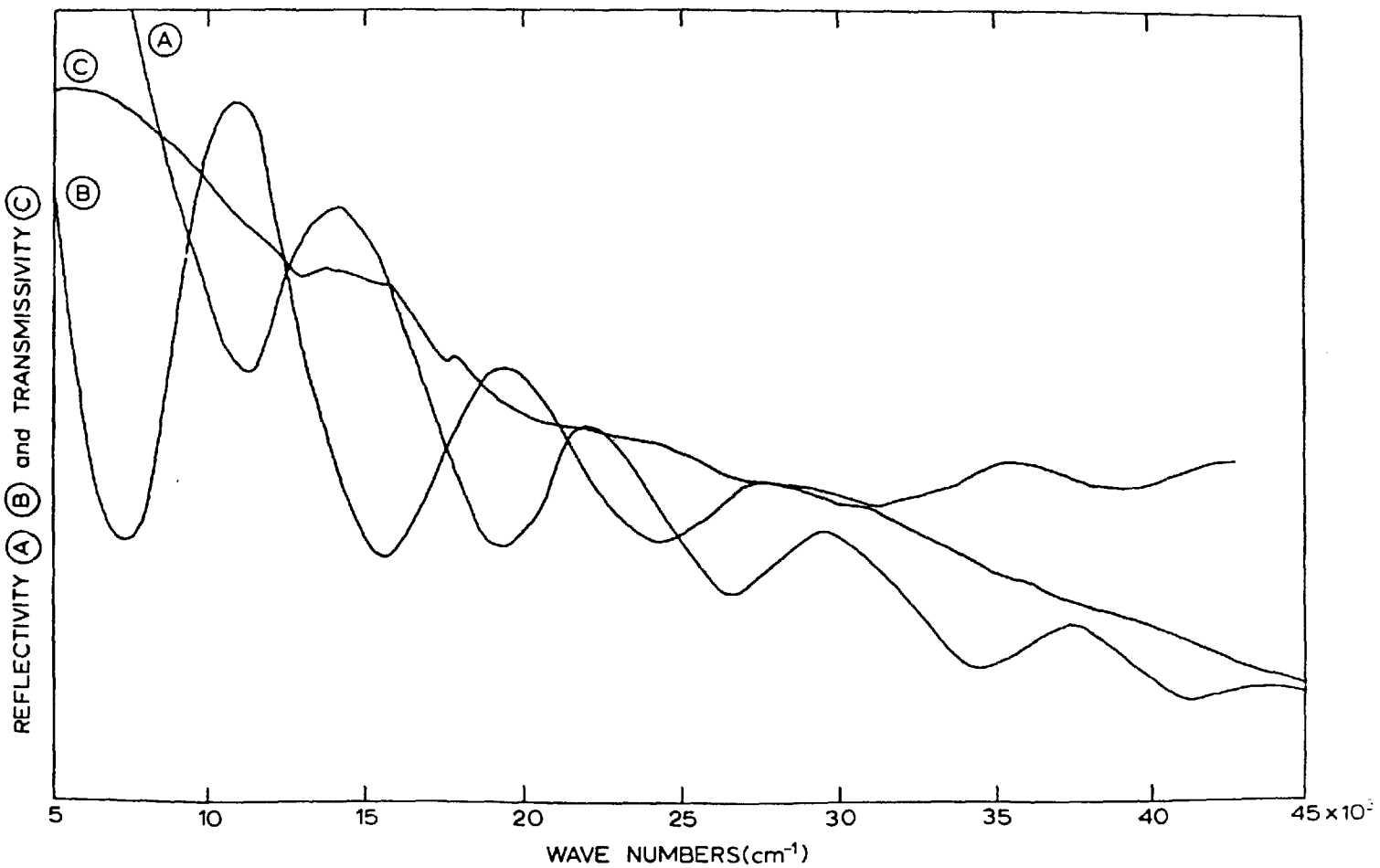

Fig.17 Reflectivity of anodized Al (A) and reflectivity (B) and transmissivity (C) of anodic Al oxide (300 v. film, un-etched Al)

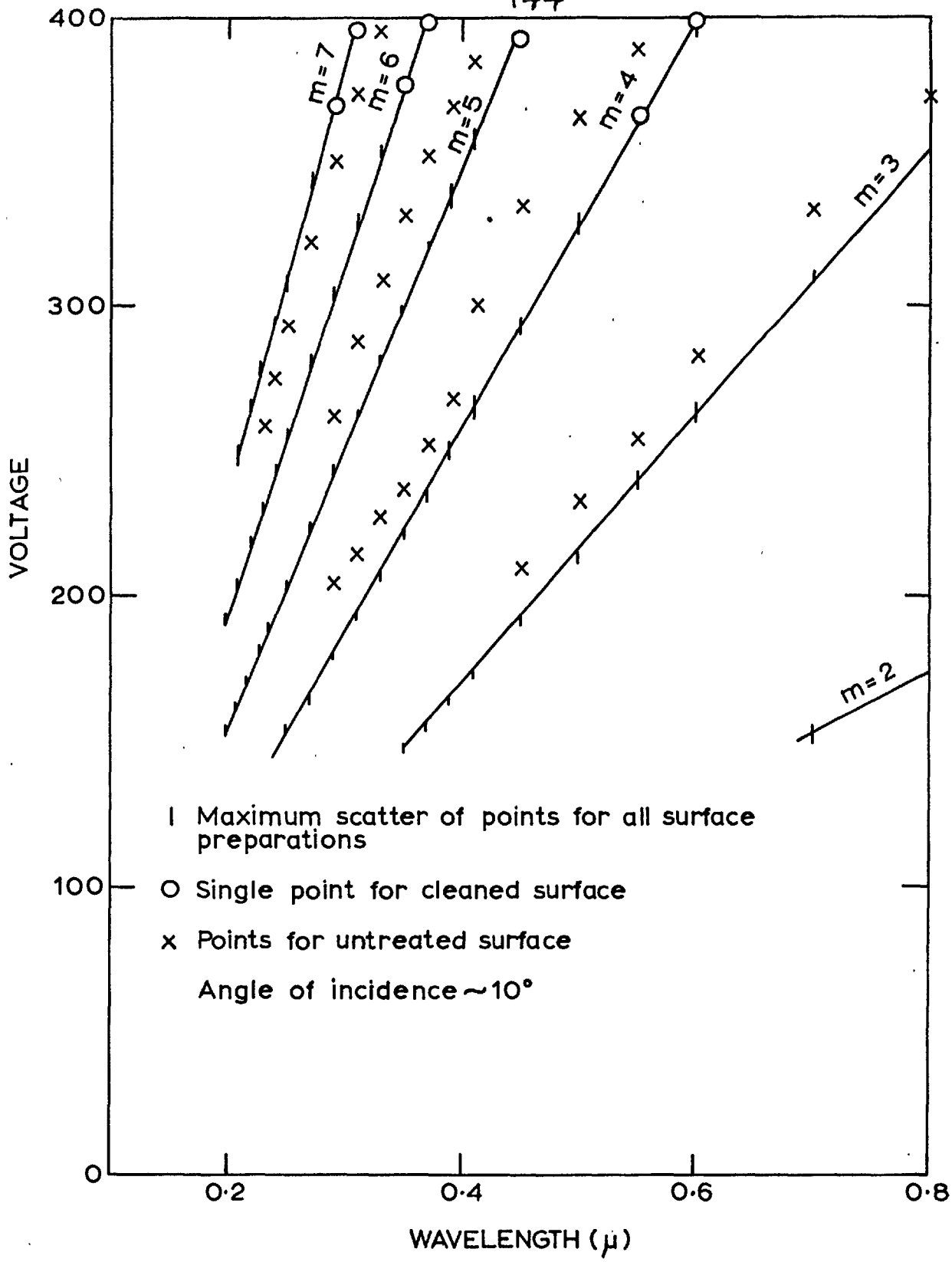

Fig.18. Voltage versus reflectivity minimum for oxide films stripped from anodized Al

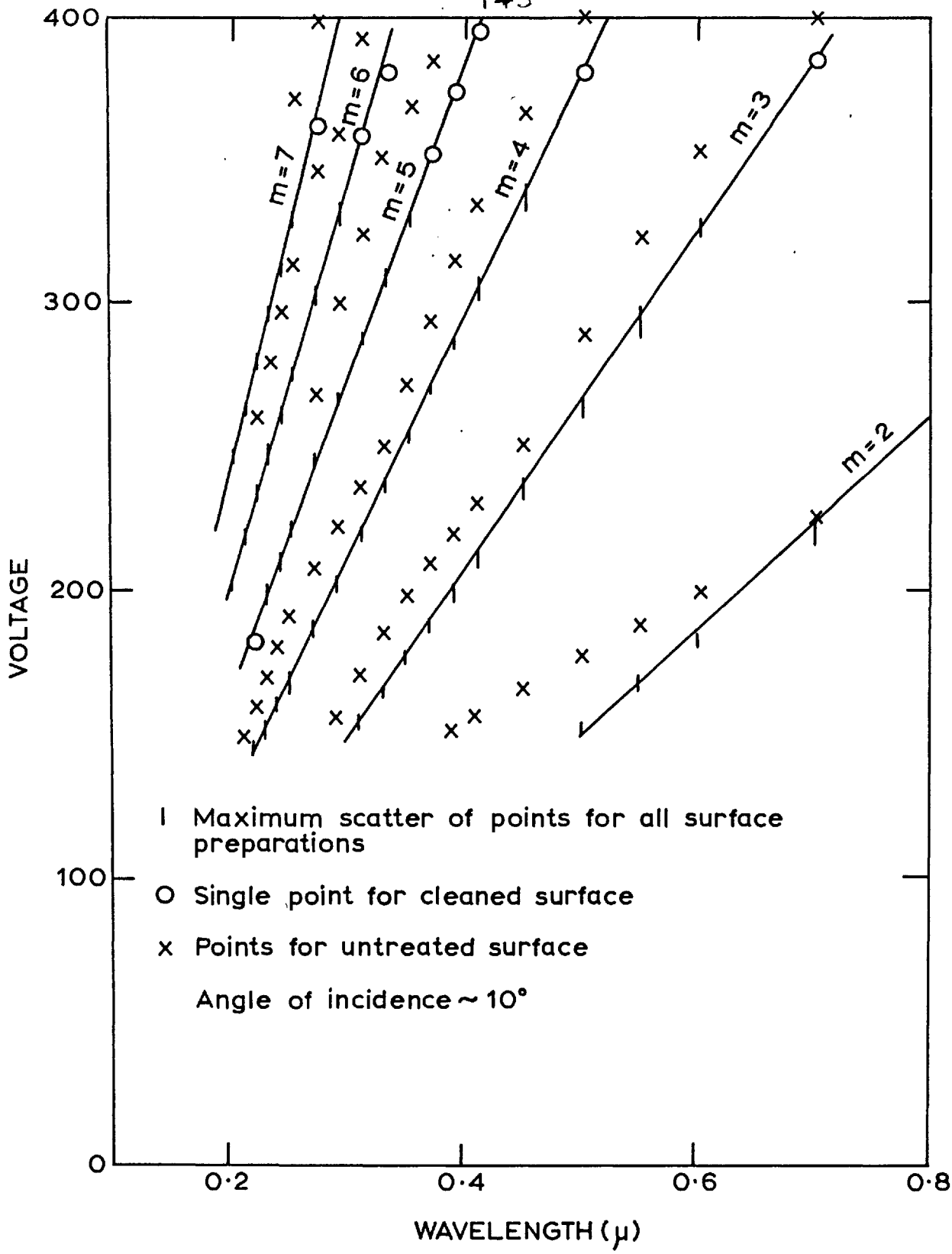

Fig. 19. Voltage versus reflectivity for anodized Al surfaces

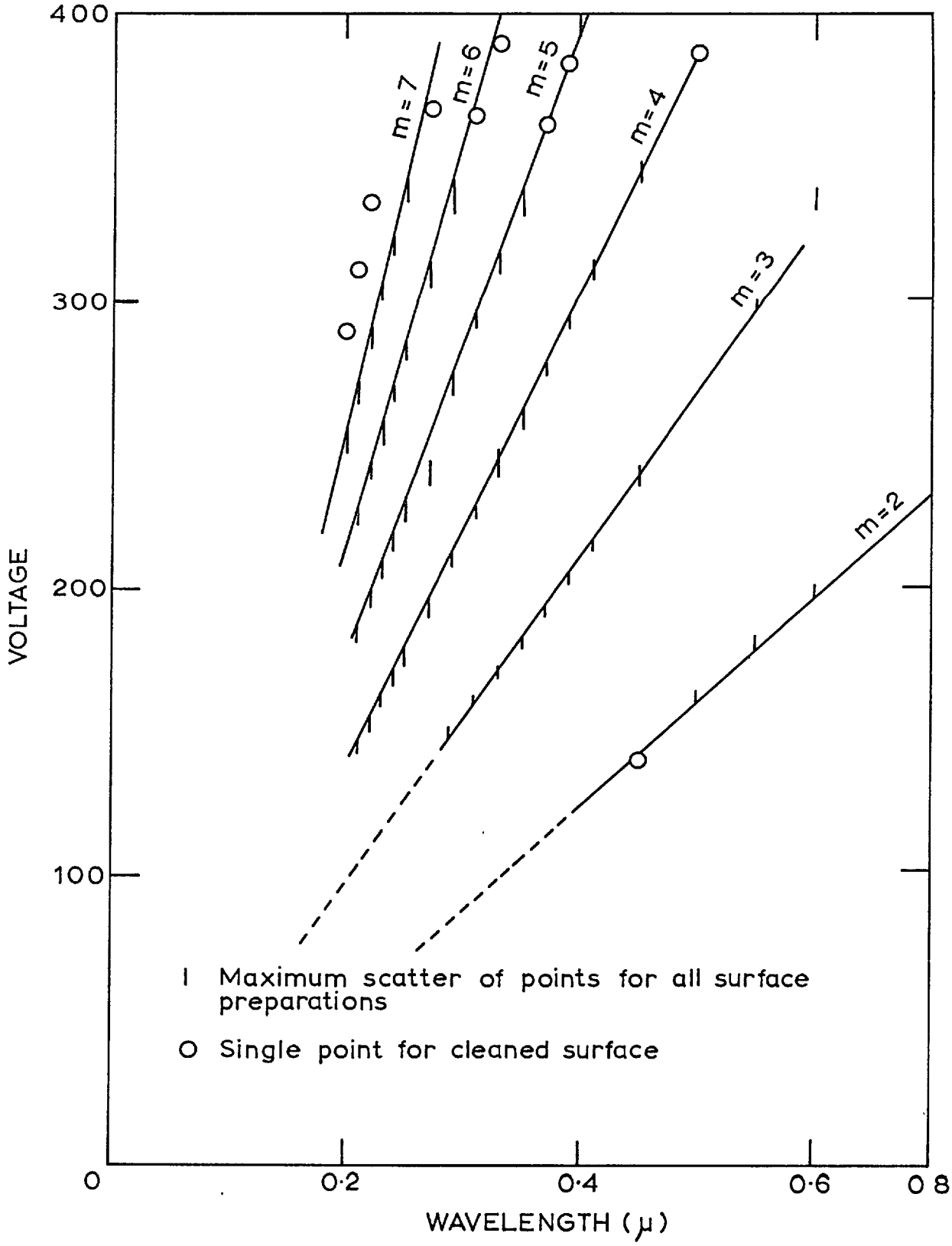

FIG. 20. Voltage versus transmissivity minimum for oxide film stripped from anodized Al.

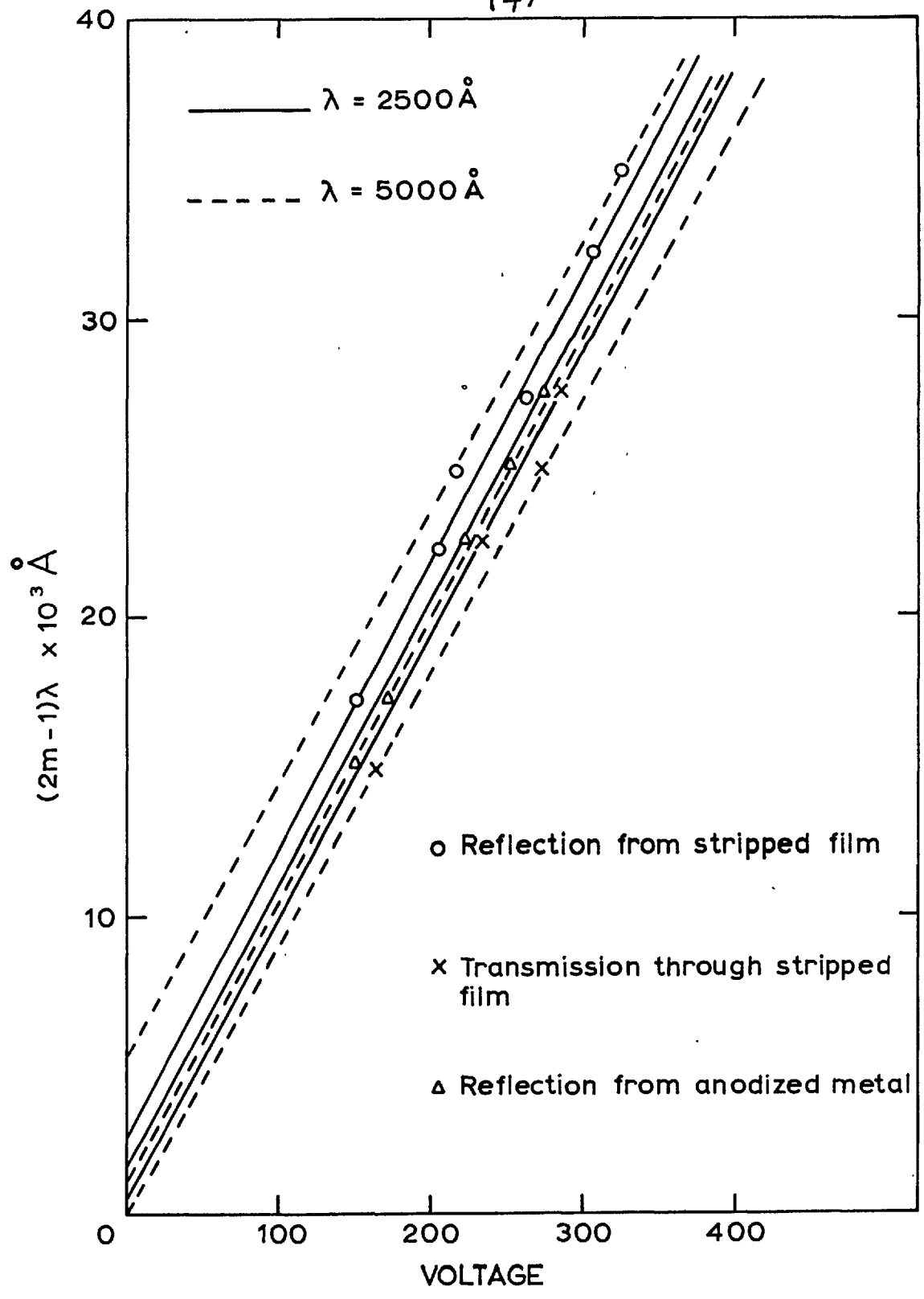

Fig.21. $(2m-1)\lambda$ versus voltage for anodic Al oxide films (Al electropolished in $HClO_4$)

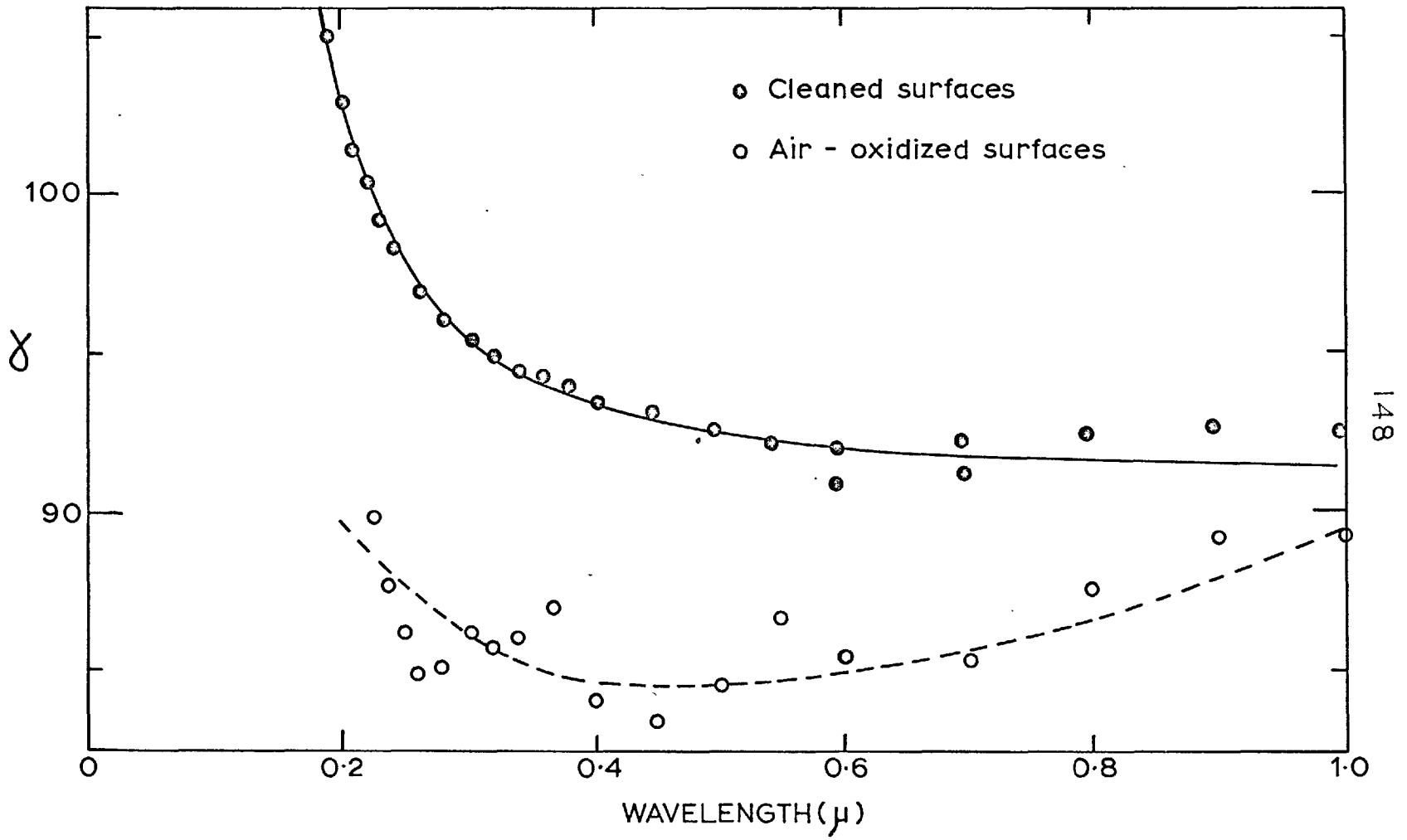

Fig.22. Change of α with μ for anodic oxide films on Al.

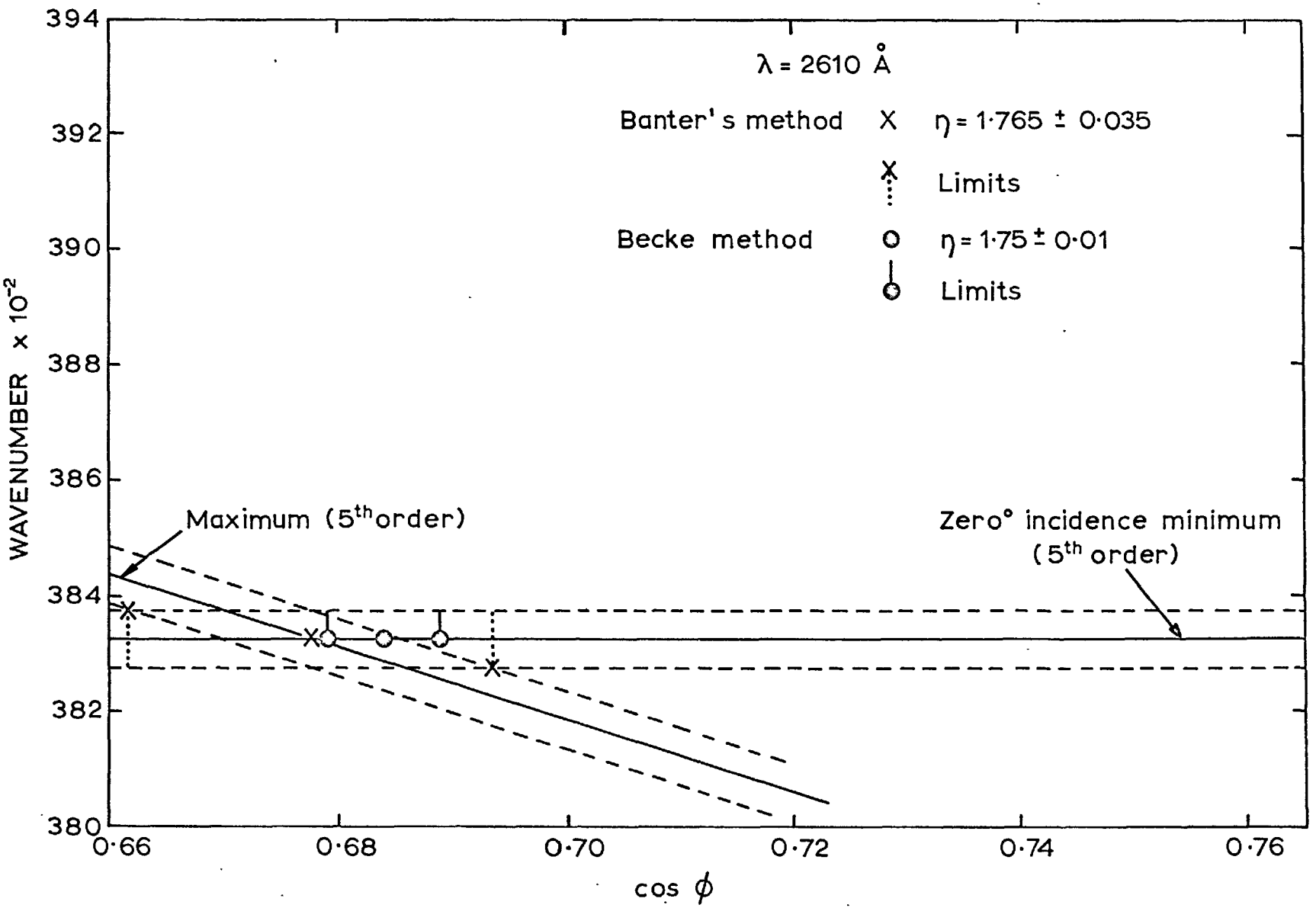

Fig. 23. Wavenumber versus cos ϕ

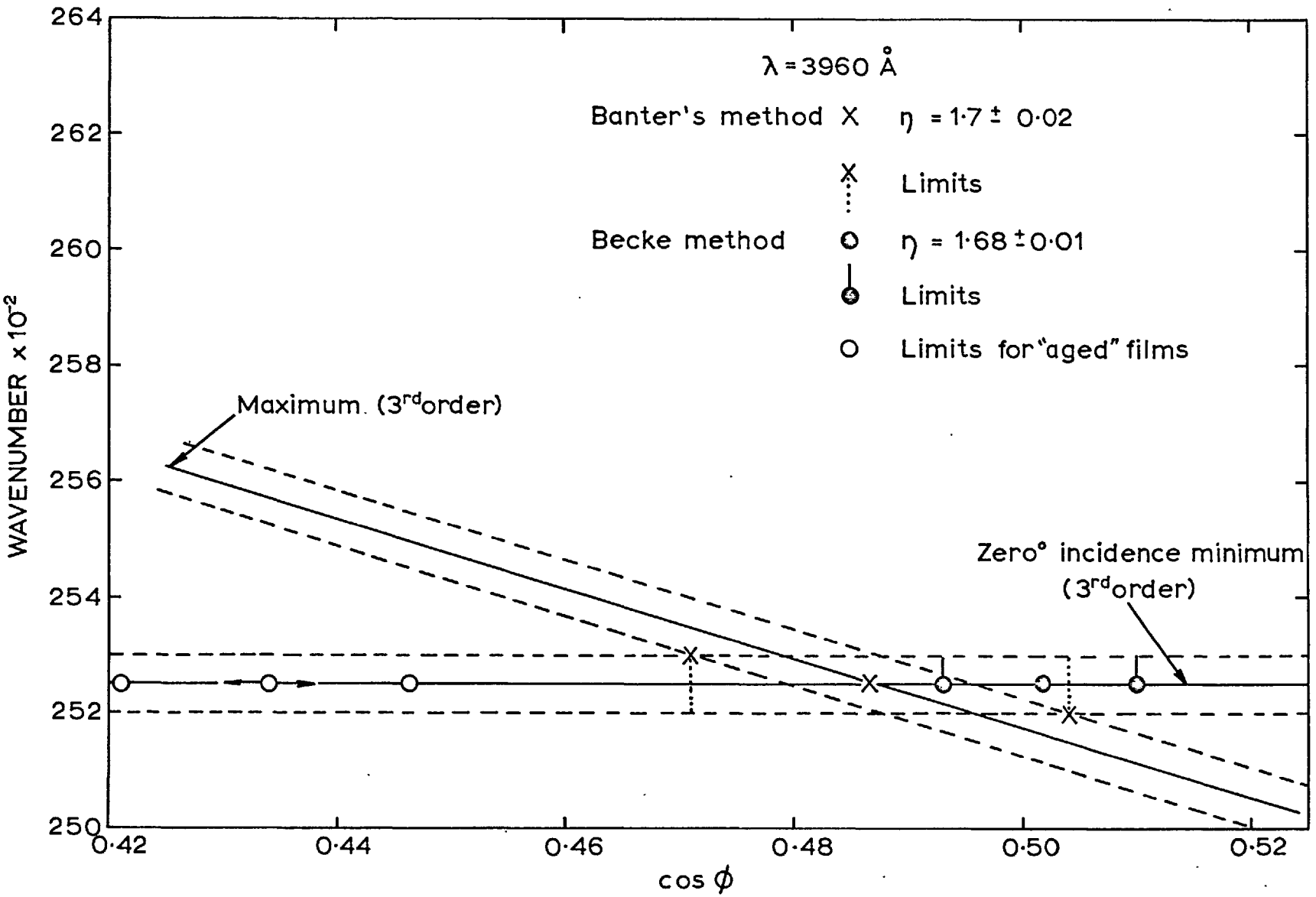

Fig.24. Wavenumber versus cos ϕ

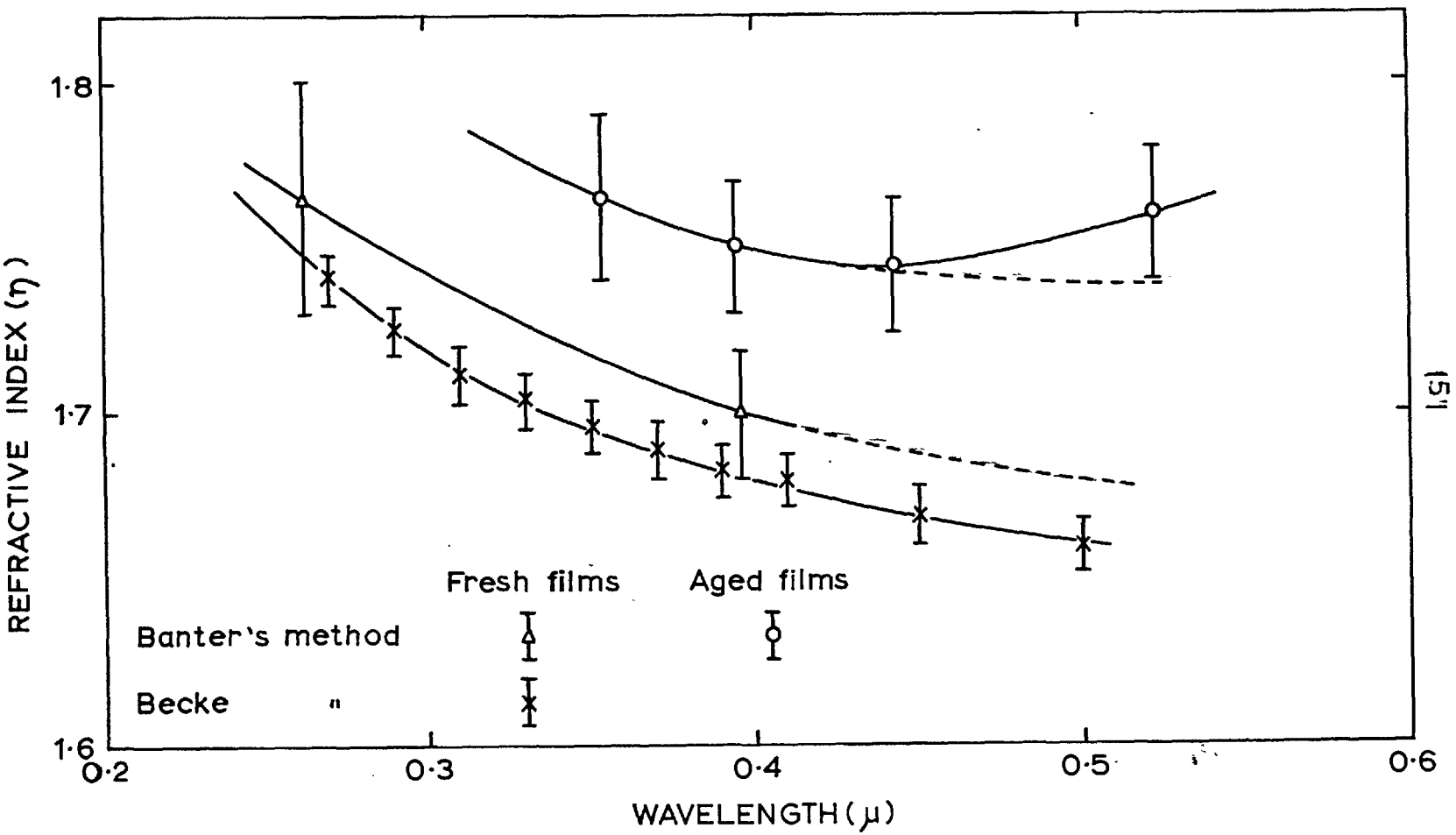
1·8
1·7
1·6
REFRACTIVE INDEX (η)
0·2
0·3
0·4
0·5
0·6
WAVELENGTH (μ)
Fresh films
Aged films
Banter's method
Becke "

Fig. 25.

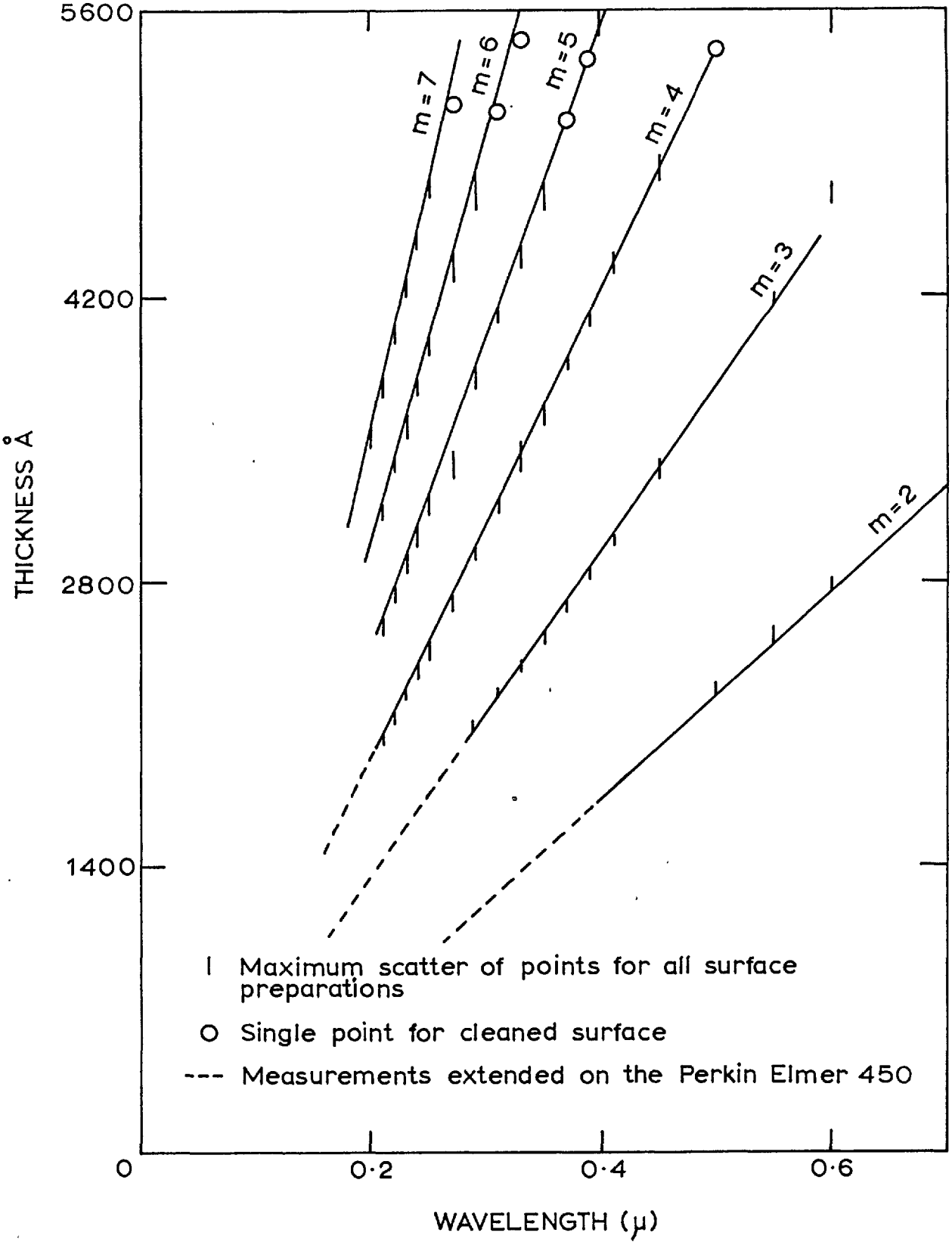

Fig.26. Thickness versus transmissivity minimum for oxide film stripped from anodized Al

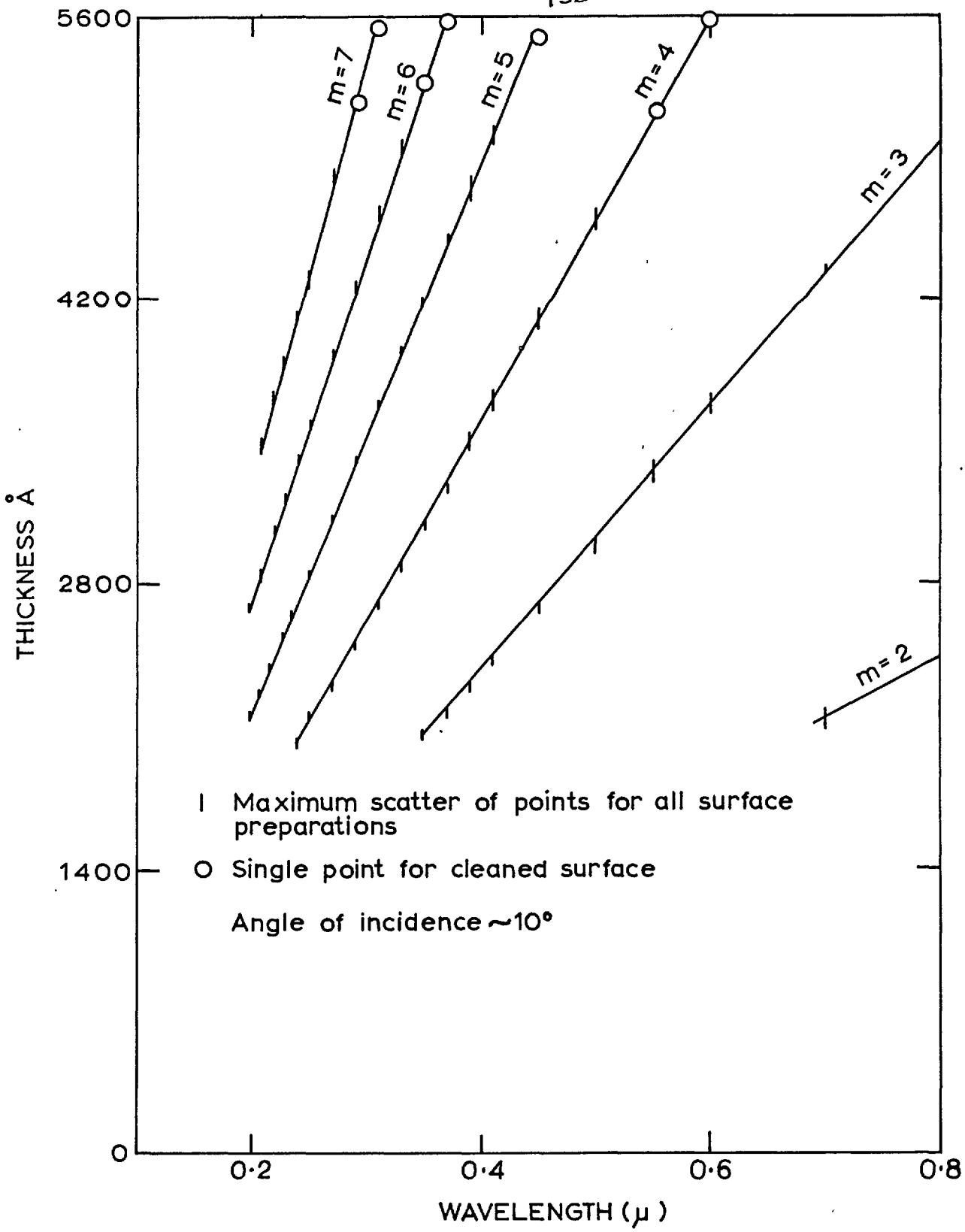

Fig.27. Thickness versus reflectivity minimum for oxide films stripped from anodized Al

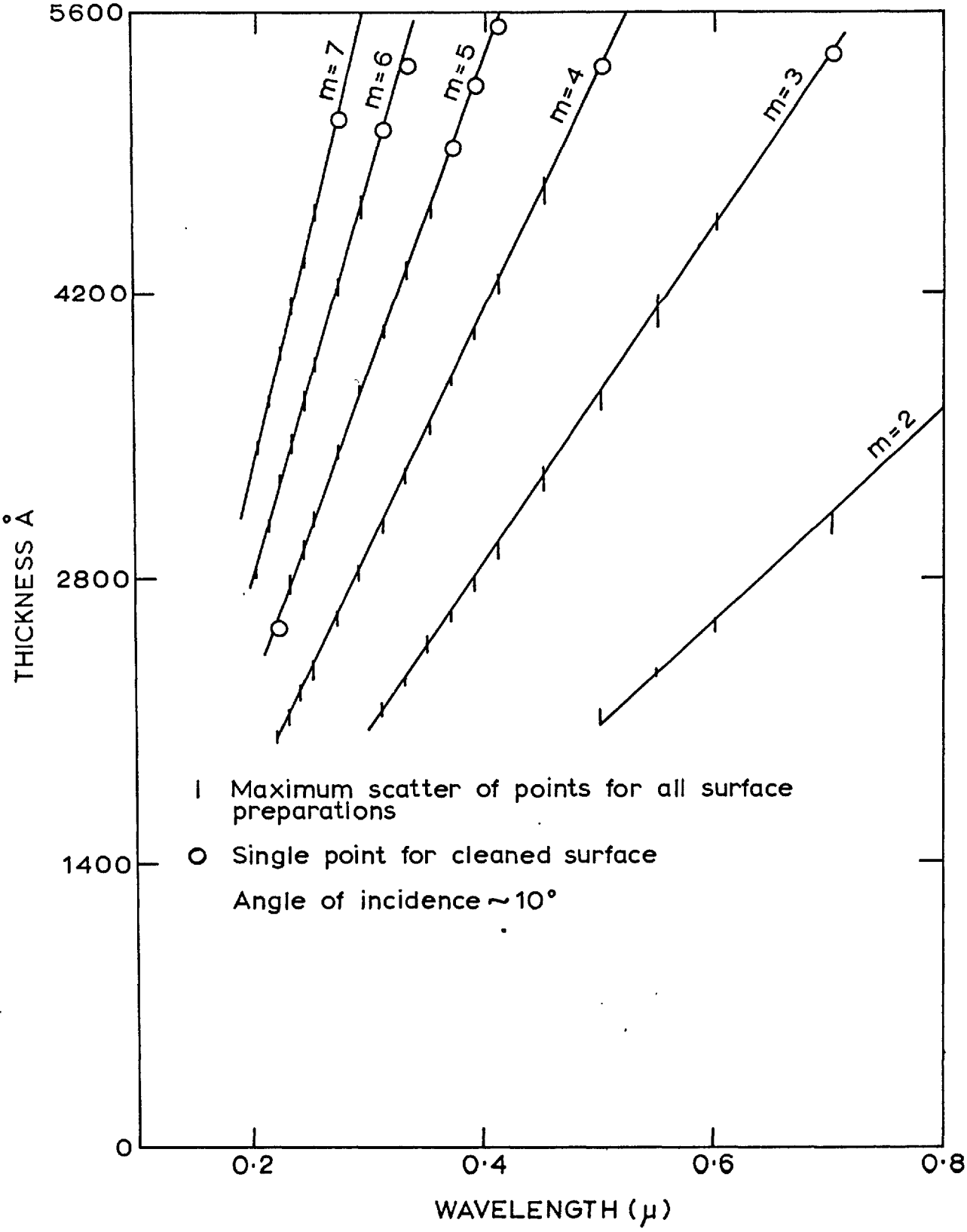

Fig.28. Thickness versus reflectivity minimum for anodized Al surfaces

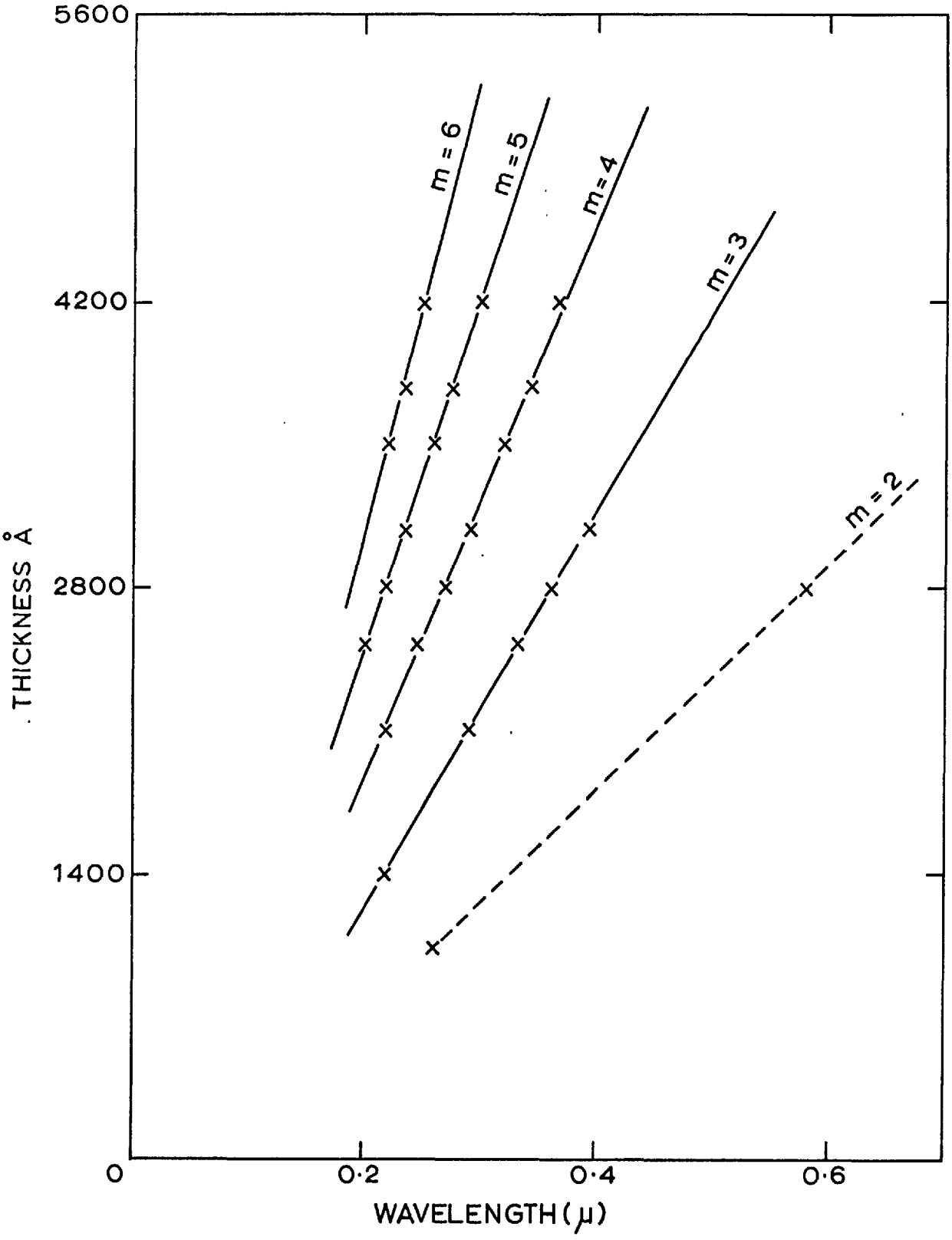

Fig.29. Thickness versus reflectivity for anodized Al surfaces (angle of incidence ~45°)

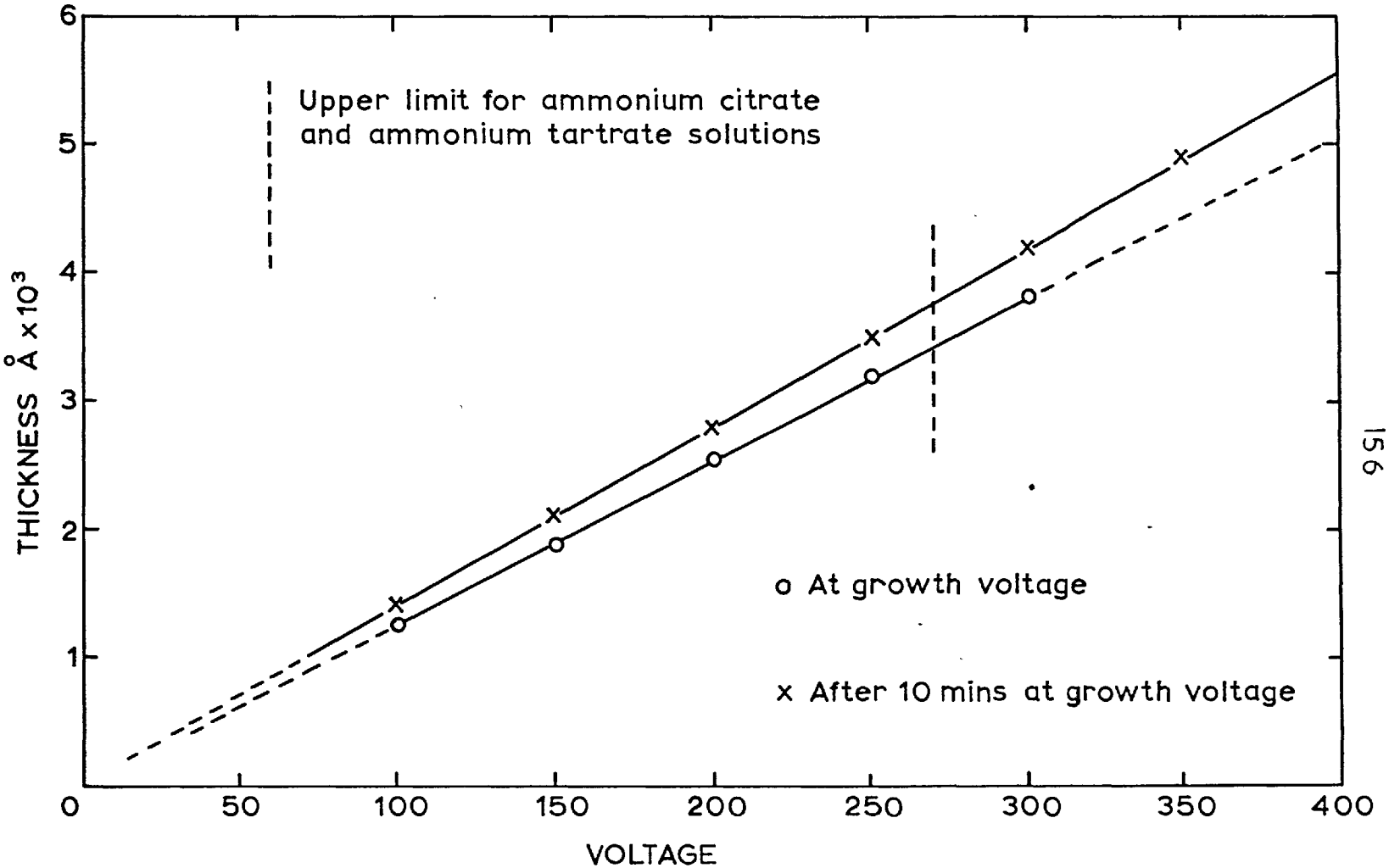

Fig.30. Optical thickness versus anodizing voltage (1·0mA/cm²) employing prepared surfaces (30g/l ammonium borate pH 9)

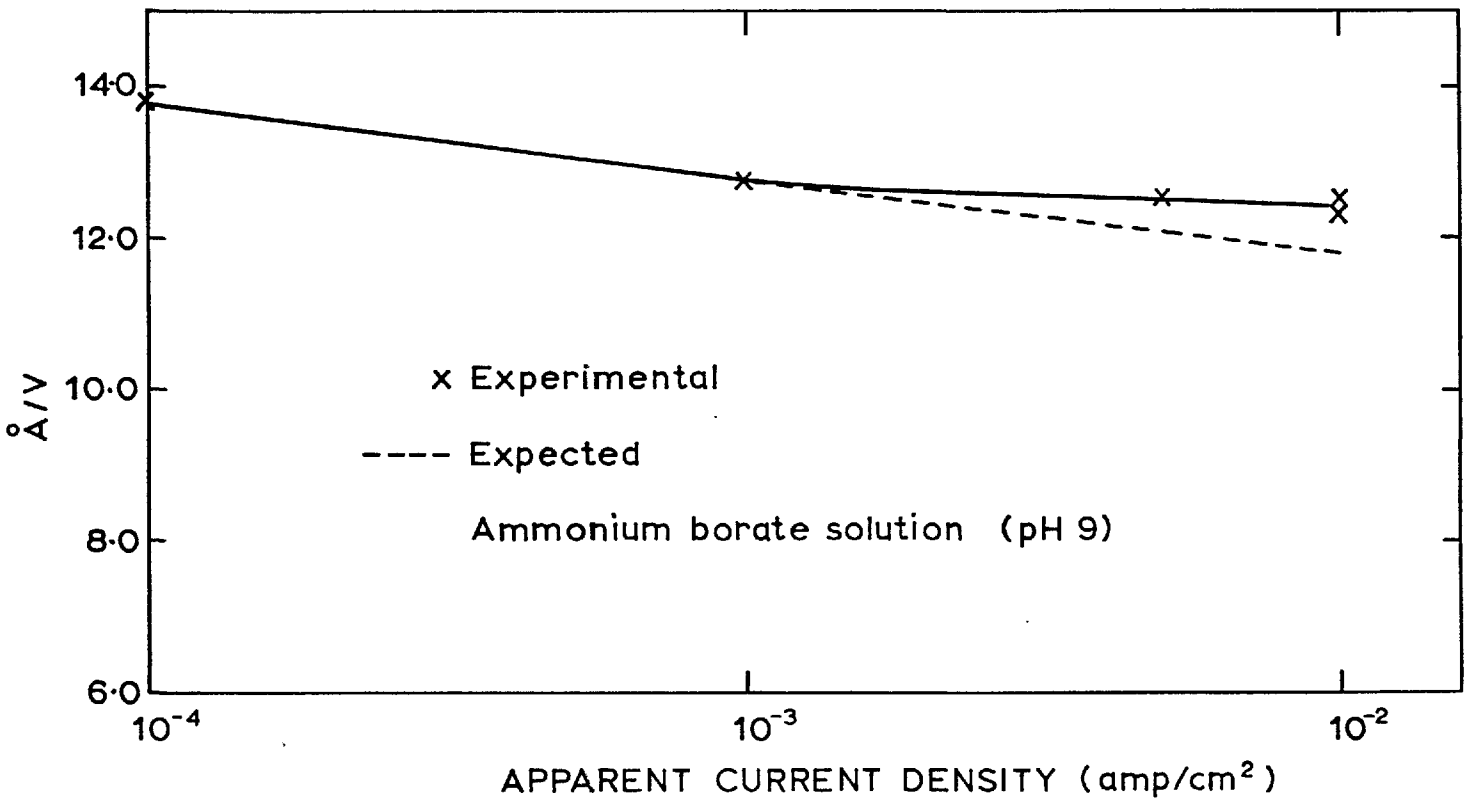
14·0
12·0
10·0
8·0
6·0
Å/V
x Experimental
---- Expected
Ammonium borate solution (pH 9)
10^{-4}
10^{-3}
10^{-2}
APPARENT CURRENT DENSITY (amp/cm²)

FIG.31.

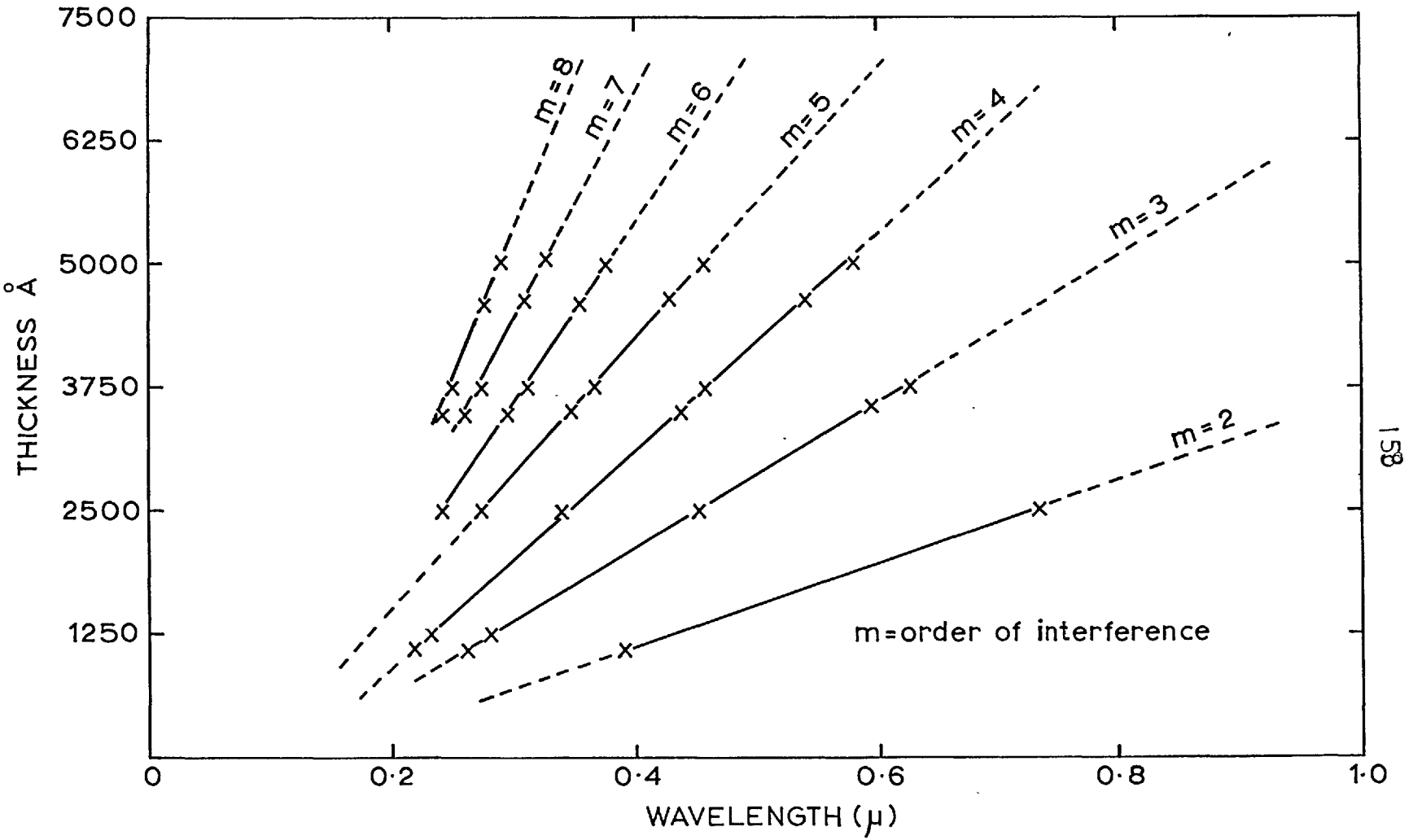

Fig.32. Thickness versus reflectivity minimum for anodized zirconium (angle of incidence ~45°)

Fig.33.

Magnification (950x).Reflection electron micrograph of 300 volts anodic alumina film formed on an etched (NaOH) aluminium foil, showing (a) upper dark part; film on the metal (b) lower white part; film stripped off the metal. (30 g/l ammonium borate, pH9, 1mA/cm^2, at voltage for 10 minutes)

Fig.34.

Magnification (36,300x) Transmission electron micrograph of 50 volts anodic alumina film formed on an etched (NaOH) aluminium foil (30 g/l ammonium borate pH9, 1mA/cm^2, at voltage for 10 minutes), showing globular features characteristic of the chemical etch.

Fig.35.

Magnification (19,200x); Transmission electron micrograph of anodic alumina film (same as in Fig.34) showing arrangement of globular features at a rolling line of the foil.

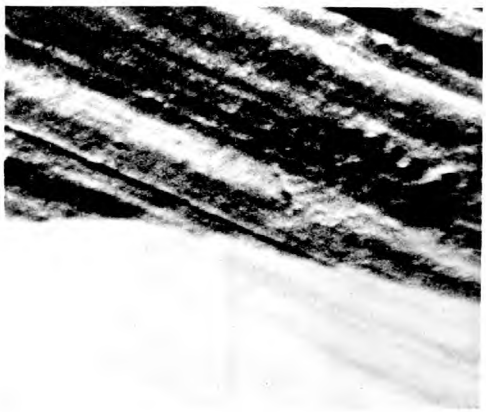

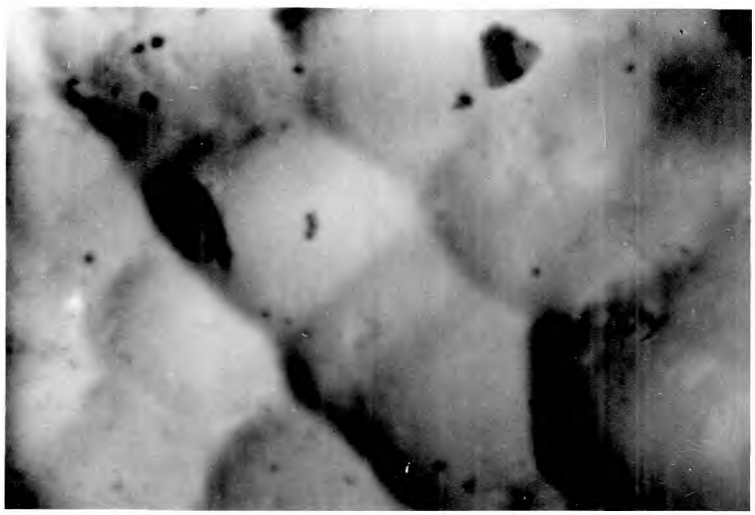

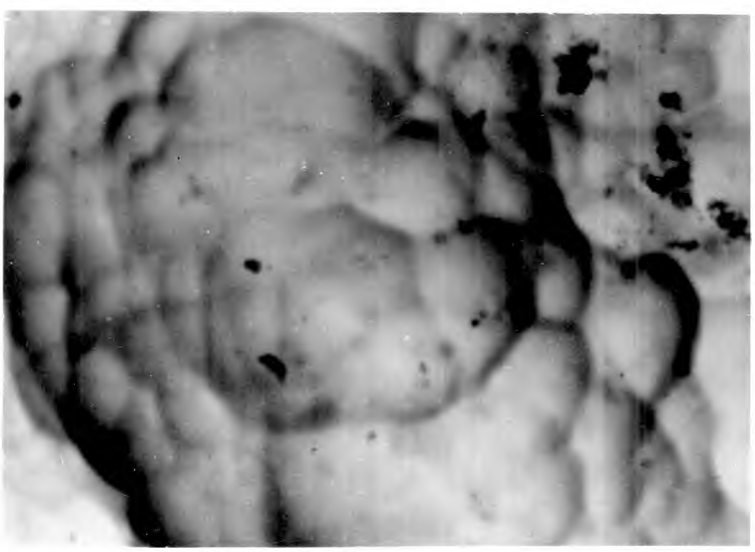

Fig.36.

Magnification (75,000x); Transmission electron micrograph of 75 volts anodic alumina film formed on an electropolished (Chromic - phosphoric - sulphuric acids) aluminium foil (30 g/l ammonium borate, pH9, 1mA/cm^2 at voltage for 10 minutes) showing hexagonal cell pattern, characteristic of the **electropolishing bath.**

Fig.37.

Magnification (75,000x); Transmission electron micrograph of 50 volts anodic alumina film formed on an electropolished (perchloric acid - ethyl alcohol) specimen, showing pore - type features and some right through pores. (the growth conditions, same as for the above films).

Fig.38.

Magnification (75,000x); Transmission electron micrograph of 75 volts anodic alumina film formed on an air - annealed (350^{o}C, 60 mins.,) aluminium foil, showing (a) pores and (b) crystalline spots (the growth conditions same as for the above films).

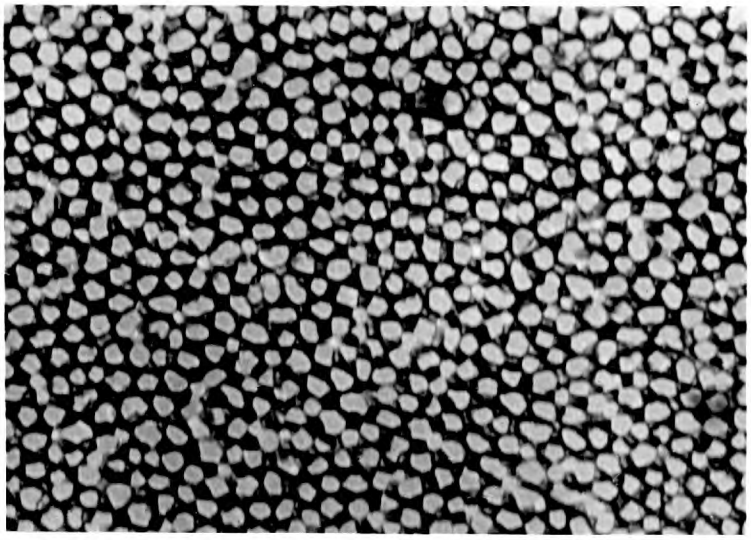

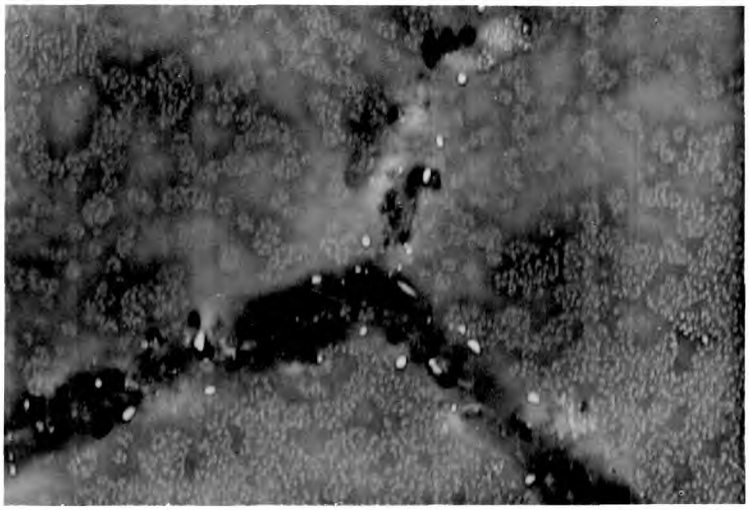

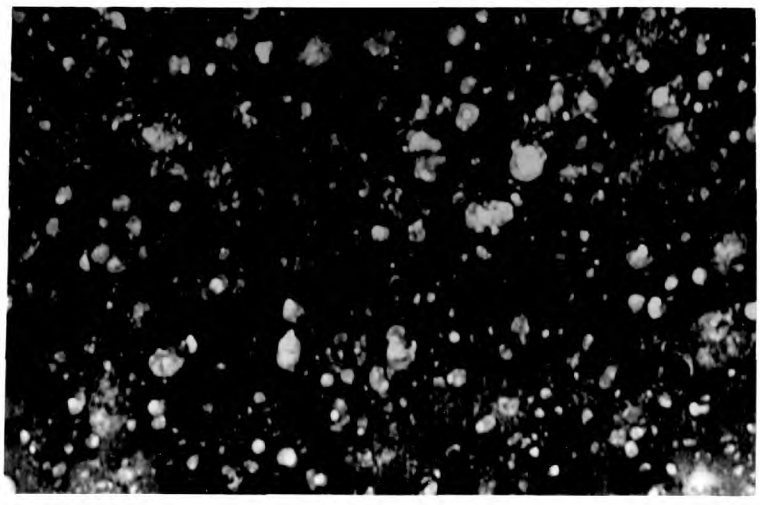

Fig.39.

Magnification (15,000x); Transmission electron micrograph of 150 volts anodic alumina film formed on an electropolished (perchloric acid - ethyl alcohol) specimen, showing initial growth of crystallites. (the formation conditions same as for previous films).

Fig.40.

Magnification (9,000x); Transmission electron micrograph of 100 volts anodic alumina film formed on an electropolished (perchloric acid - ethyl alcohol) specimen, showing crystallites formation (the oxide film formed in 3% tartaric acid, pH 5.5, $1mA/cm^2$, 10 mins. at voltage)

Fig.41.

Magnification (15,000x); Transmission electron micrograph of 150 volts anodic alumina film formed on an etched (NaOH) foil, showing random distribution and enhanced growth of crystallites (30 g/l ammonium borate, pH 9.0, $1mA/cm^2$, 10 minutes at voltage)

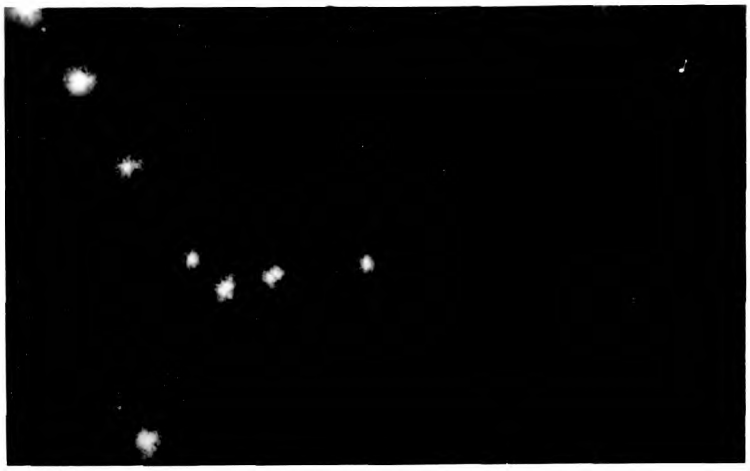

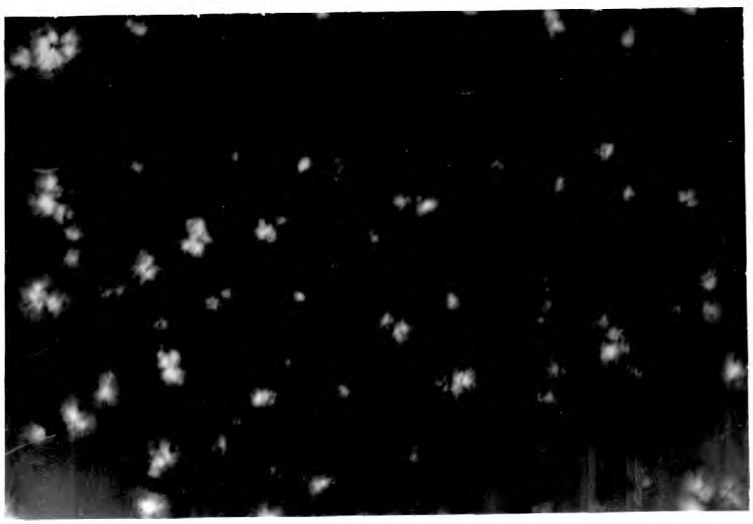

Fig.42.

Magnification (3,750x); Transmission electron micrograph of 250 volts anodic alumina film formed on an electropolished (perchloric acid - ethyl alcohol) specimen. (The film thinned about 10% in pH 9.7 buffer solution) showing enhanced growth of crystallites at the sites corresponding to the original grain boundaries of the metal. (30 g/l ammonium borate pH 9.0, 1mA/cm^2, 10 minutes at voltage)

Fig.42A.

Magnification (3,600x); Transmission electron micrograph of 300 volts anodic alumina film formed as the above film, showing growth of crystallites above some grains of the metal.

Fig.43.

Magnification (19,200x); Transmission electron micrograph of the film as in Fig.42., at high magnification.

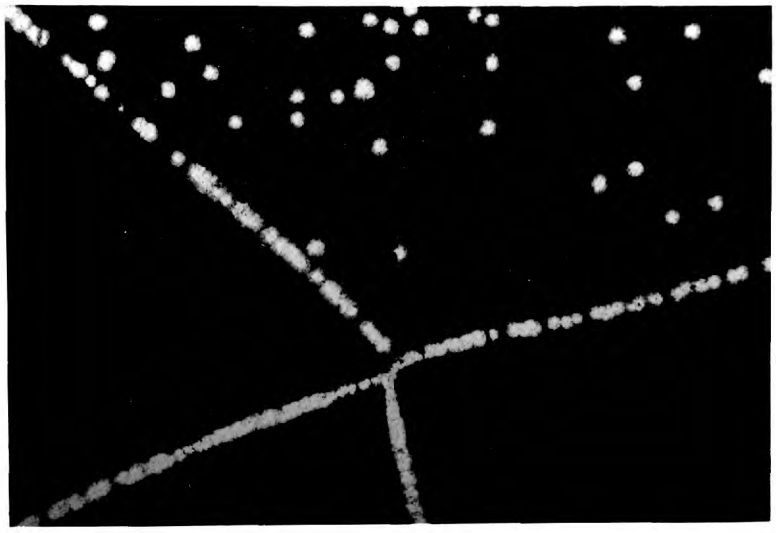

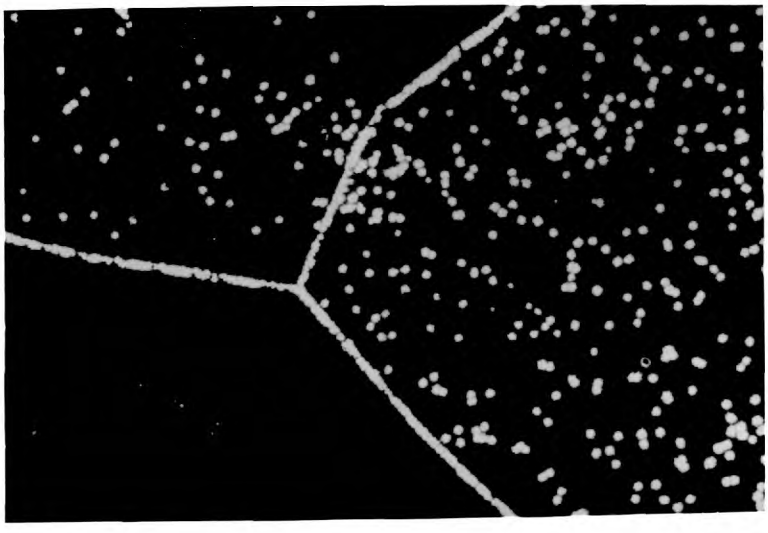

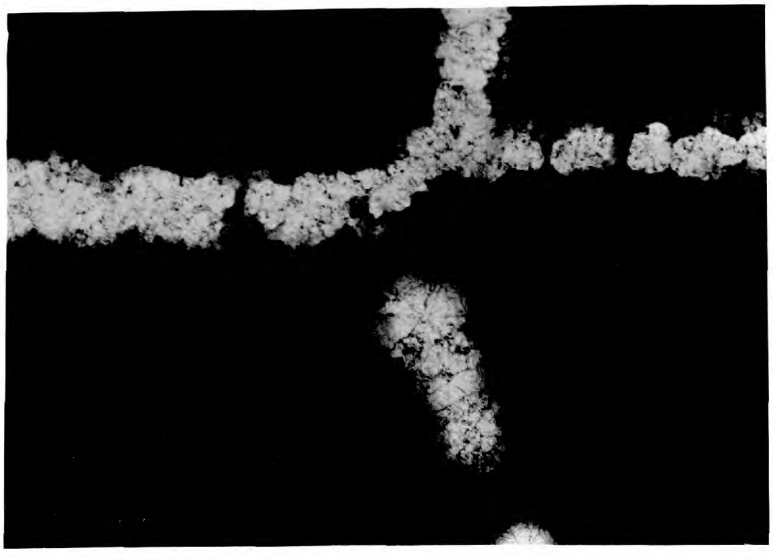

Fig.44.

Magnification (60,000x); Transmission electron micrograph of the film as in Fig.39. at high magnification, showing the initial structure of the crystallites.

Fig.45.

Magnification (32,000x); Transmission electron micrograph of 300 volts anodic alumina film formed on an etched (NaOH) foil, (The film thinned about 15% in pH 9.7 buffer solution) showing structure of crystallites with increased thickness of the film. (The conditions of film growth came as for the above film in Fig.44).

Fig.46.

Magnification (19,200x); Transmission electron micrograph of the film examined in Fig.42.

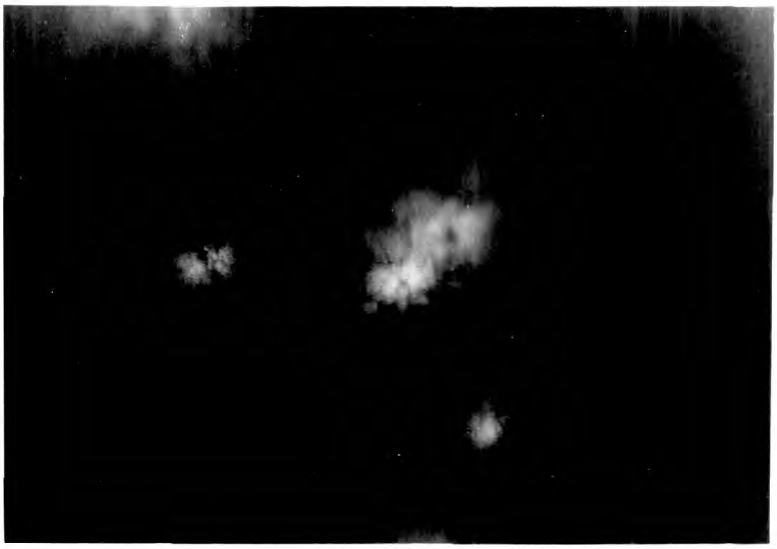

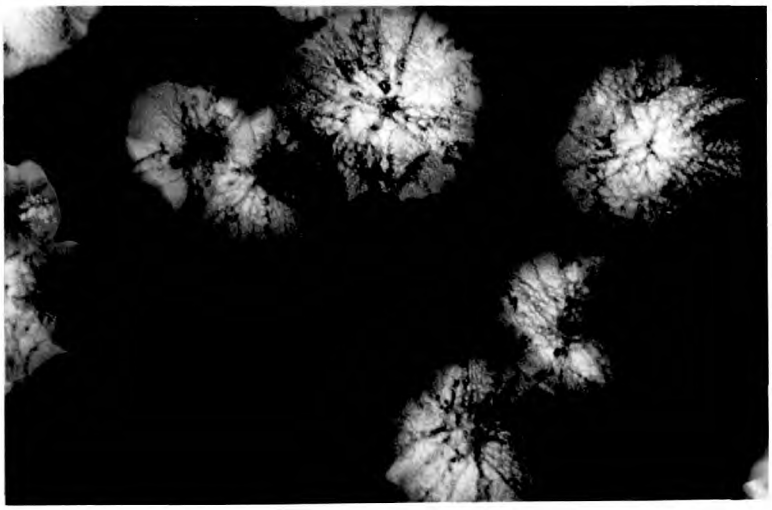

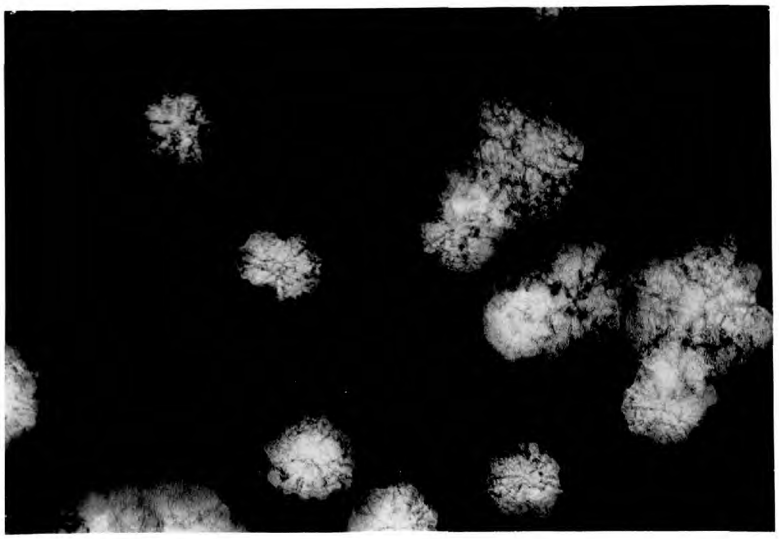

Fig.47.

Magnification (109,300x); Transmission electron micrograph for the film examined in Figs.42 and 46, showing a single crystalline spot.

Fig.48.

Transmission electron diffraction pattern for the 50 volts anodic alumina film examined in Figs.34 and 35.

Fig.49.

Selected area transmission electron diffraction pattern for the 250 volts film examined in Figs.42 and 43.

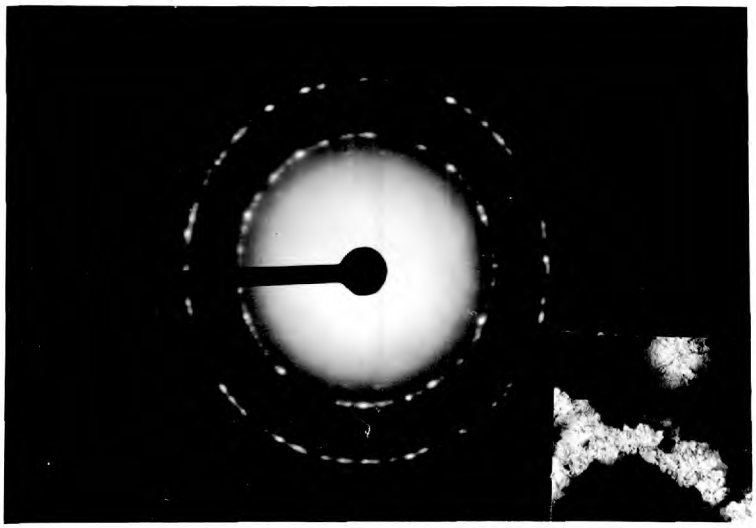

Fig.50.

Slected area transmission electron diffraction pattern for 300 volts anodic alumina formed on an etched specimen (NaOH). (Film thinned down about 20% in pH 9.7 buffer.) The film was originally formed in 30 g/l ammonium borate, $1mA/cm^2$, 10 minutes at voltage.

Fig.51.

A general transmission electron diffraction pattern 300 volts anodic alumina film formed as above and thinned about 40% in pH 9.7 buffer solution, by immersing the stripped oxide window in the solution.

Fig.52.

Magnification (30,000x); Transmission electron micrograph of the film examined in Fig.51, showing pores developed at the crystalline spots within the amorpheus bulk oxide.

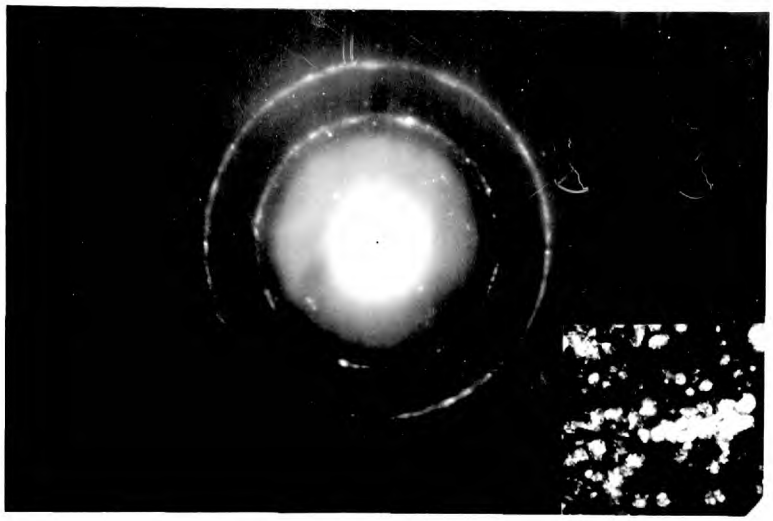

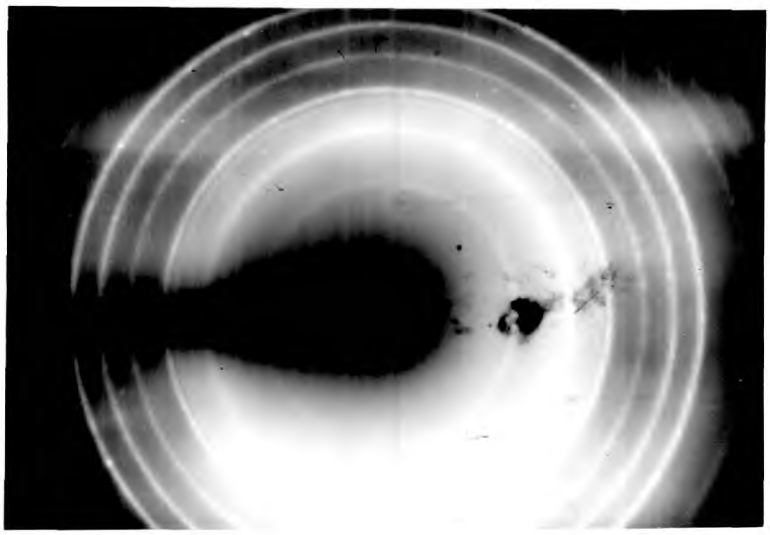

Fig.53.

Magnification (30,000x); Transmission electron micrograph of 300 volts anodic alumina film thinned down in pH 9.7 buffer solution, showing the development of pores due to thinning. (The film was formed on an etched specimen).

Fig.54.

Magnification (75,000x); Transmission electron micrograph of 300 volts anodic alumina film formed on an electropolished (perchloric acid - ethyl alcohol) specimen, showing pores due to thinning in pH 9.7 buffer solution. An oxide "window" was used as for all other thinning experiments.

Fig.55.

Magnification (30,000x); Transmission electron micrograph of 300 volts anodic alumina film formed on an electropolished (perchloric acid - ethyl alcohol) specimen and thinned down after stripping in potassium chromate solution pH 13.

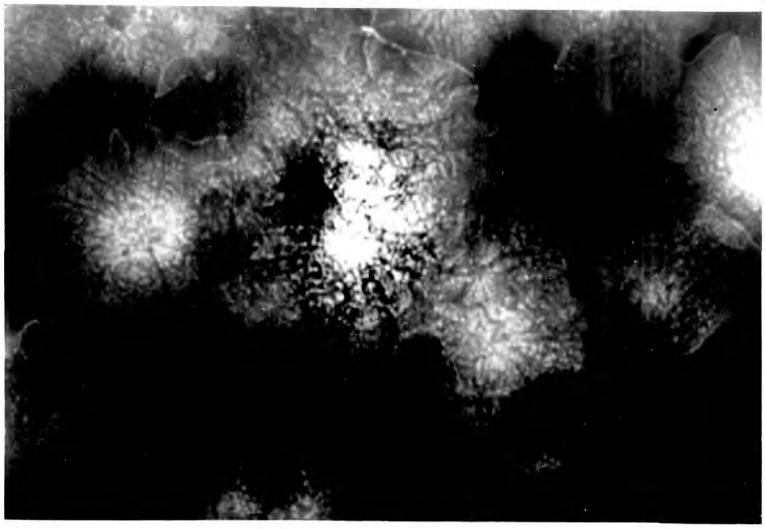

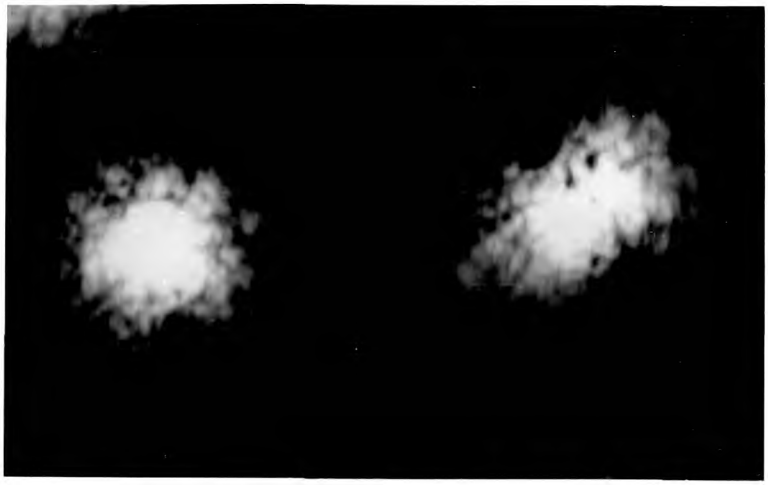

Fig.56.

Magnification (3,000x); Transmission electron micrograph of 300 volts anodic film formed on an etched (NaOH) specimen and thinned for about two minutes in the chromic - phosphoric acids mixture at 80°C after stripping it off the metal base. (The film was originally formed in 30 g/l ammonium borate solution pH 9.0 at $1mA/cm^2$ for 10 minutes at voltage). Thickness loss as indicated by spectrophotometry was about 25%.

Fig.57.

Magnification (15,000x); Transmission electron micrograph of the film as above at high magnification.

Fig.58.

Magnification (30,000x); Transmission electron micrograph of 200 volts anodic alumina film formed on an etched specimen (NaOH) and thinned down for about two minutes as above, after stripping it off the metal base. (The film was originally formed in 3.0% tartaric acid solution pH 5.5) Spectrophotometric measurement indicated about 30% loss of thickness.

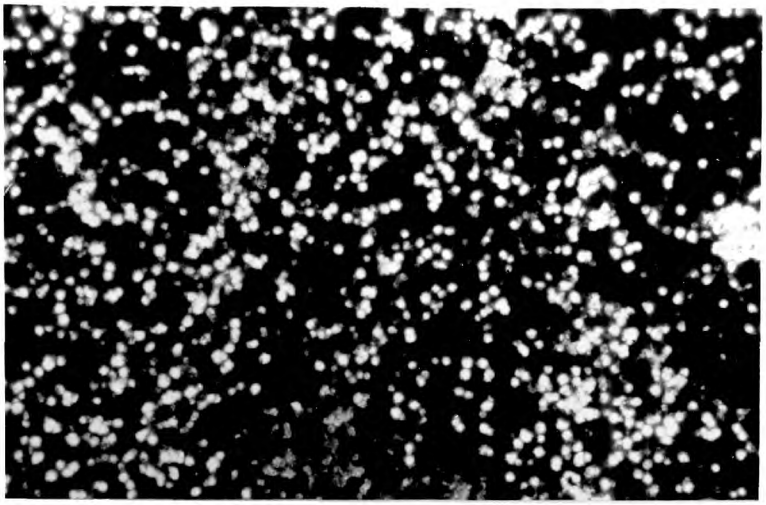

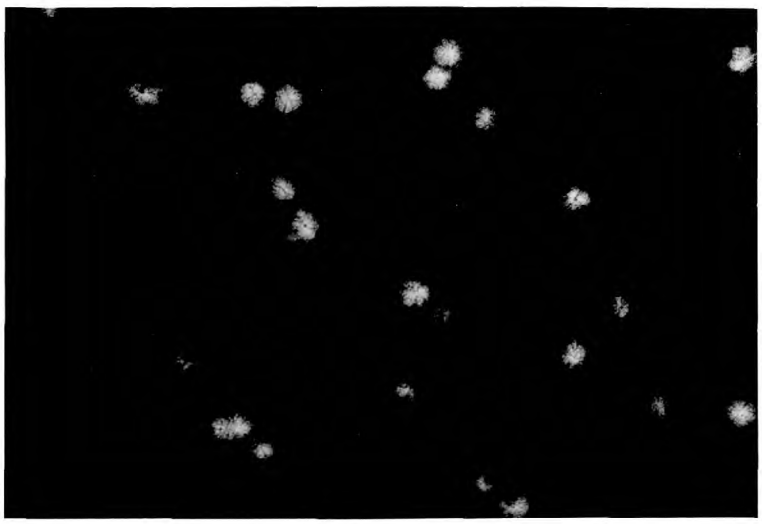

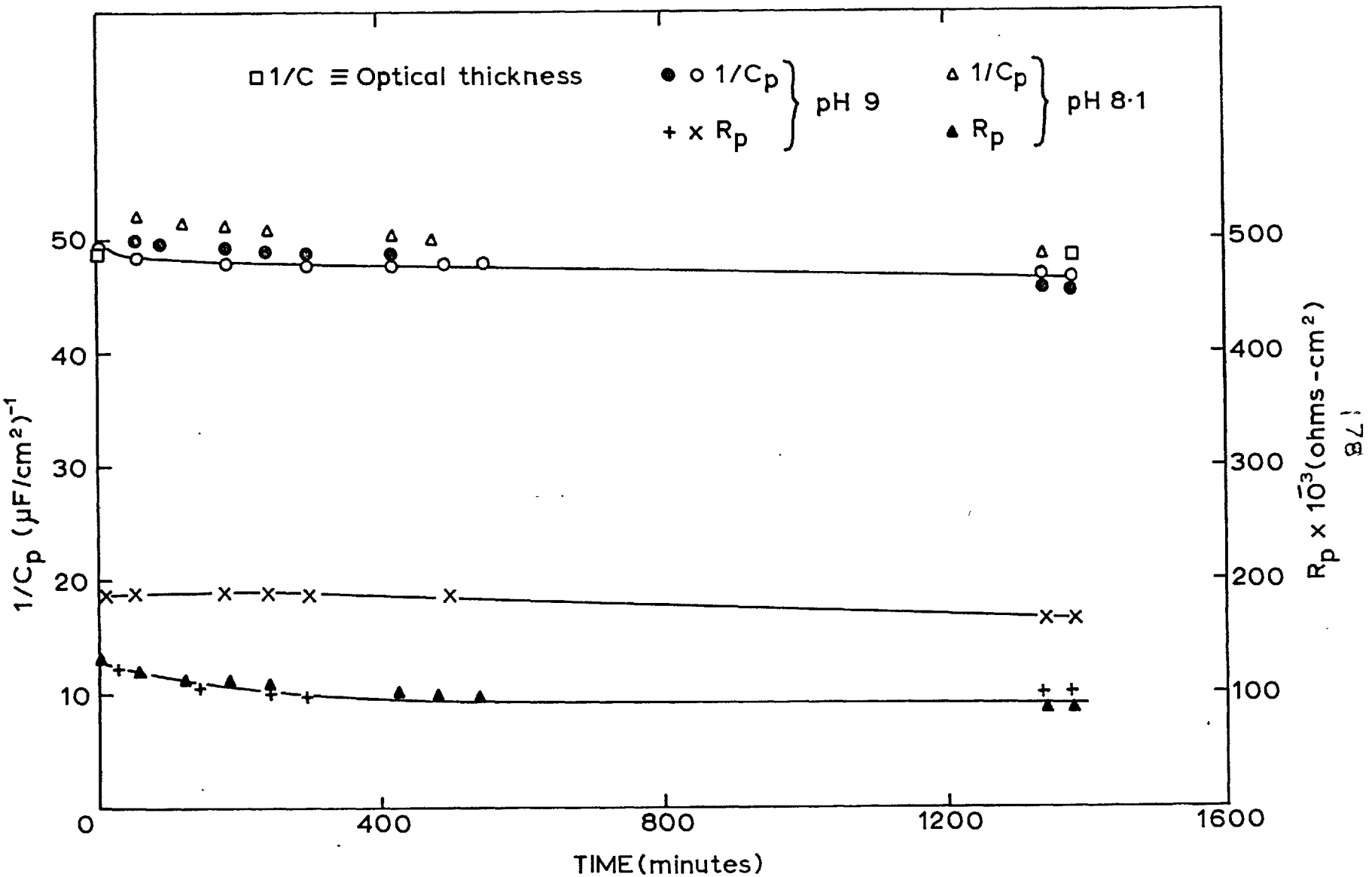

Fig. 59. $1/C_p$ and R_p versus time of immersion of anodized Al in anodizing solution

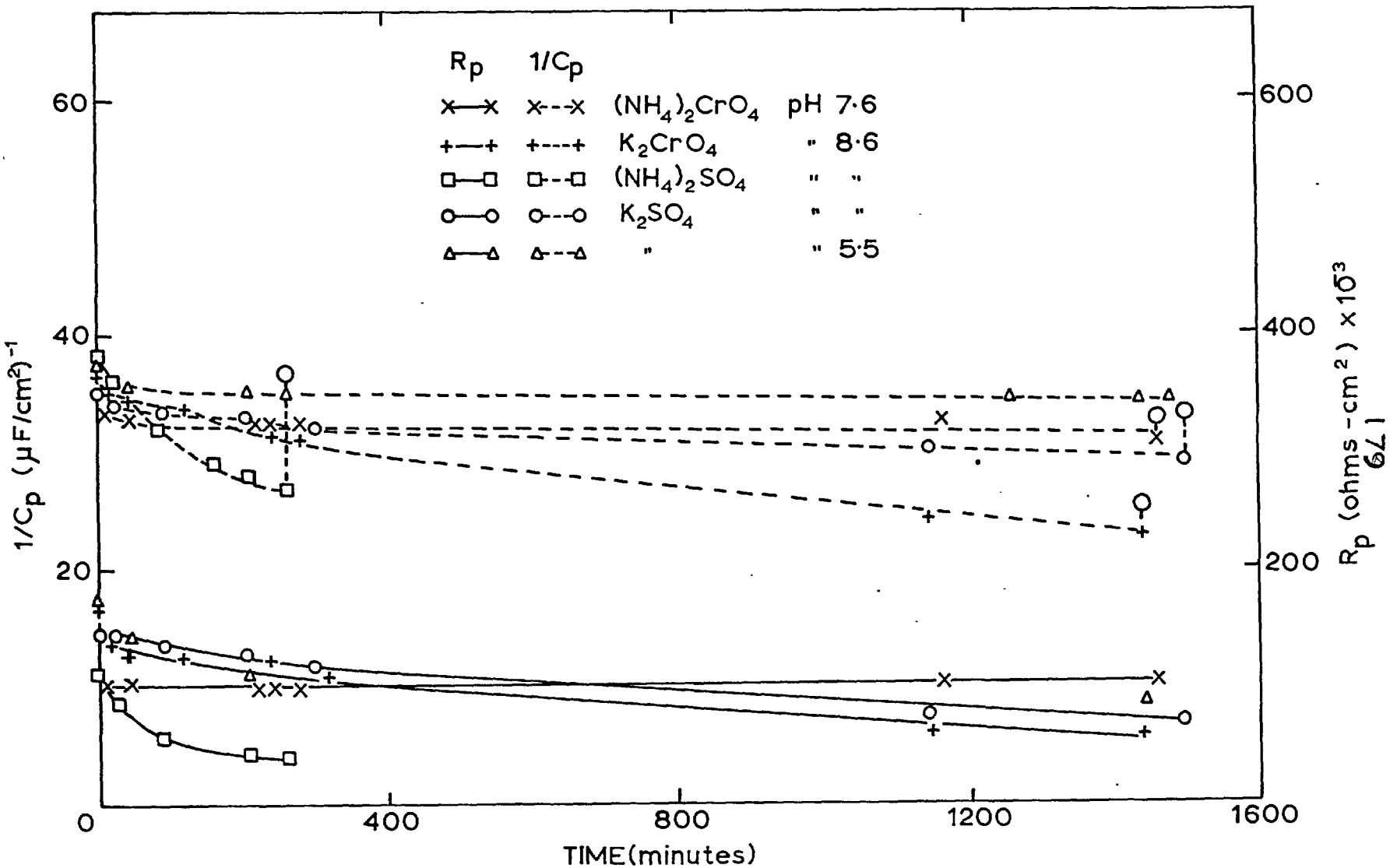

Fig.60. $1/C_p$ and R_p versus time of immersion of anodized Al in 0·1M. CrO_4^{--} and SO_4^{--} solutions pH range 5·5 - 8·6

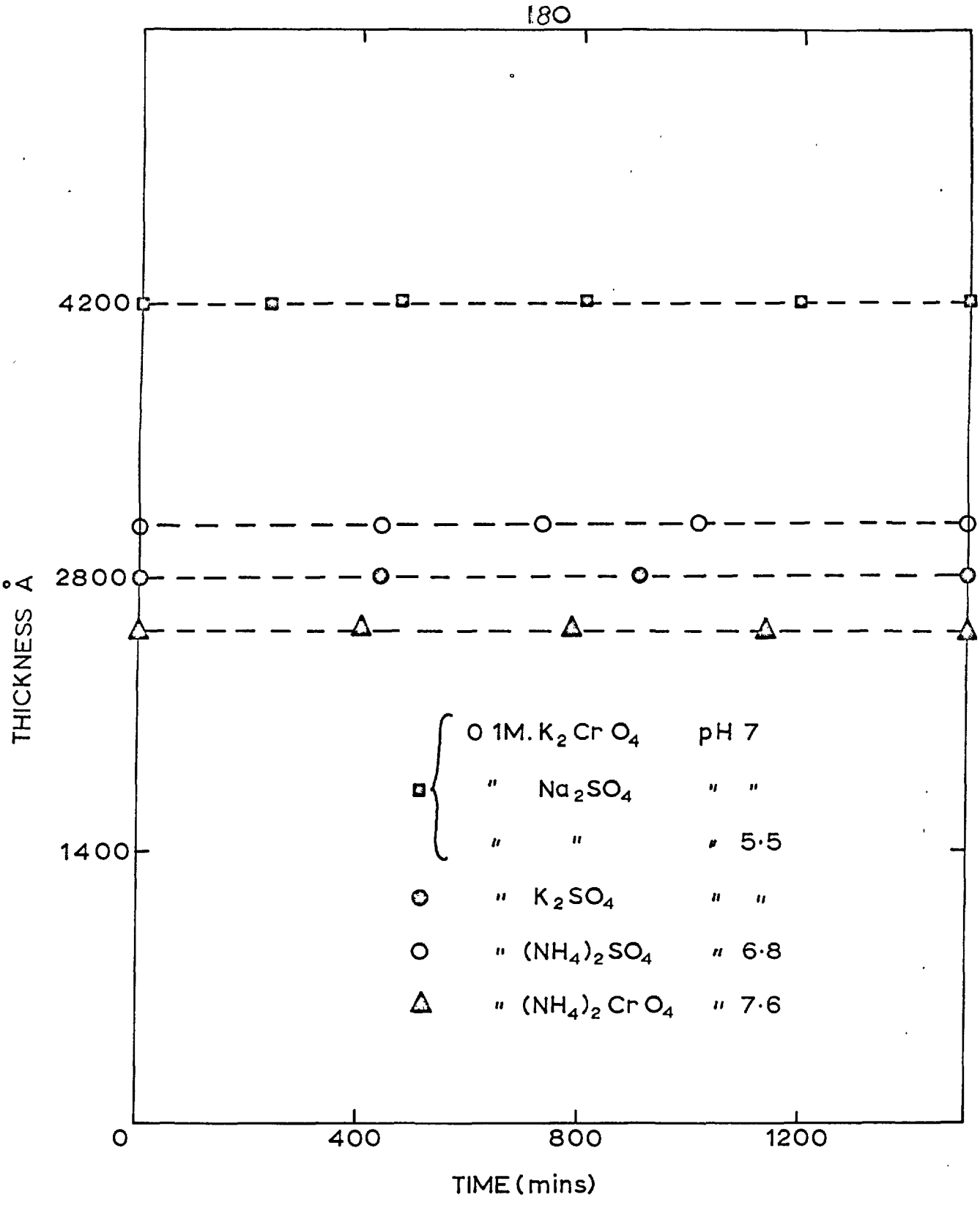

Fig.61. Oxide thickness versus time of immersion in different solutions (pH 5·5-7·6)

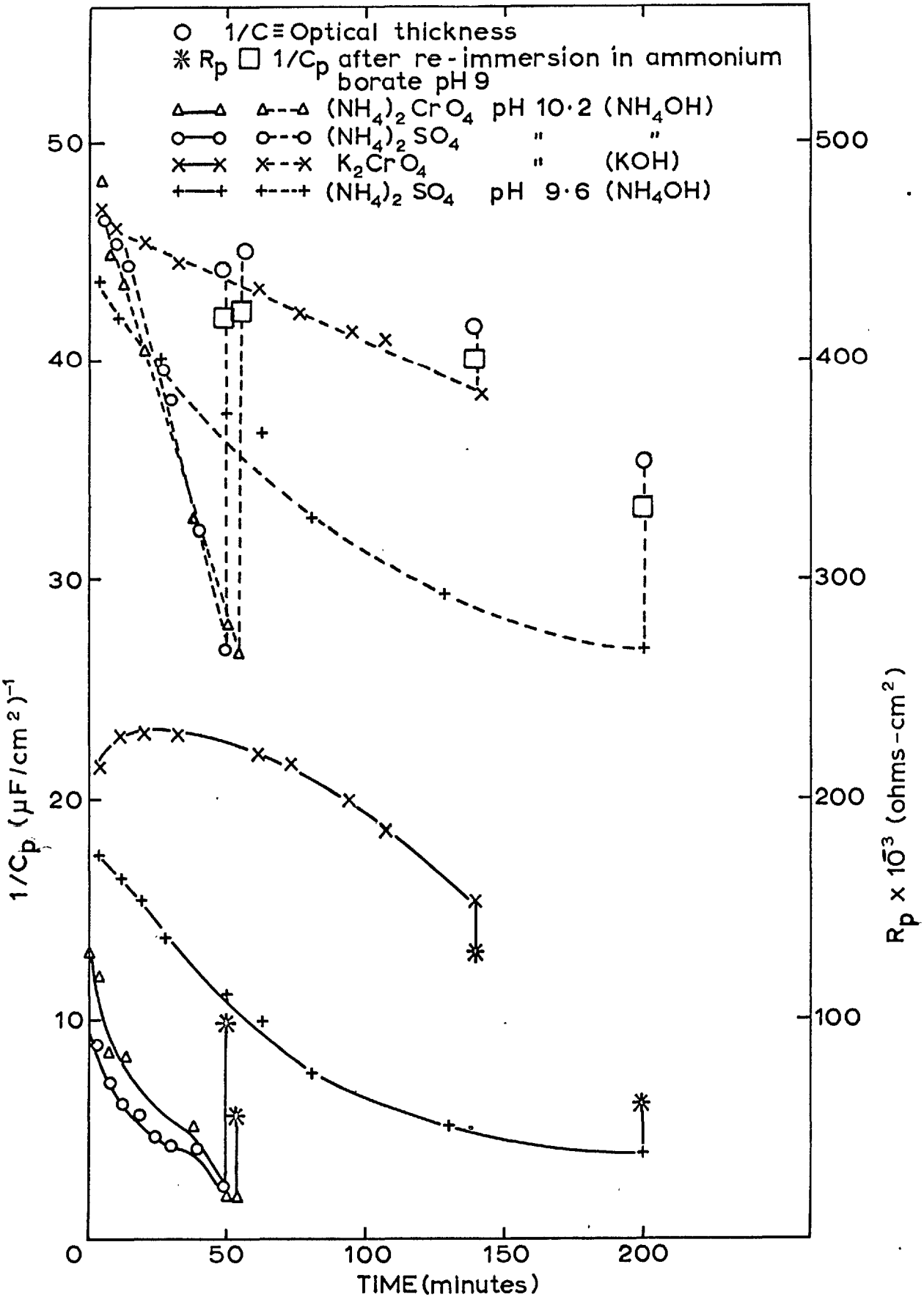

Fig. 62. $1/C_p$ and R_p versus time of immersion in 0·1 M. CrO_4^{--} and SO_4^{--} solutions pH 9·6 and 10·2

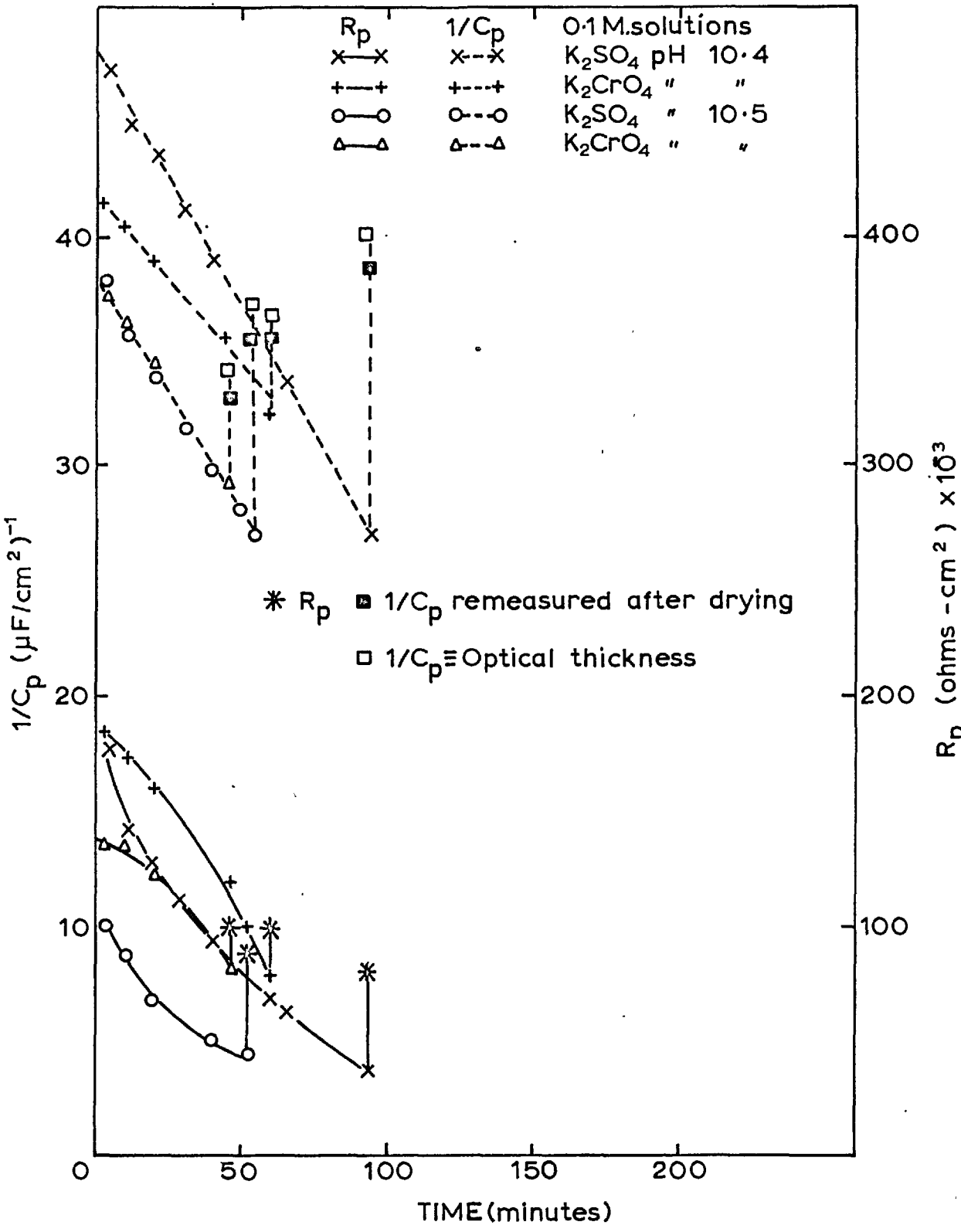

Fig.63. $1/C_p$ and R_p versus time of immersion of anodized Al in K_2CrO_4 and K_2SO_4

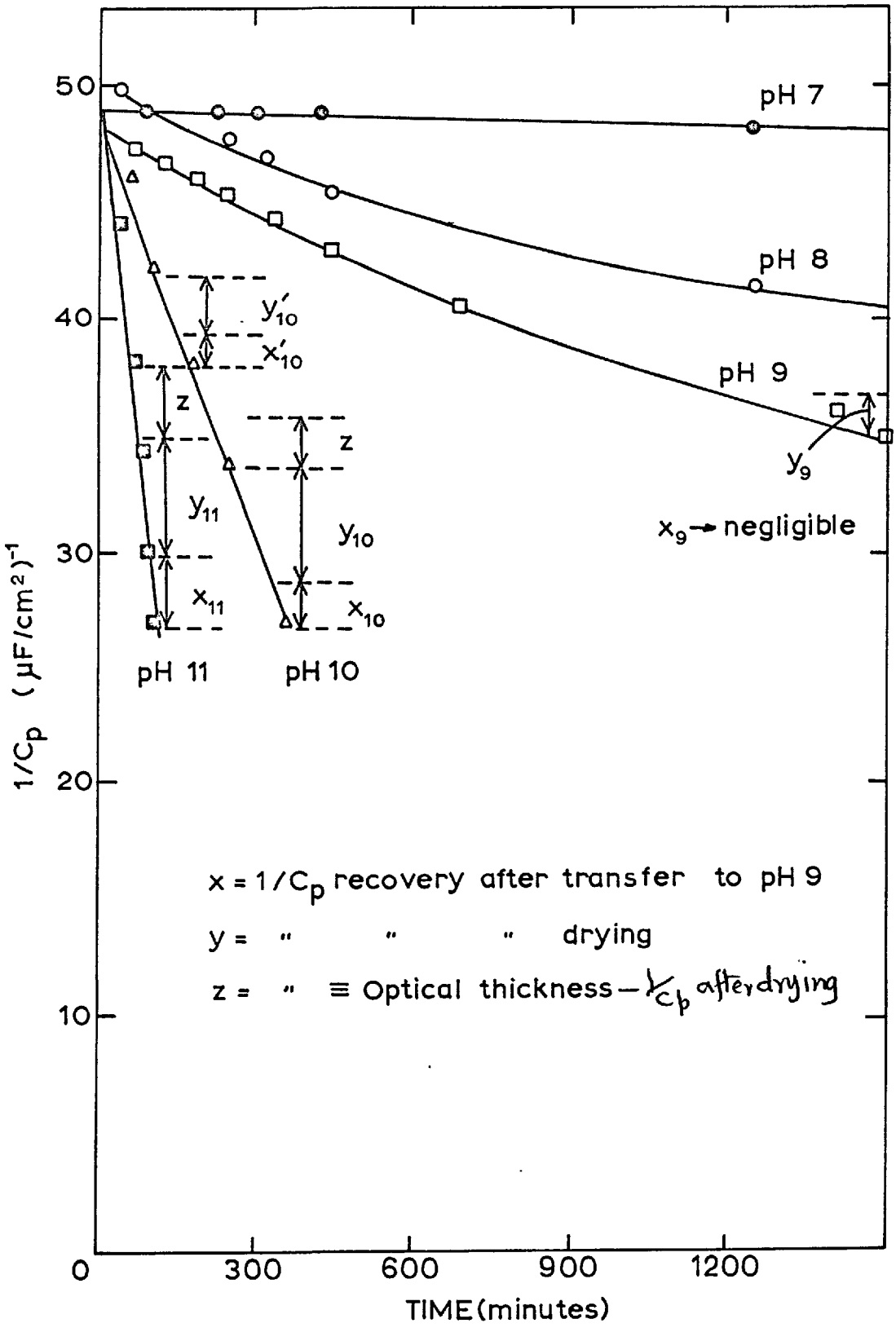

Fig.64. $1/C_p$ versus time of immersion of anodized Al in 0·1M.K_2CrO_4 solutions (pH range 7-11)

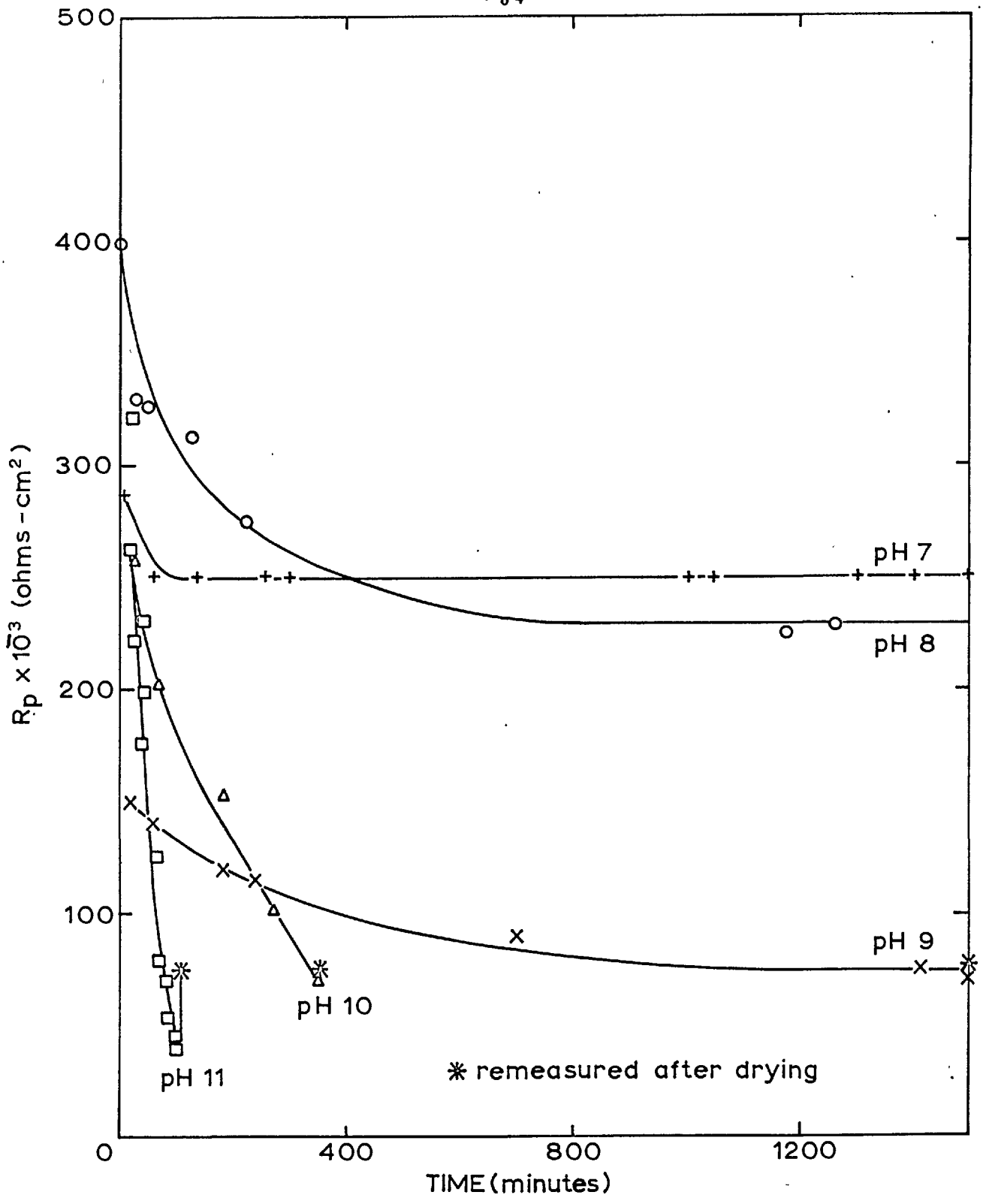

Fig.65. Resistance versus time of immersion of anodized Al in 0·1M. K_2CrO_4 solutions

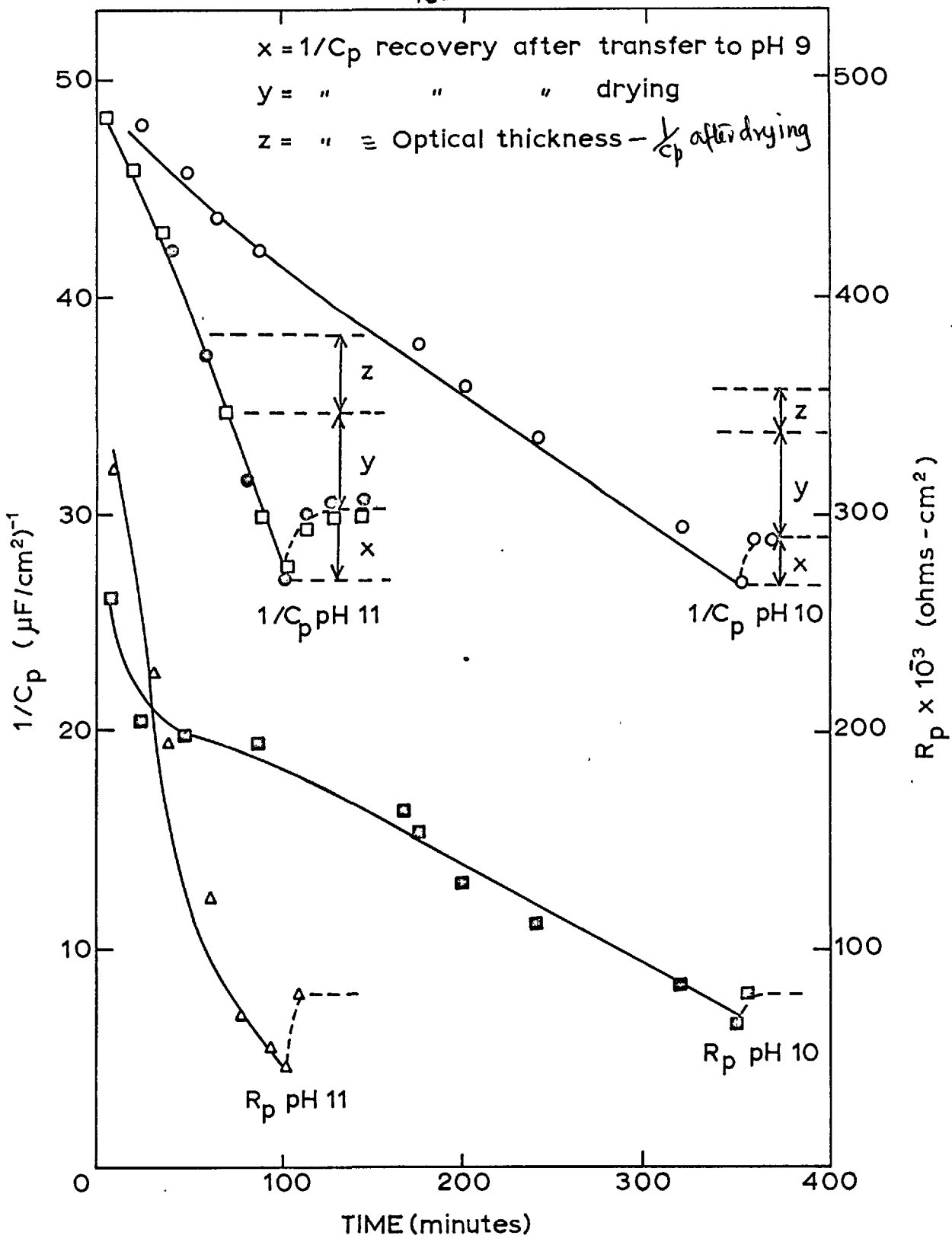

Fig.66. $1/C_p$ and R_p versus time of immersion in 0·1M. K_2CrO_4 solutions.

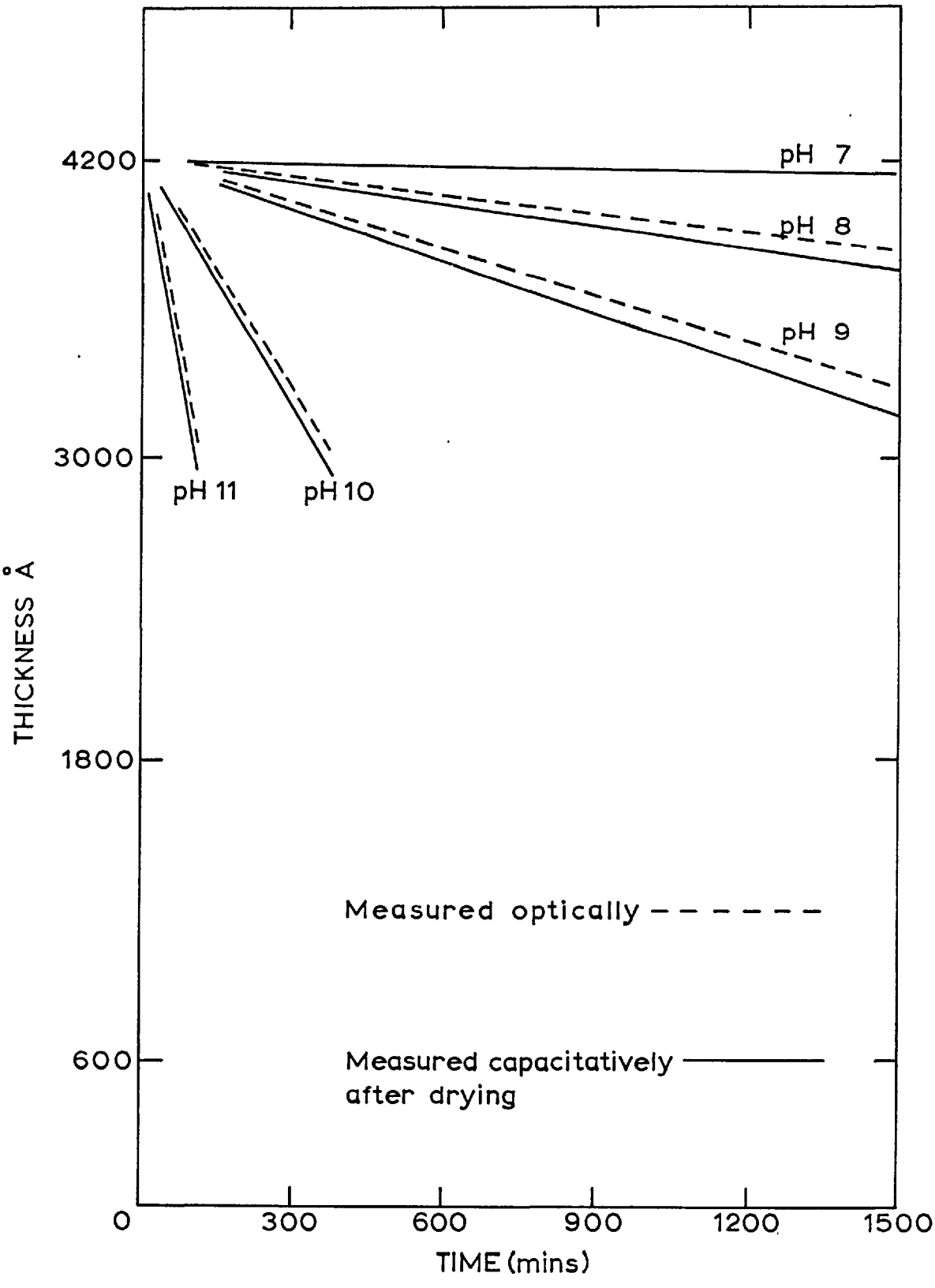

Fig.67. Rate of thinning of alumina film on the metal immersed in 0·1M. K_2CrO_4 at various pH values

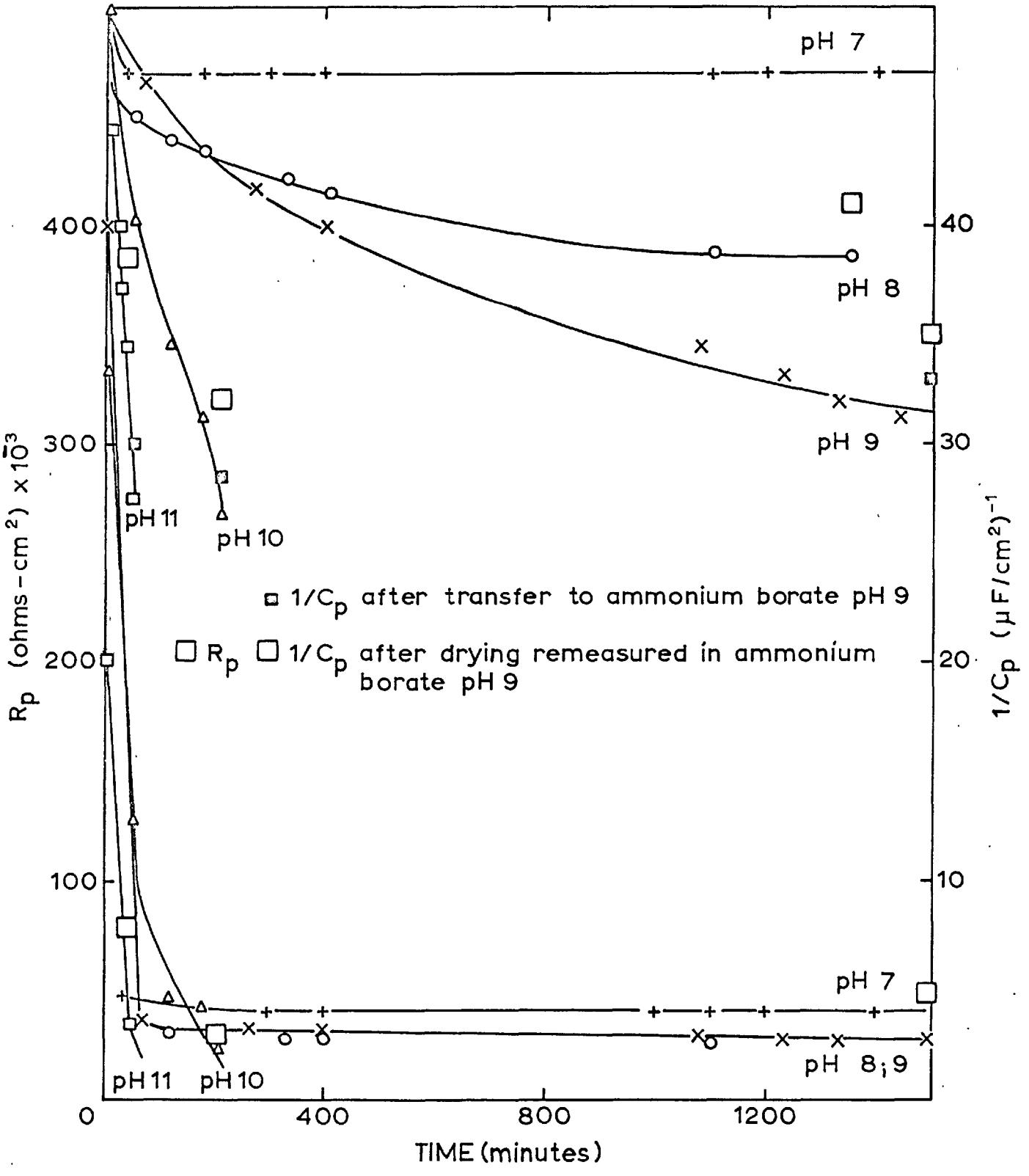

Fig. 68. $1/C_p$ and R_p versus time of immersion in 0·1M.KCl + 0·1M. K_2CrO_4 solution at various pH's for anodized Al

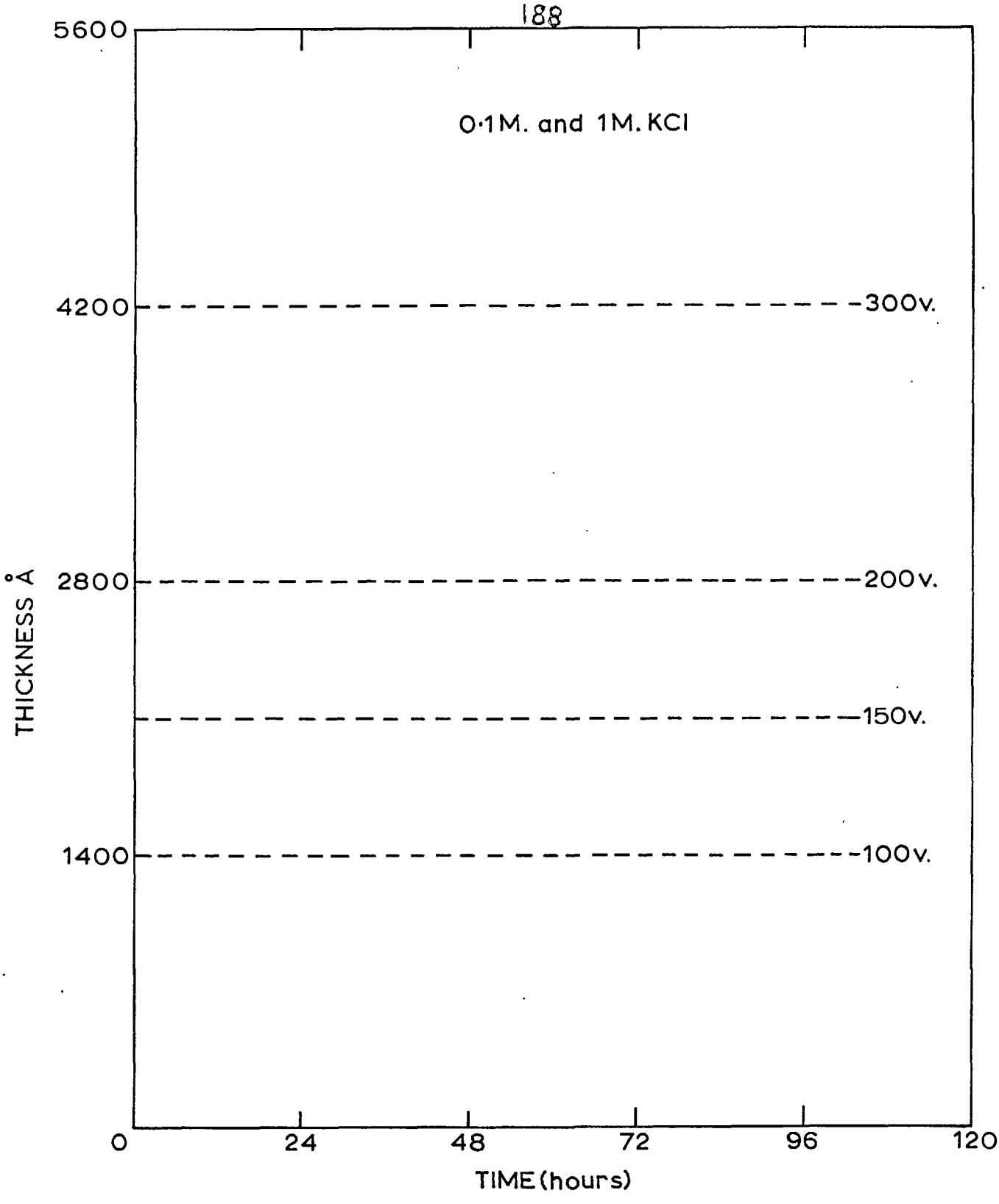

Fig.69. Optical thickness versus time of immersion in KCl solutions for anodized Al

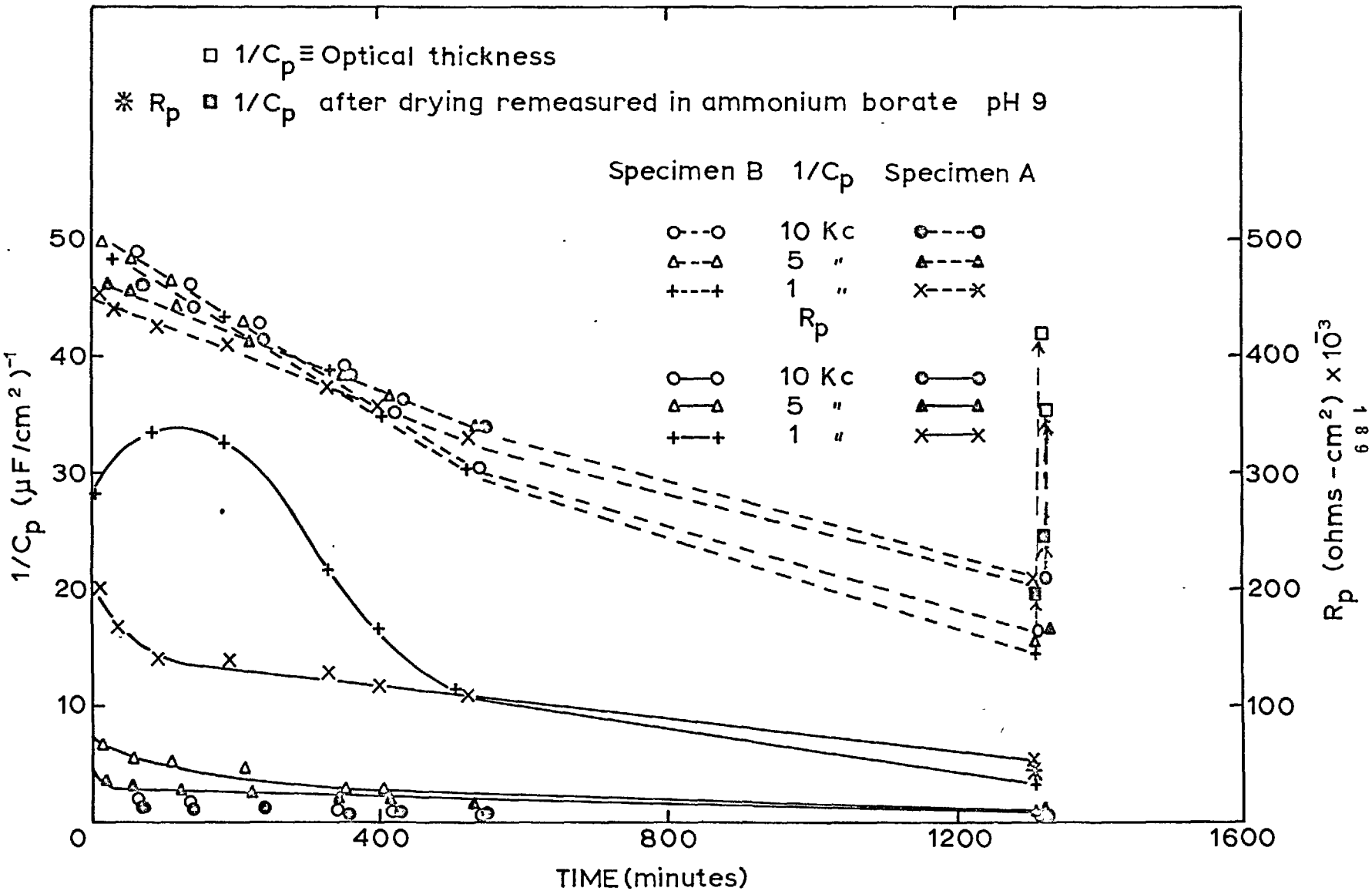

Fig.70. $1/C_p$ and R_p versus time of immersion in pH 9·7 buffer solution at different frequencies.

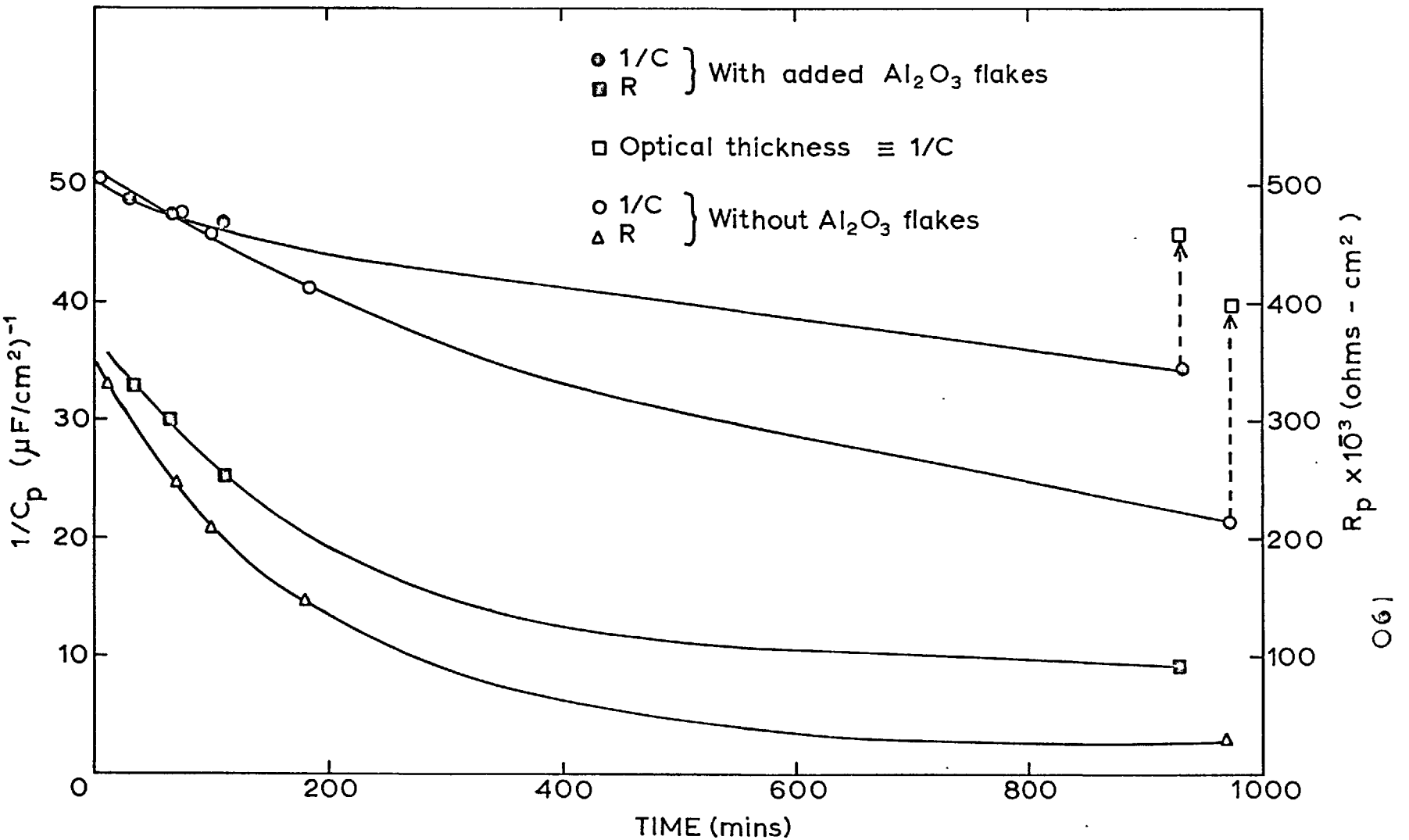

Fig. 71. $1/C_p$ and R_p versus time of immersion of anodized Al in buffer solution pH 9·7

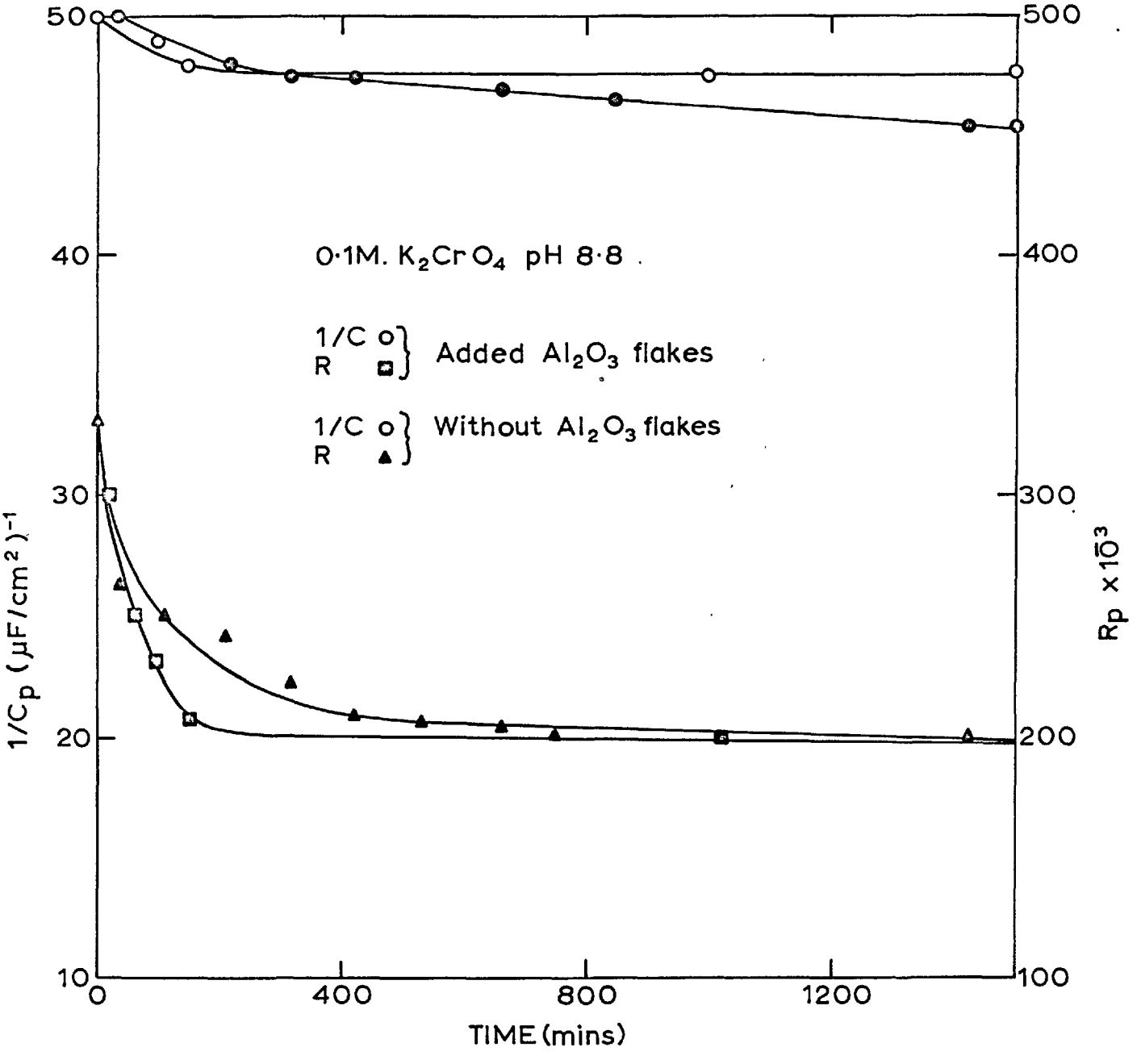

Fig. 72. $1/C_p$ and R_p versus time of immersion in 0·1M. K_2CrO_4 for anodized Al

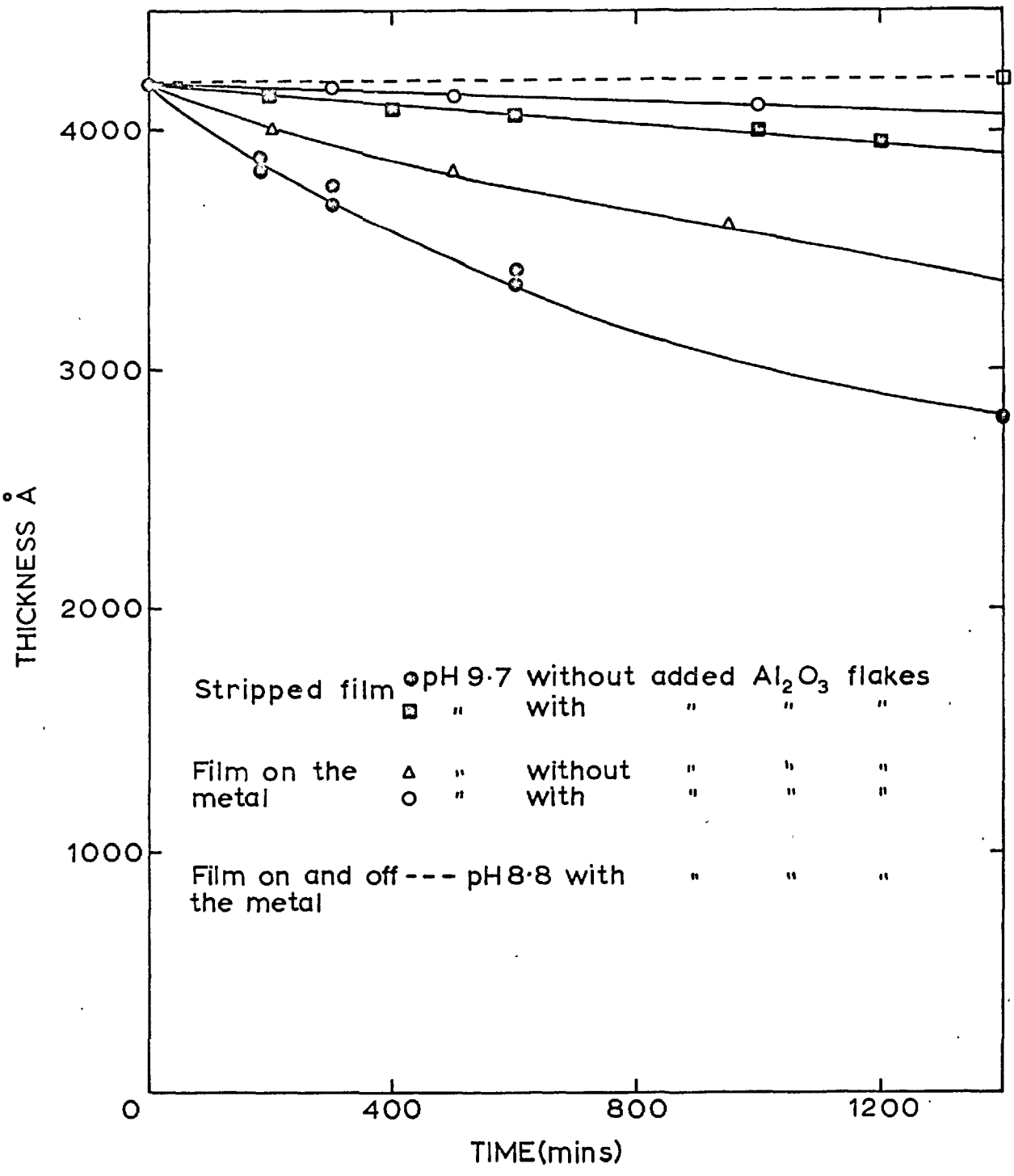

Fig.73. Optical thickness versus time of immersion in pH 8·8 0·1M. K_2CrO_4 and pH 9·7 buffer solutions

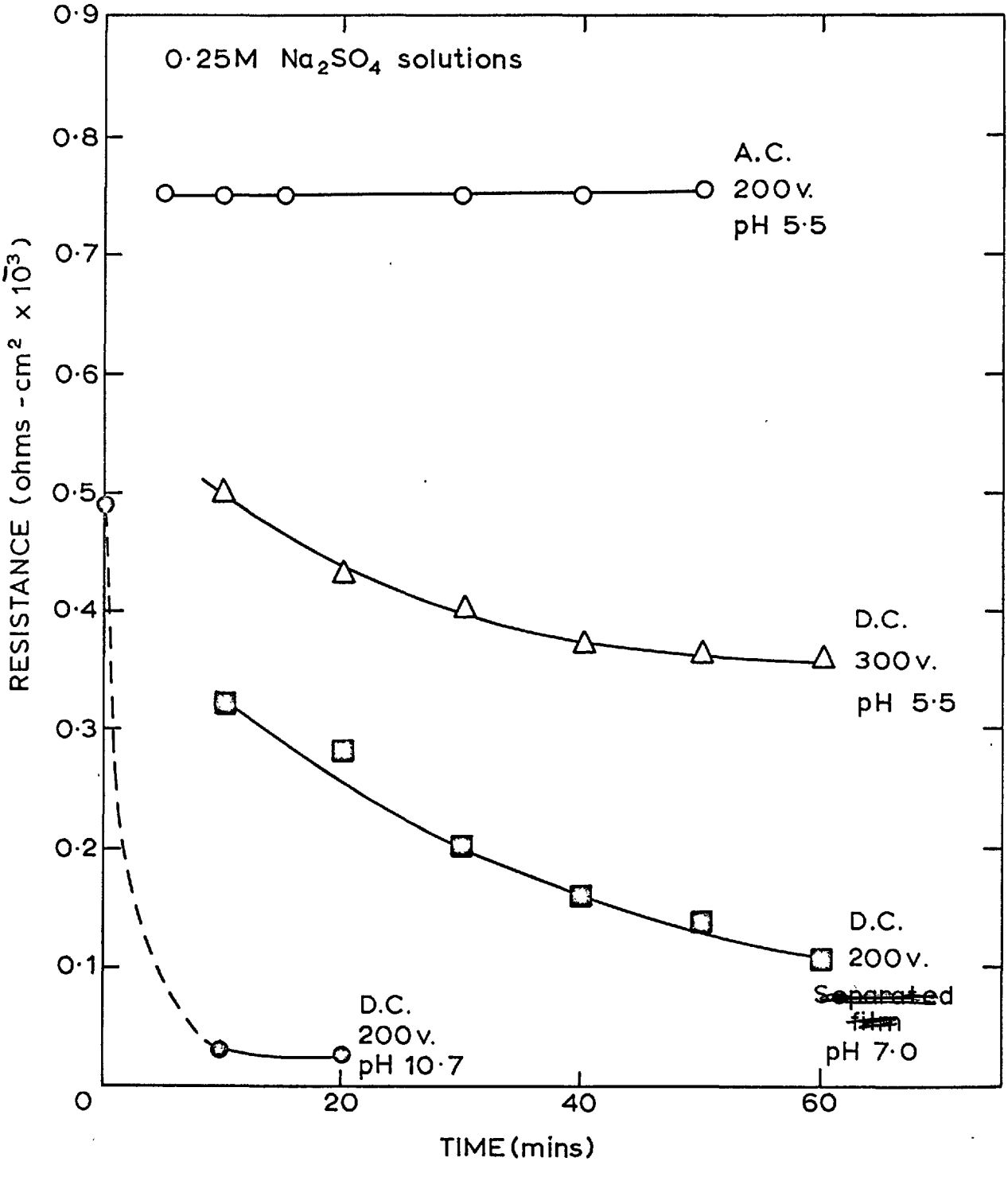

Fig.74. Resistance versus time of measurements for stripped oxide films by A.C. and D.C. methods

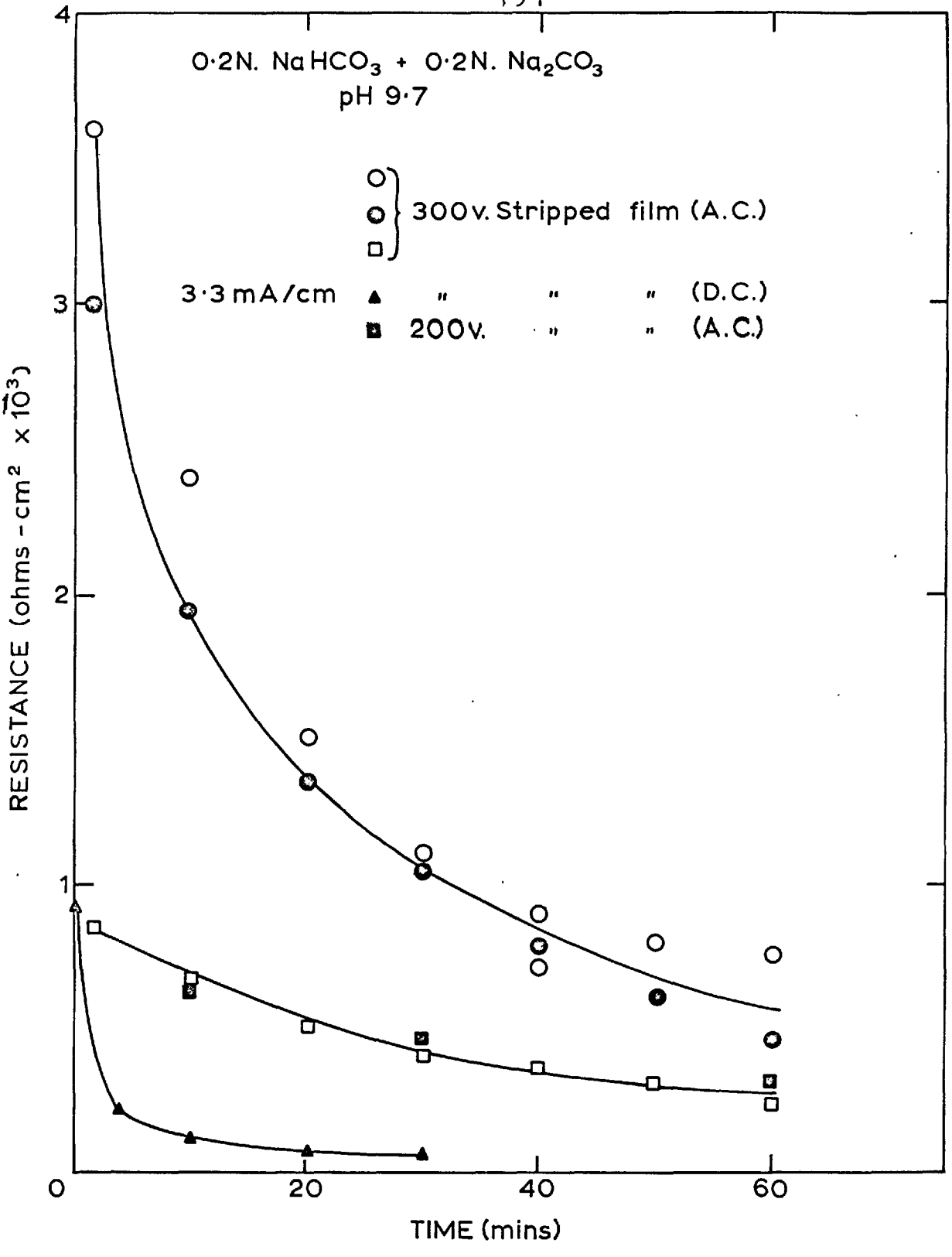

Fig.75. Resistance versus time of measurements for stripped films

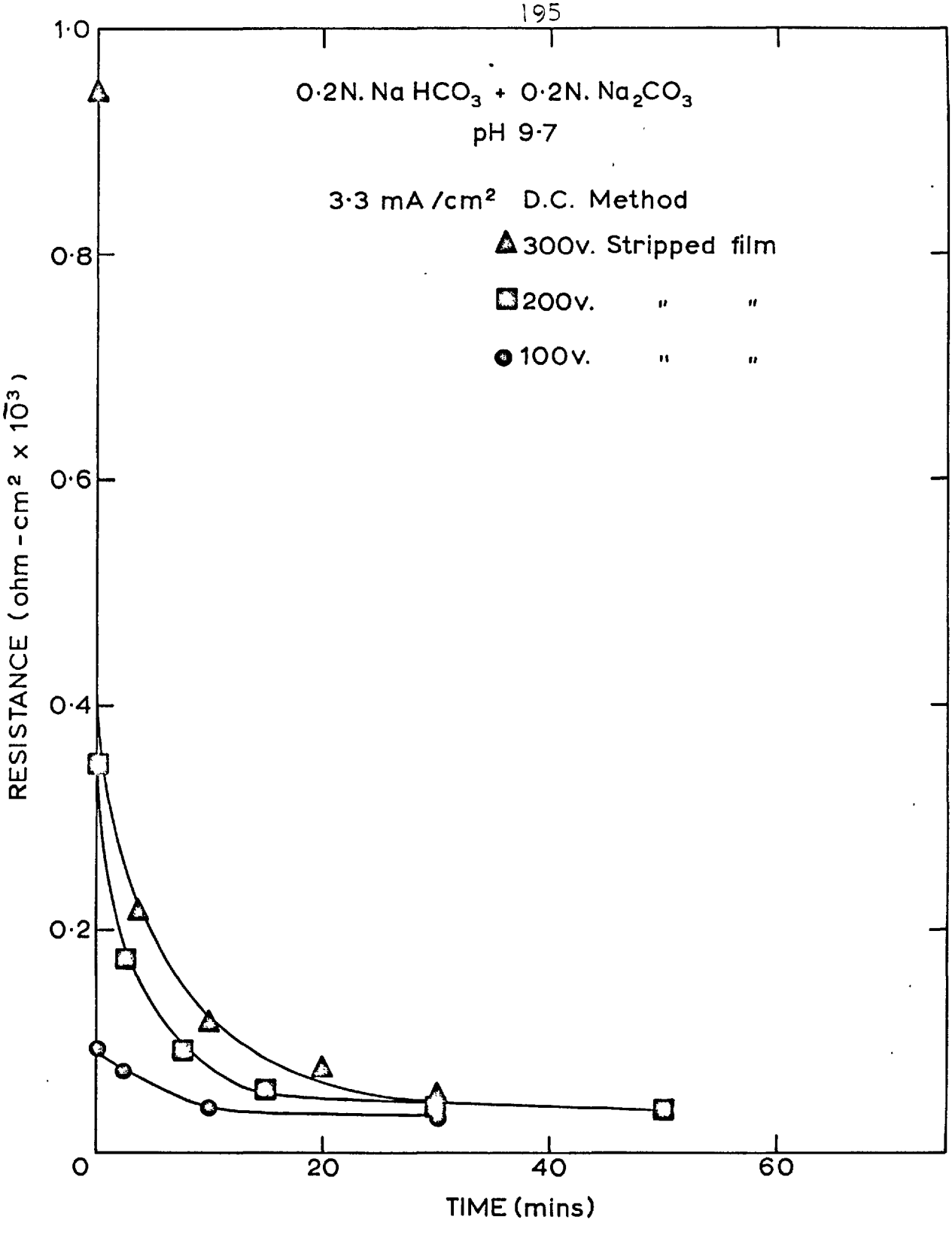

Fig. 76. Resistance versus time of measurements for stripped films

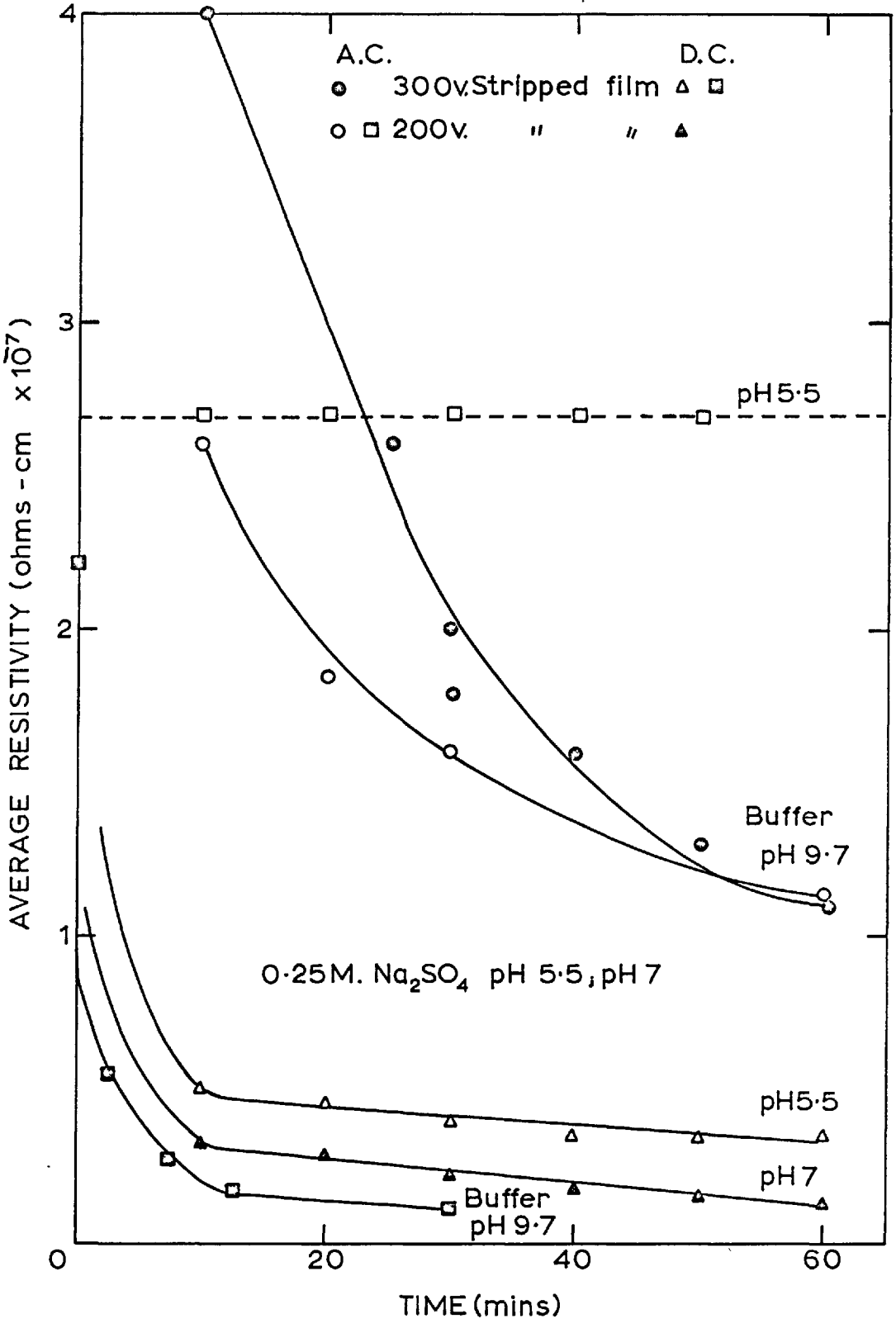

Fig.77. Resistivity versus time of measurements of stripped films in various solutions

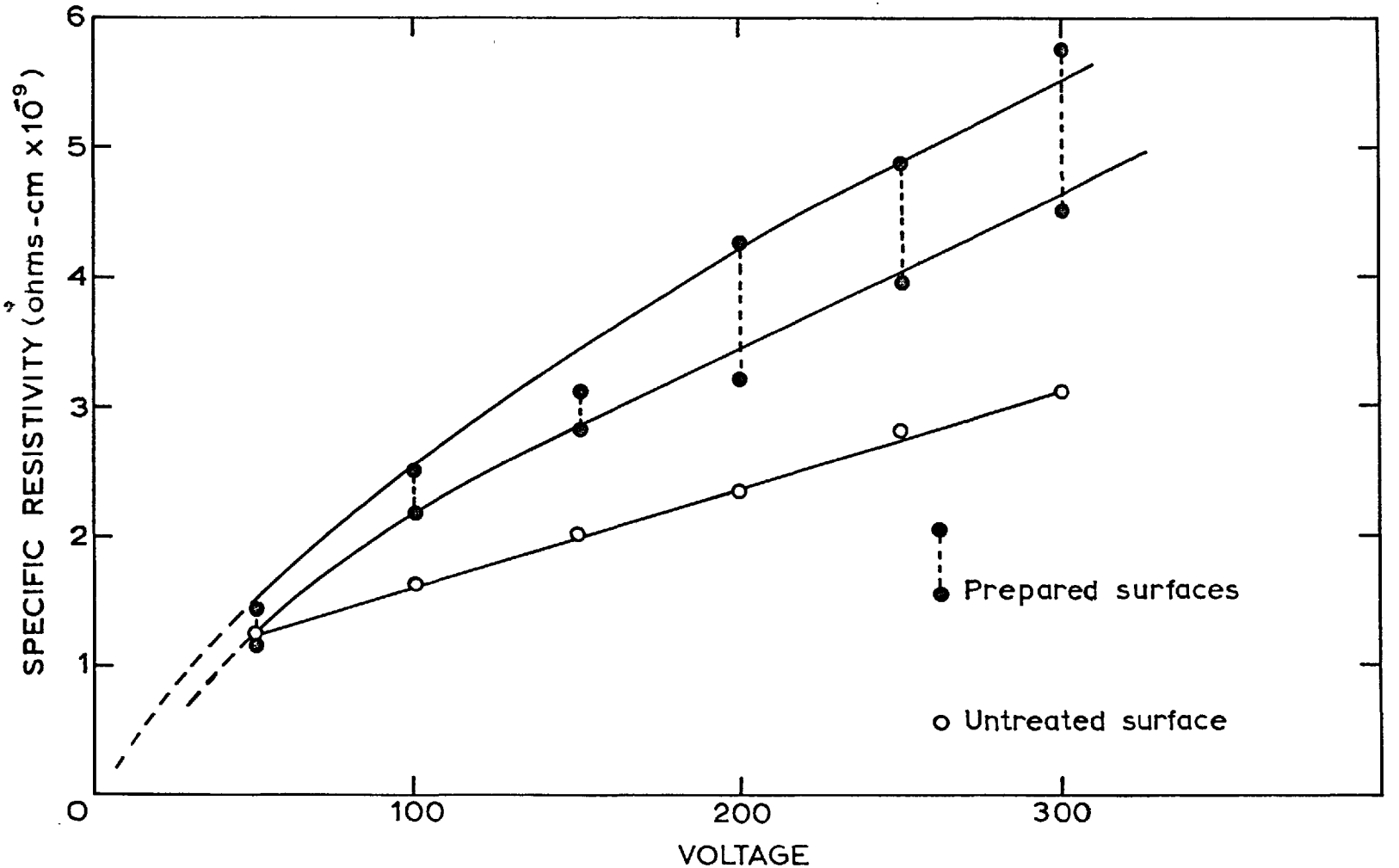

Fig.78. Specific resistivity versus voltage for alumina film formed on various surfaces (1592 c.p.s)

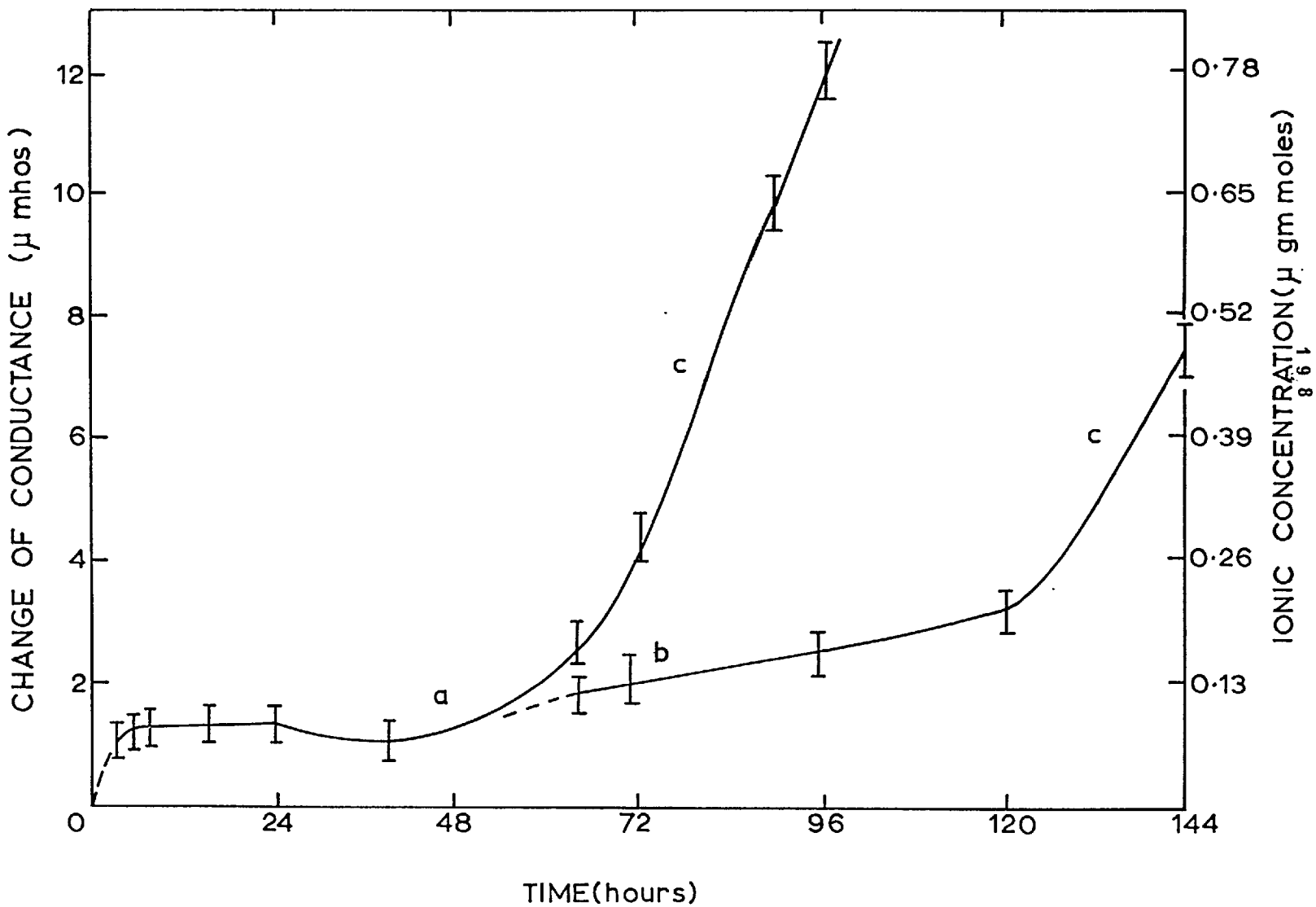

Fig.79. Conductance and ionic concentration versus time of permeation through stripped Al_2O_3 (300v., $1cm^2$, 1M.KCl)

Fig.80.

Magnification (30,000x); Transmission electron micrograph of 300 volts stripped film mounted for permeation experiment for one week as a diaphragm, showing pores developed

Fig.81.

Magnification (180x); Transmission optical micrograph of 300 volts stripped film mounted as diaphragm for permeation test as above for six days and finally a d.c. potential was applied across it for 10 minutes, showing damage caused by the field and the chloride ions.

Fig.82.

Magnification (180x); Reflection optical micrograph of the film as above, showing the appearance of damaged spots by reflection.

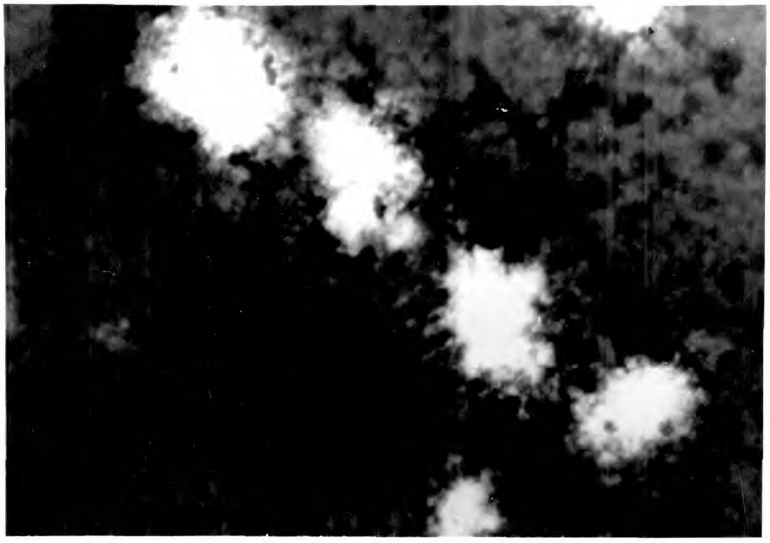

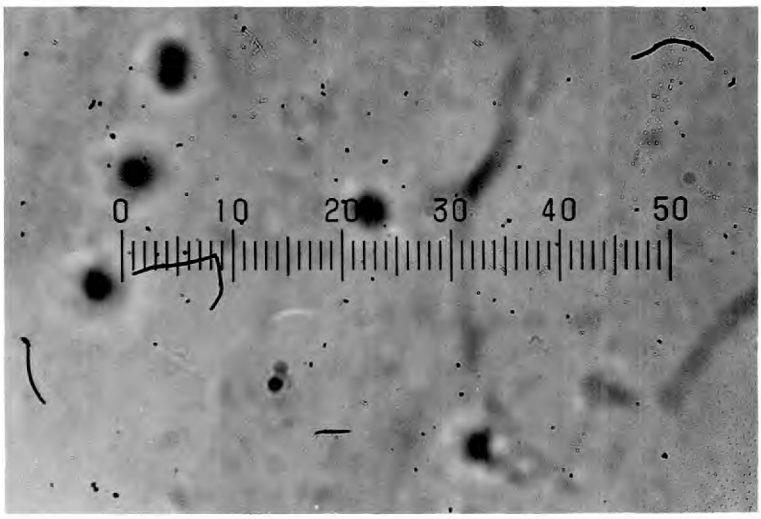
0
10
20
30
40
50

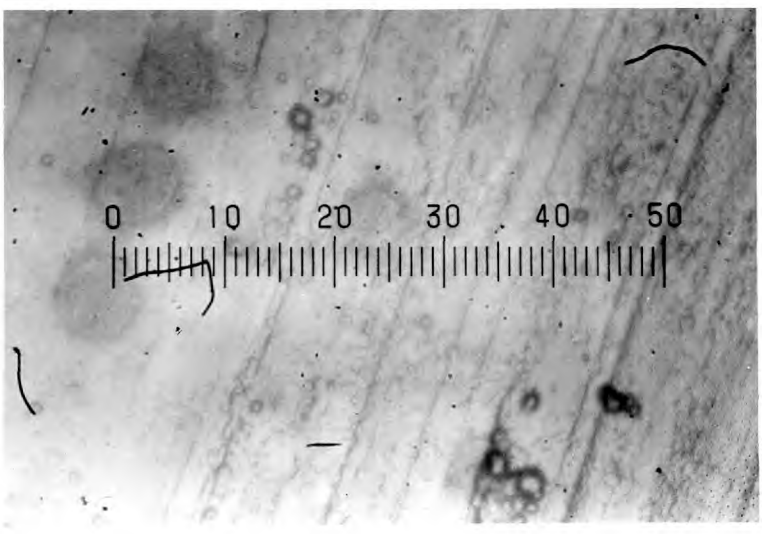
0
10
20
30
40
50